NBS TECHNICAL NOTE

366

An Analysis of the Brayton Cycle As a Cryogenic Refrigerator

U. S. DEPARTMENT OF COMMERCE
National Bureau of Standards

NATIONAL BUREAU OF STANDARDS

The National Bureau of Standards[1] was established by an act of Congress March 3, 1901. Today, in addition to serving as the Nation's central measurement laboratory, the Bureau is a principal focal point in the Federal Government for assuring maximum application of the physical and engineering sciences to the advancement of technology in industry and commerce. To this end the Bureau conducts research and provides central national services in three broad program areas and provides central national services in a fourth. These are: (1) basic measurements and standards, (2) materials measurements and standards, (3) technological measurements and standards, and (4) transfer of technology.

The Bureau comprises the Institute for Basic Standards, the Institute for Materials Research, the Institute for Applied Technology, and the Center for Radiation Research.

THE INSTITUTE FOR BASIC STANDARDS provides the central basis within the United States of a complete and consistent system of physical measurement, coordinates that system with the measurement systems of other nations, and furnishes essential services leading to accurate and uniform physical measurements throughout the Nation's scientific community, industry, and commerce. The Institute consists of an Office of Standard Reference Data and a group of divisions organized by the following areas of science and engineering:

Applied Mathematics—Electricity—Metrology—Mechanics—Heat—Atomic Physics—Cryogenics[2]—Radio Physics[2]—Radio Engineering[2]—Astrophysics[2]—Time and Frequency.[2]

THE INSTITUTE FOR MATERIALS RESEARCH conducts materials research leading to methods, standards of measurement, and data needed by industry, commerce, educational institutions, and government. The Institute also provides advisory and research services to other government agencies. The Institute consists of an Office of Standard Reference Materials and a group of divisions organized by the following areas of materials research:

Analytical Chemistry—Polymers—Metallurgy — Inorganic Materials — Physical Chemistry.

THE INSTITUTE FOR APPLIED TECHNOLOGY provides for the creation of appropriate opportunities for the use and application of technology within the Federal Government and within the civilian sector of American industry. The primary functions of the Institute may be broadly classified as programs relating to technological measurements and standards and techniques for the transfer of technology. The Institute consists of a Clearinghouse for Scientific and Technical Information,[3] a Center for Computer Sciences and Technology, and a group of technical divisions and offices organized by the following fields of technology:

Building Research—Electronic Instrumentation — Technical Analysis — Product Evaluation—Invention and Innovation— Weights and Measures — Engineering Standards—Vehicle Systems Research.

THE CENTER FOR RADIATION RESEARCH engages in research, measurement, and application of radiation to the solution of Bureau mission problems and the problems of other agencies and institutions. The Center for Radiation Research consists of the following divisions:

Reactor Radiation—Linac Radiation—Applied Radiation—Nuclear Radiation.

---

[1] Headquarters and Laboratories at Gaithersburg, Maryland, unless otherwise noted; mailing address Washington, D. C. 20234.
[2] Located at Boulder, Colorado 80302.
[3] Located at 5285 Port Royal Road, Springfield, Virginia 22151.

UNITED STATES DEPARTMENT OF COMMERCE
C. R. Smith, Secretary
NATIONAL BUREAU OF STANDARDS • A. V. Astin, Director

TECHNICAL NOTE 366

ISSUED AUGUST 1968

AN ANALYSIS OF THE BRAYTON CYCLE AS A CRYOGENIC REFRIGERATOR

R. C. MUHLENHAUPT AND T. R. STROBRIDGE

Cryogenics Division
Institute for Basic Standards
National Bureau of Standards
Boulder, Colorado 80302

For sale by the Superintendent of Documents, U.S. Government Printing Office, Washington, D.C., 20402
Price $1.25

TABLE OF CONTENTS

		Page
ABSTRACT		1
1.	Introduction	1
2.	Refrigerants	2
3.	Nomenclature List	2
4.	Discussion of Process	4
5.	Parameter Values	4
6.	Ideal Gas Calculations	8
7.	Real Gas Calculations	15
8.	Pressure Drop	16
9.	Results	18
10.	Discussion of Results	19
11.	Conclusions	30
12.	References	33
13.	Appendix	34

List of Figures

Figure 1.	Schematic Flow Diagram of the Modified Brayton Refrigeration Cycle	5
Figure 2.	Temperature-Entropy Diagram of the Modified Brayton Refrigeration Cycle	6
Figure 3.	Temperature-Entropy Diagram of an Ideal Brayton Refrigerator	7

TABLE OF CONTENTS (CONTINUED)

Page

Figure 4. Schematic Diagram of the Brayton Refrigerator Performance with an Ideal Gas as the Working Fluid . . 12

Figure 5. Schematic Diagram of the Brayton Refrigerator Performance Showing a Double Minimum Curve 22

Figure 6. Schematic Diagram of Enthalpy Difference as a Function of High Pressure For Parahydrogen 24

Figure 7. Schematic Diagram of Brayton Refrigerator Performance with an Ideal Gas as the Working Fluid - Single and Double Minimum Curves 25

Figure 8. Brayton Refrigerator Performance - Helium Refrigerant - 300 K Cycle Inlet Temperature - 100% Expander Efficiency - No Pressure Drop 39

Figure 9. Brayton Refrigerator Performance - Helium Refrigerant - 300 K Cycle Inlet Temperature - 90% Expander Efficiency - No Pressure Drop 40

Figure 10. Brayton Refrigerator Performance - Helium Refrigerant - 300 K Cycle Inlet Temperature - 70% Expander Efficiency - No Pressure Drop 41

Figure 11. Brayton Refrigerator Performance - Helium Refrigerant - 300 K Cycle Inlet Temperature - 50% Expander Efficiency - No Pressure Drop 42

Figure 12. Brayton Refrigerator Performance - Helium Refrigerant - 77.36 K Cycle Inlet Temperature - 100% Expander Efficiency - No Pressure Drop 43

Figure 13. Brayton Refrigerator Performance - Helium Refrigerant - 77.36 K Cycle Inlet Temperature - 90% Expander Efficiency - No Pressure Drop 44

Figure 14. Brayton Refrigerator Performance - Helium Refrigerant - 77.36 K Cycle Inlet Temperature - 70% Expander Efficiency - No Pressure Drop 45

TABLE OF CONTENTS (CONTINUED)

Page

Figure 15. Brayton Refrigerator Performance - Helium Refrigerant - 77.36 K Cycle Inlet Temperature - 50% Expander Efficiency - No Pressure Drop 46

Figure 16. Brayton Refrigerator Performance - Helium Refrigerant - 20.27 K Cycle Inlet Temperature - 100% Expander Efficiency - No Pressure Drop 47

Figure 17. Brayton Refrigerator Performance - Helium Refrigerant - 20.27 K Cycle Inlet Temperature - 90% Expander Efficiency - No Pressure Drop 48

Figure 18. Brayton Refrigerator Performance - Helium Refrigerant - 20.27 K Cycle Inlet Temperature - 70% Expander Efficiency - No Pressure Drop 49

Figure 19. Brayton Refrigerator Performance - Helium Refrigerant - 20.27 K Cycle Inlet Temperature - 50% Expander Efficiency - No Pressure Drop 50

Figure 20. Brayton Refrigerator Performance - Parahydrogen Refrigerant - 300 K Cycle Inlet Temperature - 100% Expander Efficiency - No Pressure Drop 51

Figure 21. Brayton Refrigerator Performance - Parahydrogen Refrigerant - 300 K Cycle Inlet Temperature - 90% Expander Efficiency - No Pressure Drop 52

Figure 22. Brayton Refrigerator Performance - Parahydrogen Refrigerant - 300 K Cycle Inlet Temperature - 70% Expander Efficiency - No Pressure Drop 53

Figure 23. Brayton Refrigerator Performance - Parahydrogen Refrigerant - 300 K Cycle Inlet Temperature - 50% Expander Efficiency - No Pressure Drop 54

Figure 24. Brayton Refrigerator Performance - Parahydrogen Refrigerant - 77.36 K Cycle Inlet Temperature - 100% Expander Efficiency - No Pressure Drop 55

TABLE OF CONTENTS (CONTINUED)

Page

Figure 25. Brayton Refrigerator Performance - Parahydrogen Refrigerant - 77.36 K Cycle Inlet Temperature - 90% Expander Efficiency - No Pressure Drop 56

Figure 26. Brayton Refrigerator Performance - Parahydrogen Refrigerant - 77.36 K Cycle Inlet Temperature - 70% Expander Efficiency - No Pressure Drop 57

Figure 27. Brayton Refrigerator Performance - Parahydrogen Refrigerant - 77.36 K Cycle Inlet Temperature - 50% Expander Efficiency - No Pressure Drop 58

Figure 28. Brayton Refrigerator Performance - Nitrogen Refrigerant - 300 K Cycle Inlet Temperature - 100% Expander Efficiency - 2 K Heat Exchanger Temperature Difference - No Pressure Drop 59

Figure 29. Brayton Refrigerator Performance - Nitrogen Refrigerant - 300 K Cycle Inlet Temperature - 90% Expander Efficiency - 2 K Heat Exchanger Temperature Difference - No Pressure Drop 60

Figure 30. Brayton Refrigerator Performance - Nitrogen Refrigerant - 300 K Cycle Inlet Temperature- 70% Expander Efficiency - 2 K Heat Exchanger Temperature Difference - No Pressure Drop 61

Figure 31. Brayton Refrigerator Performance - Nitrogen Refrigerant - 300 K Cycle Inlet Temperature - 50% Expander Efficiency - 2 K Heat Exchanger Temperature Difference - No Pressure Drop 62

Figure 32. Brayton Refrigerator Performance - Nitrogen Refrigerant - 300 K Cycle Inlet Temperature - 100% Expander Efficiency - 4 K Heat Exchanger Temperature Difference - No Pressure Drop 63

Page

Figure 33. Brayton Refrigerator Performance - Nitrogen Refrigerant - 300 K Cycle Inlet Temperature - 90% Expander Efficiency - 4 K Heat Exchanger Temperature Difference - No Pressure Drop 64

Figure 34. Brayton Refrigerator Performance - Nitrogen Refrigerant - 300 K Cycle Inlet Temperature - 70% Expander Efficiency - 4 K Heat Exchanger Temperature Difference - No Pressure Drop 65

Figure 35. Brayton Refrigerator Performance - Nitrogen Refrigerant - 300 K Cycle Inlet Temperature - 50% Expander Efficiency - 4 K Heat Exchanger Temperature Difference - No Pressure Drop 66

Figure 36. Brayton Refrigerator Performance - Nitrogen Refrigerant - 300 K Cycle Inlet Temperature - 100% Expander Efficiency - 6 K Heat Exchanger Temperature Difference - No Pressure Drop 67

Figure 37. Brayton Refrigerator Performance - Nitrogen Refrigerant - 300 K Cycle Inlet Temperature - 90% Expander Efficiency - 6 K Heat Exchanger Temperature Difference - No Pressure Drop 68

Figure 38. Brayton Refrigerator Performance - Nitrogen Refrigerant - 300 K Cycle Inlet Temperature - 70% Expander Efficiency - 6 K Heat Exchanger Temperature Difference - No Pressure Drop 69

Figure 39. Brayton Refrigerator Performance - Nitrogen Refrigerant - 300 K Cycle Inlet Temperature - 50% Expander Efficiency - 6 K Heat Exchanger Temperature Difference - No Pressure Drop 70

Figure 40. Brayton Refrigerator Performance - Nitrogen Refrigerant - 300 K Cycle Inlet Temperature - 100% Expander Efficiency - 10 K Heat Exchanger Temperature Difference - No Pressure Drop 71

TABLE OF CONTENTS (CONTINUED)

Page

Figure 41. Brayton Refrigerator Performance - Nitrogen Refrigerant - 300 K Cycle Inlet Temperature - 90% Expander Efficiency - 10 K Heat Exchanger Temperature Difference - No Pressure Drop 72

Figure 42. Brayton Refrigerator Performance - Nitrogen Refrigerant - 300 K Cycle Inlet Temperature - 70% Expander Efficiency - 10 K Heat Exchanger Temperature Difference - No Pressure Drop 73

Figure 43. Brayton Refrigerator Performance - Nitrogen Refrigerant - 300 K Cycle Inlet Temperature - 50% Expander Efficiency - 10 K Heat Exchanger Temperature Difference - No Pressure Drop 74

Figure 44. Brayton Refrigerator Performance - Helium Refrigerant - 300 K Cycle Inlet Temperature - 70% Expander Efficiency - Pressure Drop. 75

Figure 45. Brayton Refrigerator Performance - Helium Refrigerant - 300 K Cycle Inlet Temperature - 50% Expander Efficiency - Pressure Drop. 76

Figure 46. Brayton Refrigerator Performance - Helium Refrigerant - 77.36 K Cycle Inlet Temperature - 70% Expander Efficiency - Pressure Drop. 77

Figure 47. Brayton Refrigerator Performance - Helium Refrigerant - 77.36 K Cycle Inlet Temperature - 50% Expander Efficiency - Pressure Drop. 78

Figure 48. Brayton Refrigerator Performance - Helium Refrigerant - 20.27 K Cycle Inlet Temperature - 70% Expander Efficiency - Pressure Drop. 79

Figure 49. Brayton Refrigerator Performance - Helium Refrigerant - 20.27 K Cycle Inlet Temperature - 50% Expander Efficiency - Pressure Drop. 80

Page

Figure 50. Brayton Refrigerator Performance - Parahydrogen Refrigerant - 300 K Cycle Inlet Temperature - 70% Expander Efficiency - Pressure Drop. 81

Figure 51. Brayton Refrigerator Performance - Parahydrogen Refrigerant - 300 K Cycle Inlet Temperature - 50% Expander Efficiency - Pressure Drop. 82

Figure 52. Brayton Refrigerator Performance - Parahydrogen Refrigerant - 77.36 K Cycle Inlet Temperature - 70% Expander Efficiency - Pressure Drop. 83

Figure 53. Brayton Refrigerator Performance - Parahydrogen Refrigerant - 77.36 K Cycle Inlet Temperature - 50% Expander Efficiency - Pressure Drop. 84

Figure 54. Brayton Refrigerator Performance - Nitrogen Refrigerant - 300 K Cycle Inlet Temperature - 70% Expander Efficiency - 2.0 K Heat Exchanger Temperature Difference - Pressure Drop. 85

Figure 55. Brayton Refrigerator Performance - Nitrogen Refrigerant - 300 K Cycle Inlet Temperature - 50% Expander Efficiency - 2.0 K Heat Exchanger Temperature Difference - Pressure Drop. 86

Figure 56. Brayton Refrigerator Performance - Nitrogen Refrigerant - 300 K Cycle Inlet Temperature - 70% Expander Efficiency - 4.0 K Heat Exchanger Temperature Difference - Pressure Drop. 87

Figure 57. Brayton Refrigerator Performance - Nitrogen Refrigerant - 300 K Cycle Inlet Temperature - 50% Expander Efficiency - 4.0 K Heat Exchanger Temperature Difference - Pressure Drop. 88

Figure 58. Brayton Refrigerator Performance - Nitrogen Refrigerant - 300 K Cycle Inlet Temperature - 70% Expander Efficiency - 6.0 K Heat Exchanger Temperature Difference - Pressure Drop. 89

TABLE OF CONTENTS (CONTINUED)

Page

Figure 59. Brayton Refrigerator Performance - Nitrogen Refrigerant - 300 K Cycle Inlet Temperature - 50% Expander Efficiency - 6.0 K Heat Exchanger Temperature Difference - Pressure Drop 90

Figure 60. Brayton Refrigerator Performance - Nitrogen Refrigerant - 300 K Cycle Inlet Temperature - 70% Expander Efficiency - 10.0 K Heat Exchanger Temperature Difference - Pressure Drop 91

Figure 61. Brayton Refrigerator Performance - Nitrogen Refrigerant - 300 K Cycle Inlet Temperature - 50% Expander Efficiency - 10.0 K Heat Exchanger Temperature Difference - Pressure Drop 92

Figure 62. Expander Performance - Helium Refrigerant - 100% Expander Efficiency - No Pressure Drop 93

Figure 63. Expander Performance - Helium Refrigerant - 90% Expander Efficiency - No Pressure Drop 94

Figure 64. Expander Performance - Helium Refrigerant - 70% Expander Efficiency - No Pressure Drop 95

Figure 65. Expander Performance - Helium Refrigerant - 50% Expander Efficiency - No Pressure Drop 96

Figure 66. Expander Performance - Parahydrogen Refrigerant - 100% Expander Efficiency - No Pressure Drop 97

Figure 67. Expander Performance - Parahydrogen Refrigerant - 90% Expander Efficiency - No Pressure Drop 98

Figure 68. Expander Performance - Parahydrogen Refrigerant - 70% Expander Efficiency - No Pressure Drop 99

Page

Figure 69. Expander Performance - Parahydrogen Refrigerant - 50% Expander Efficiency - No Pressure Drop 100

Figure 70. Expander Performance - Helium Refrigerant - 70% Expander Efficiency - Pressure Drop. 101

Figure 71. Expander Performance - Helium Refrigerant - 50% Expander Efficiency - Pressure Drop. 102

Figure 72. Expander Performance - Parahydrogen Refrigerant - 70% Expander Efficiency - Pressure Drop. 103

Figure 73. Expander Performance - Parahydrogen Refrigerant - 50% Expander Efficiency - Pressure Drop. 104

Figure 74. Specific Flow Rate - Helium Refrigerant 105

Figure 75. Specific Flow Rate - Parahydrogen Refrigerant 106

AN ANALYSIS OF THE BRAYTON CYCLE AS A CRYOGENIC REFRIGERATOR

R. C. Muhlenhaupt and T. R. Strobridge

The performance of a Brayton-cycle refrigerator has been computed taking into account the efficiencies of the various components. The results are presented in graphical form. These charts give the input power requirements, mass flow rate, pertinent temperatures, and allow selection of the optimum high pressure for a given set of component characteristics.

Key Words: Brayton, cryogenics, refrigeration

1. Introduction

In 1873 a Boston engineer, George Brayton, conceived an ideal heat engine which, when operating in a thermodynamic system, combines constant pressure and constant entropy processes. In actual practice, the real machine differs from this ideal because of fluid friction in the flow passages, heat transfer with the surroundings, and irreversibilities in the expansion machine, compressor, and heat exchanger.

In the same year Brayton, using the principles learned in the development of his heat engine, designed a refrigeration machine which operated on a reversed Brayton cycle. The working fluid in such a machine receives heat at some low pressure and temperature and then rejects heat at some higher pressure and temperature. Brayton's cycle is sometimes referred to as the Joule or the air-standard cycle. This is because Joule, working independently of Brayton, proposed the same cycle, and air is commonly used as the working fluid.

During the past several years, the Brayton cycle, operating as an open cycle refrigerator, has been used extensively in aircraft cooling, and the cycle is considered by many to be the prime candidate

for space power systems (Bernatowicz, [1963]; Harrach and Caldwell, [1963]; Glassman and Stewart, [1964]; Schultz and Melber, [1964]; and Glassman et al., [1965]). A modified version of this refrigeration cycle has been analyzed and will be considered here.

Analytical expressions are derived to determine values for flow rate, high pressure, evaporator inlet temperature, and figure of merit (the power input per unit of refrigeration) for selected values of expander efficiency, cycle inlet temperature, evaporator outlet temperature, and cycle temperature difference (the temperature differential across the warm end of the heat exchanger). The resulting data are presented in figures 8 thru 75.

2. Refrigerants

Fluids considered in this analysis are nitrogen, parahydrogen, and helium. The state equations of Strobridge, [1962], Roder and Goodwin, [1961], and Mann, [1962] were used to calculate the required thermodynamic properties. Data were obtained for refrigeration at, and above, the normal boiling points of each fluid which are 77.364 K for nitrogen, 20.269 K for parahydrogen and 4.214 K for helium.

3. Nomenclature List

C_p	specific heat at constant pressure	(J/g mole•K)
C_v	specific heat at constant volume	(J/g mole•K)
F	volumetric flow rate	(scfm)
F/Q	compressor flow per unit refrigeration	(scfm/kW)
M	molecular weight	(He 4.0028 g/g mole) (H_2 2.016 g/g mole) (N_2 28.016 g/g mole)

P	pressure	(atm)
R	universal gas constant	(8.3143 J/g mole•K)
T	temperature	(K)
T_a	ambient temperature	(300 K)
ΔT_{1-5}	temperature difference between the fluid streams at warm end of heat exchanger ($T_1 - T_5$)	(K)
W_c/Q	figure of merit (compressor power per unit of refrigeration)	(W/W)
W_e/F	expander power per unit flow	(W/scfm)
h	specific enthalpy	(J/g)
k	specific heat ratio (C_p/C_v)	(unitless)
m	mass flow rate	(g/s)
s	specific entropy	(J/g•K)
scfm	standard cubic feet per minute measured at 273.15 K and 1.0 atmosphere	(ft^3/min)
v	specific volume	(cm^3/g)
v_{std}	specific volume of the gas at 273.15 K and 1.0 atmosphere	(cm^3/g)
η_c	isothermal compressor efficiency	(unitless)
Q	unit of refrigeration	(W)

η_e	isentropic expander efficiency	(unitless)
ρ	density	(g mole/ℓ)
101.3278	a multiplication factor	(J/ℓ•atm)
0.002119	a multiplication factor	(J•scfm/cm^3•W)

4. Discussion of Process

A schematic flow diagram of the modified Brayton refrigeration cycle is shown in figure 1, and the process paths are illustrated on temperature-entropy coordinates in figure 2. The thermodynamic processes involved are isobaric cooling between stations 1 and 2, adiabatic expansion between 2 and 3, isobaric heat absorption of the refrigeration load between 3 and 4, isobaric heating between 4 and 5, and isothermal compression at ambient temperature between the low and high pressures[1].

For comparison, figure 3 shows the process paths of Brayton's ideal refrigeration cycle. The main difference between the two figures occurs in the ideal compression and expansion processes which are isentropic in figure 3 rather than isothermal and adiabatic as shown in figure 2.

5. Parameter Values

The performance of the refrigerator depends on the fluid used as the refrigerant, the pressure levels in the fluid circuit, the refrigeration temperature, the temperature at the warm inlet of the heat exchanger, and the efficiencies of the compressor, heat exchanger, and expansion

[1] The process path shown in figure 2 between stations 5 and 1 is not isothermal, indicating that a finite temperature difference will exist in the heat exchanger of an actual refrigerator. It is assumed that the temperature of the fluid at the inlet of the compressor will be the same as the discharge due to heat transfer with the surroundings through the interconnecting piping.

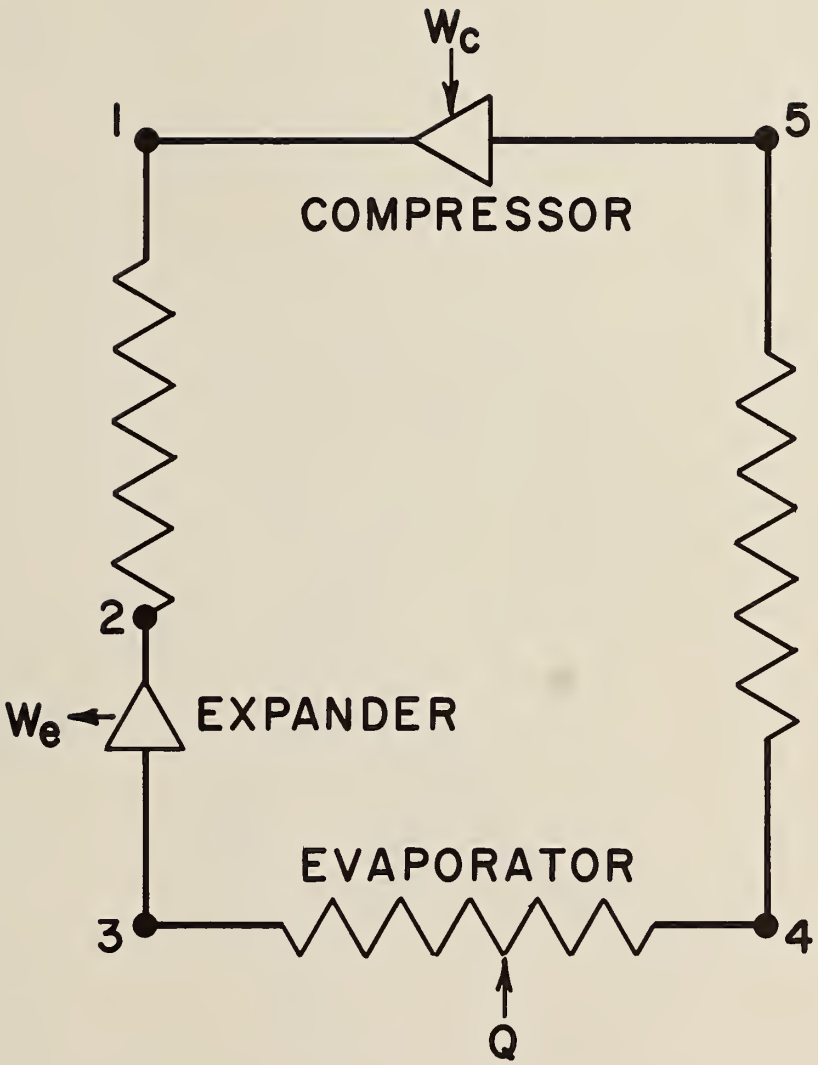

Figure 1. Schematic Flow Diagram of the Modified Brayton Refrigeration Cycle.

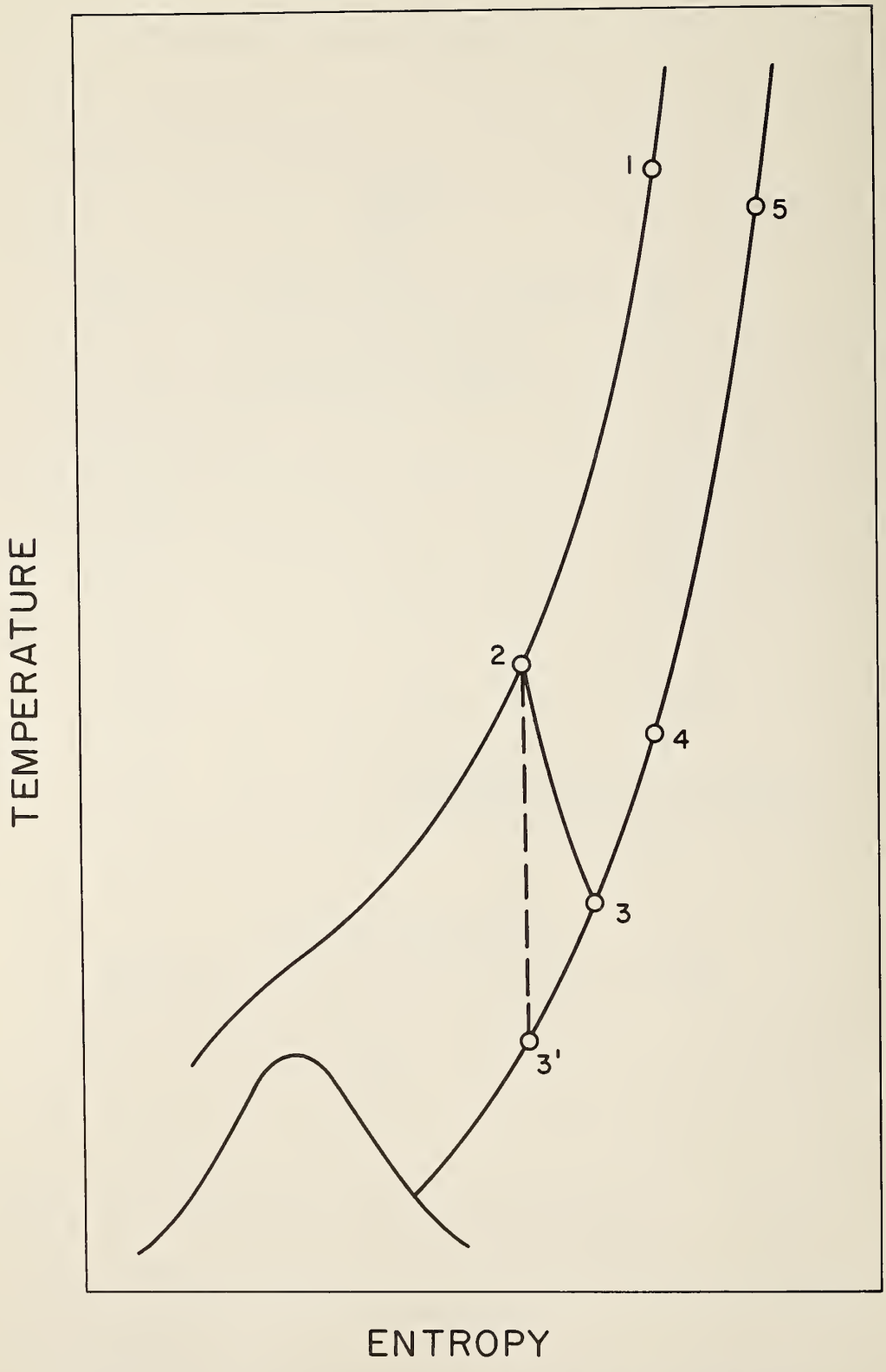

Figure 2. Temperature-Entropy Diagram of the Modified Brayton Refrigeration Cycle.

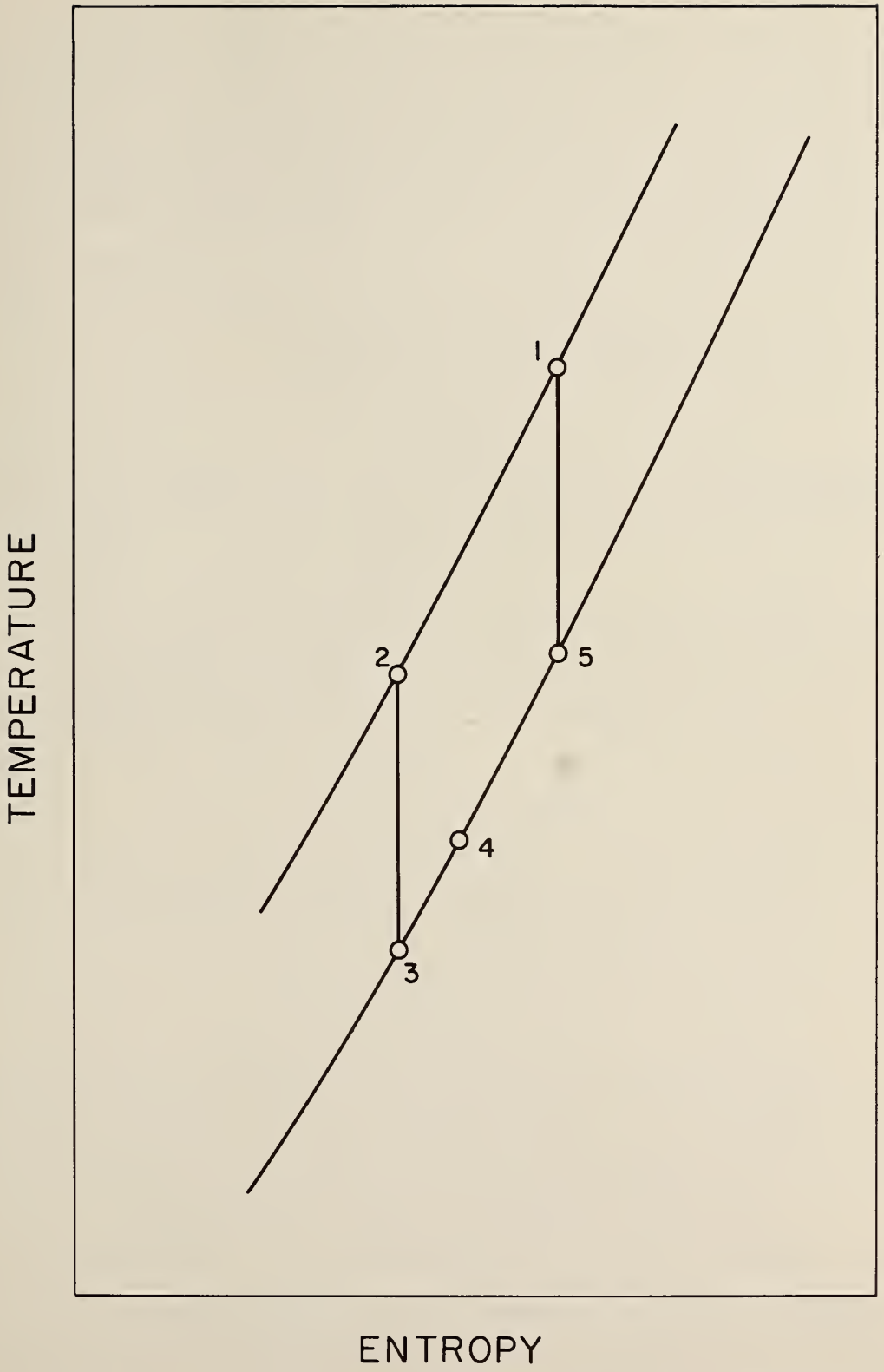

Figure 3. Temperature-Entropy Diagram of an Ideal Brayton Refrigerator.

engine. The power required for the compressor was in all instances calculated from the relation for the 100 percent efficient isothermal compression of an ideal gas at 300 K between the appropriate pressure levels. The results presented here must therefore be corrected to take into account the isothermal efficiency of actual compressors. The efficiency of the heat exchanger is reflected by the temperature difference between the fluid streams at the warm end of the heat exchanger. Table I lists the values of the parameters used in the analysis.

TABLE I

Parameter	Variations
T_1	300.0, 77.36, & 20.27 K
T_4	8-100 K (helium)
	78-100 K (nitrogen)
	22-100 K (parahydrogen)
ΔT_{1-5}	0.5, 1.0, 2.0, 3.0, 4.0, 6.0 & 10.0 K
P_1	2-60 atm
P_5	1 and 1.2 atm
η_e	50, 70, 90 & 100%

6. Ideal Gas Calculations

Charts showing the performance of the modified Brayton refrigerator assuming that the refrigerants behave as ideal gases are useful in two ways. First, such charts, and the relations from which they are derived, are helpful in explaining the characteristics of the various curves. Second, when the ideal gas performance charts are prepared as transparent overlays to graphs calculated from real gas properties, the direct visual comparison shows the necessity for using real gas properties if accurate results are required.

The efficiency (or the figure of merit, as it is commonly called) of a refrigeration device is usually defined as the ratio of the net power input to the refrigeration effect. For the purpose of this analysis, the figure of merit is defined as the ratio of the isothermal compressor power input (rather than the net power input) to the refrigeration effect. Thus,

$$\frac{W_c}{Q} = -\frac{RT_a \ln\left(\frac{P_1}{P_5}\right)}{\eta_c C_p (T_4 - T_3)} \quad . \tag{1}$$

The compressor power W_c is negative because it represents power transferred to the system. However, for convenience, the absolute value is always used in this analysis.

Since the efficiencies of the expander and the heat exchanger are important considerations to the refrigerator designer, these properties must be included. An expression equivalent to (1) is

$$\frac{W_c}{Q} = \frac{T_a \ln\left(\frac{P_1}{P_5}\right)^{\frac{k-1}{k}}}{\eta_c \left\{\eta_e \left[1 - \left(\frac{P_1}{P_5}\right)^{-\frac{k-1}{k}}\right]\left[T_4 + \Delta T_{1-5}\right] - \Delta T_{1-5}\right\}} \quad . \tag{2}$$

For a given set of parameters (i.e., T_4, ΔT_{1-5}, η_e, and the refrigerant), there is an optimum high pressure which will require a minimum amount of compressor power to produce a unit of refrigeration. This fact can be demonstrated by differentiating (2). Thus

$$\left[\frac{d\left(\frac{W_c}{Q}\right)}{dP_1}\right]_{T_1} = \frac{T_a \eta_c \frac{k-1}{k} \left\{\eta_e \left[1 - \left(\frac{P_1}{P_5}\right)^{-\frac{k-1}{k}}\right]\left[T_4 + \Delta T_{1-5}\right] - \Delta T_{1-5}\right\}}{\eta_c^2 P_1 \left\{\eta_e \left[1 - \left(\frac{P_1}{P_5}\right)^{-\frac{k-1}{k}}\right]\left[T_4 + \Delta T_{1-5}\right] - \Delta T_{1-5}\right\}^2}$$

$$- \frac{T_a \eta_c \eta_e \frac{k-1}{k} \left(T_4 + \Delta T_{1-5}\right) \left(\frac{P_1}{P_5}\right)^{-\frac{2k-1}{k}} \left(\frac{P_1}{P_5}\right) \ell n \left(\frac{P_1}{P_5}\right)^{\frac{k-1}{k}}}{\eta_c^2 P_1 \left\{\eta_e \left[1 - \left(\frac{P_1}{P_5}\right)^{-\frac{k-1}{k}}\right]\left[T_4 + \Delta T_{1-5}\right] - \Delta T_{1-5}\right\}^2}$$

which becomes

$$\left[\frac{d\left(\frac{W_c}{Q}\right)}{dP_1}\right]_{T_1} = \frac{T_a \eta_e \left(T_4 + \Delta T_{1-5}\right)(k-1)}{\eta_c P_1 k}$$

$$\times \frac{\left\{\left[1 - \frac{\Delta T_{1-5}}{\eta_e \left(T_4 + \Delta T_{1-5}\right)}\right] - \left(\frac{P_1}{P_5}\right)^{-\frac{k-1}{k}} \left[1 + \ell n \left(\frac{P_1}{P_5}\right)^{\frac{k-1}{k}}\right]\right\}}{\left\{\eta_e \left[1 - \left(\frac{P_1}{P_5}\right)^{-\frac{k-1}{k}}\right]\left[T_4 + \Delta T_{1-5}\right] - \Delta T_{1-5}\right\}^2}. \quad (3)$$

For simplification, two terms in the numerator are defined as follows:

$$A = 1 - \frac{\Delta T_{1-5}}{\eta_e \left(T_4 + \Delta T_{1-5}\right)} \qquad \text{and}$$

$$B = \left(\frac{P_1}{P_5}\right)^{-\frac{k-1}{k}} \left[1 + \ell n \left(\frac{P_1}{P_5}\right)^{\frac{k-1}{k}}\right]$$

For the combinations of component parameters, the term A is a constant greater than zero but less than one, while B varies from a maximum of one (as P_1 approaches P_5) to a minimum of zero (as P_1 approaches infinity).

At a pressure P_1 equal to P_5, the term B equals 1. For this condition only, (3) becomes

$$\left[\frac{d\left(\frac{W_c}{Q}\right)}{d P_1}\right]_{T_1} = -\frac{T_a (k-1)}{\eta_c k \Delta T_{1-5} P_1} \quad . \tag{4}$$

The terms in (4) are positive; therefore, the slope is negative, and the curve is decreasing with increasing pressure. Referring to (3), as the pressure ratio is increased, B decreases causing the slope to increase until some pressure $P_{1(i)}$ is reached where A and B are equal. Here the slope goes to zero establishing a minimum point on the curve. Beyond this pressure the difference between A and B is always positive; therefore, the slope is also positive. As the pressure is increased further, the slope, still remaining positive, begins to decrease and continues to do so until the pressure becomes infinite. Here the slope goes to zero.

Equation (2) was evaluated holding ΔT_{1-5}, η_e, η_c, and P_5 constant while varying P_1 and T_4. The results were plotted as a function of P_1. The general shape of the curves is shown schematically in figure 4. For each T_4 at constant ΔT_{1-5} the optimum high pressure can be found. For each ΔT_{1-5} at constant T_4 again the optimum pressure can be calculated. Therefore, it is possible to plot the locus of optimum pressures for both constant T_4 and constant ΔT_{1-5}.

To determine these optimum pressures, (3) is set equal to zero, and after simplification, the expression becomes

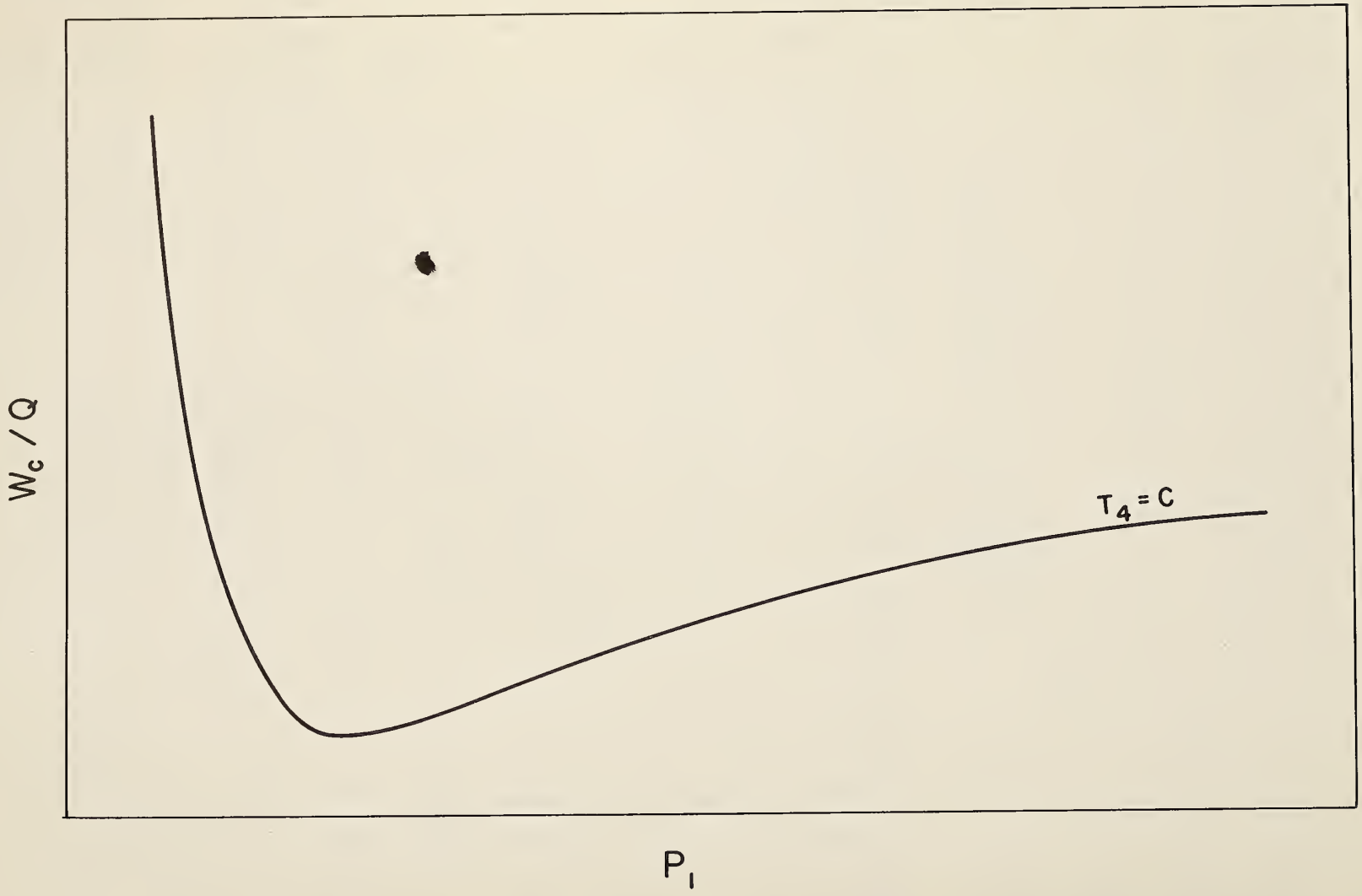

Figure 4. Schematic Diagram of the Brayton Refrigerator Performance with an Ideal Gas as the Working Fluid.

$$\left\{1 - \frac{\Delta T_{1-5}}{\eta_e (T_4 + \Delta T_{1-5})} - \left(\frac{P_1}{P_5}\right)^{-\frac{k-1}{k}} \left[1 + \ell n \left(\frac{P_1}{P_5}\right)^{\frac{k-1}{k}}\right]\right\} = 0. \quad (5)$$

The optimum pressure P_1 was then calculated through an iteration process for several sets of P_1, T_4, and ΔT_{1-5} for the ideal gas refrigerants, helium and hydrogen. For comparison to the corresponding real gas data, these charts are shown as transparent overlays to figures 8 thru 11 and 20 thru 23.

For additional information, a family of evaporator inlet (or expander outlet) temperature T_3 curves is included on these ideal gas, optimum operating pressure plots. The efficiency of the expansion device is defined as

$$\eta_e = \frac{T_2 - T_3}{T_2 - T_{3'}} \quad , \quad (6)$$

and the temperature-pressure relationship for an isentropic expansion is

$$\frac{T_2}{T_{3'}} = \left(\frac{P_2}{P_{3'}}\right)^{\frac{k-1}{k}} \quad . \quad (7)$$

In addition

$$T_2 = T_4 + \Delta T_{1-5} \quad (8)$$

for an ideal gas. Substituting (8) and (7) into (6) and rearranging, gives

$$T_3 = (T_4 + \Delta T_{1-5}) \left\{ \eta_e \left[\left(\frac{P_1}{P_5} \right)^{-\frac{k-1}{k}} - 1 \right] + 1 \right\} , \qquad (9)$$

where P_1 equals P_2 and P_5 equals $P_{3'}$. The evaporator inlet temperatures were calculated from (9) using the optimum high pressures determined in evaluating (5).

As ΔT_{1-5} approaches zero for all refrigeration temperatures, the optimum high pressure becomes smaller and is equal to the low pressure in the limit. Although this is an impossible operating condition, it is informative to calculate the performance since it is a lower limit for the power required per unit of refrigeration. Equation (1) cannot be evaluated explicitly for a high pressure of one atmosphere; however, it can be changed to the equivalent form

$$\frac{W_c}{Q} = \frac{T_a \ln \left(\frac{T_4}{T_{3'}} \right)}{\eta_c \eta_e (T_4 - T_{3'})} , \qquad (10)$$

where T_4 equals $T_{3'}$ when P_1 equals P_5. Although (10) also cannot be evaluated explicitly for T_4 equal to $T_{3'}$, it can be solved using L'Hospital's rule. Thus, in the limit as T_4 approaches $T_{3'}$

$$\frac{W_c}{Q} = \frac{T_a}{\eta_c \eta_e T_4} . \qquad (11)$$

Equation (11) was used to determine W_c/Q at one atmosphere high pressure for all T_4 values for both the ideal and the real gas cases.

7. Real Gas Calculations

The analysis that follows assumes no pressure loss in the system; thus, $P_2 = P_1$ and $P_3 = P_4 = P_5$ = one atmosphere. In addition T_1, η_e, and T_4 are constant. The compressor is 100 percent efficient with respect to ideal gas isothermal compression. Steady state conditions are assumed throughout and elevation and kinetic energy contributions to the fluid energy are negligible. Application of the first law of thermodynamics to the cycle gives

$$\frac{W_c}{Q} = - \frac{RT_a \ln\left(\frac{P_1}{P_5}\right)}{\eta_c M (h_4 - h_3)} . \qquad (12)$$

Again the convention of using absolute values of W_c/Q is adopted. If (12) is evaluated in the same manner as (2) and the results plotted, the curves will again exhibit the general behavior shown in figure 4.

The development of (13), used to determine optimum pressures is given in the Appendix. This expression is similar to (5) and equal to zero at optimum conditions,

$$(h_4 - h_3) + \left(\frac{101.32779}{M}\right)\left(P_1 \ln\frac{P_1}{P_5}\right)$$

$$x \left[\left(1 - \eta_e + \frac{\eta_e T_{3'}}{T_2}\right)\left(\frac{d h_1}{d P_1}\right)_{T_1} - \frac{\eta_e T_{3'}}{\rho_2 T_2}\right] = 0 . \qquad (13)$$

Equation (13) with its logarithmic term cannot be solved explicitly for P_1; therefore, an iteration process was employed to find the correct pressure within 0.01 atmosphere.

As with the ideal gas plots, a family of evaporator inlet temperature curves is given to provide additional design information. Since the temperatures at stations 2 and 3' are determined in the course of evaluating (13), the corresponding enthalpys are known. The enthalpy, and therefore the temperature, at station 3 is readily determined from the definition of efficiency

$$\eta_e = \frac{h_2 - h_3}{h_2 - h_{3'}} \quad . \tag{14}$$

As stated in the ideal gas calculations, the W_c/Q values at the one-atmosphere intercept are determined from (11).

Additional charts show the expander power per unit of volumetric flow as a function of expander inlet temperature, expander outlet temperature, and expander inlet pressure. These values were calculated directly from

$$\frac{W_e}{F} = \frac{h_2 - h_3}{0.002119}\, v_{std} \tag{15}$$

for each refrigerant.

8. Pressure Drop

The discussion thus far has centered upon a simple, two-pressure refrigeration system. Since fluid friction occurs in the flow passages, pressure losses will result. Thus, the pressures P_1 and P_2 (see figure 1) will not be equal as assumed in the previous analysis. For the same reason, the pressures P_4 and P_3 will not equal P_5. Therefore it is desirable to predict what, if any, effect this behavior has upon the parameters of interest.

The expression

$$\left[\frac{W_c}{Q}\right]_{PD} = \left[\frac{W_c}{Q}\right]_{NPD} x \left[\frac{\left\{T_2 \eta_e \left[1 - \left(\frac{P_2}{P_3}\right)^{-\frac{k-1}{k}}\right] - \Delta T_{1-5}\right\}_{NPD}}{\left\{T_2 \eta_e \left[1 - \left(\frac{P_2}{P_3}\right)^{-\frac{k-1}{k}}\right] - \Delta T_{1-5}\right\}_{PD}}\right], \qquad (16)$$

derived from (2) for pressure drop and no pressure drop conditions, predicts the change in the figure of merit W_c/Q with reasonable precision. The subscripts PD and NPD refer to pressure drop and no pressure drop conditions respectively. A similar expression predicting the corresponding shift in optimum pressure has not been developed.

It is impractical to perform a complete set of pressure drop calculations because a large number of conditions can be conceived. Therefore only a brief examination of this phase of the work was performed. Equation (13) was modified slightly to obtain the necessary optimum operating expression

$$\left[\frac{d\left(\frac{W_c}{Q}\right)}{dP_1}\right]_{T_1} = (h_4 - h_3) + \left(\frac{101.32779}{M}\right)\left(P_1 \ln \frac{P_1}{P_5}\right)$$

$$x\left[\left(1 - \eta_e + \frac{\eta_e T_{3'}}{T_2}\right)\left(\frac{dh_1}{dP_1}\right) - \left(\frac{\eta_e T_{3'}}{\rho_2 T_2}\right)\left(\frac{dP_2}{dP_1}\right)_{T_1}\right] = 0 \qquad (17)$$

Pressure drops of 10 and 20 percent in the high and low pressure streams respectively, believed to be reasonable values were selected for the calculations. As before, an iteration process was employed to determine the correct high pressure to within 0.01 atmosphere.

9. Results

The data for optimum pressure plots for helium and parahydrogen shown in figures 8 thru 27 were calculated using real gas properties. Several optimum pressure charts are also included for the ideal refrigerants helium and parahydrogen. For ease of comparison each ideal gas plot is a transparent overlay for the real gas refrigerant chart. Each graph is for a particular expander efficiency and a specific cycle inlet temperature. The isothermal compressor efficiency in all cases is 100 percent. The figure of merit W_c/Q is shown as a function of optimum pressure P_1 for a series of curves representing the evaporator outlet temperature T_4, the evaporator inlet temperature T_3, and the temperature difference between the fluid streams at the warm end of the heat exchanger ΔT_{1-5}.

None of the optimum pressure plots show an evaporator outlet temperature equal to the liquid temperature of the refrigerant. This is because the optimum pressure is either beyond the range of available data or too high to be practicable.

Most optimum pressures were beyond the range of available data for nitrogen; therefore, high pressure--rather than optimum pressure--plots were obtained for this refrigerant. This information is presented in figures 28 thru 43. Each chart is for a particular expander efficiency, a specific heat exchanger temperature difference between the fluid streams at the warm end of the heat exchanger, and an isothermal compressor efficiency of 100 percent. The figure of merit W_c/Q is shown as a function of high pressure P_1 for a series of curves representing the evaporator inlet temperature T_3, the evaporator outlet temperature T_4, the expander power per unit flow W_e/F, and the flow per unit of refrigeration F/Q.

Figures 44 thru 61 show performance data for pressure drops of 10 and 20 percent in the high and low pressure streams of the heat exchanger. These charts provide essentially the same information and cover the same general high pressure range as the corresponding ones for no pressure drop.

Additional performance information for helium and parahydrogen is given in figures 62 thru 73 which show expander power per unit flow W_e/F as a function of expander inlet temperature T_2, cycle inlet pressure P_1, and expander outlet temperature T_3. Figures 62 thru 69 are for zero pressure drop in the heat exchanger, while figures 70 thru 73 are for pressure drops of 10 and 20 percent in the high and low pressure streams respectively of the heat exchanger.

The final two plots (figures 74 and 75) show the evaporator inlet temperature T_3 as a function of evaporator outlet temperature T_4 for a family of curves representing flow rate per unit refrigeration F/Q. There are upper and lower limits on the value of T_3. It can equal (at an infinite flow rate) but not exceed T_4. Likewise, it can equal but never be less than the liquid temperature of the refrigerant (i.e., for the conditions discussed in this work).

10. Discussion of Results

The optimum pressure charts for helium show reasonable agreement with the transparent overlays since the properties of helium, especially in the high temperature, low pressure regions, are very similar to those for an ideal gas. The corresponding plots for parahydrogen demonstrate the difference between the properties of parahydrogen and the ideal gas.

The discontinuities on the 300.0 K cycle inlet temperature parahydrogen curves are in disagreement with the smooth curves on the

transparent overlays; therefore, this anomalous behavior must be examined more closely. Accordingly, a generalized equation

$$\frac{d\left(\frac{W_c}{Q}\right)_{opt}}{d(P_1)_{opt}} = \frac{RT_a\left[A_{opt} + B_{opt} + C_{opt} + D_{opt}\right]}{M(P_1)^2_{opt} A^2_{opt}} \tag{18}$$

representing the slope of the constant ΔT curves may be derived. The terms in (18) for a variable evaporator outlet temperature T_4, a constant cycle inlet temperature T_1, a constant cycle outlet temperature T_5, and a 100 percent expander efficiency (to simplify the equation) are defined as follows:

RT_a/M = a constant (approximately 1237),

$$A_{opt} = \left(\frac{T_{3'}}{T_2}\right)_{opt}\left[\left(\frac{d\,h_1}{d\,P_1}\right)_{T_1} + \left(\frac{d\,h_4}{d\,P_1}\right)_{T_1} - v_2\right]_{opt},$$

$$B_{opt} = P_1\left(\frac{T_{3'}}{T_2}\right)_{opt}\left[\left(\frac{d^2 h_1}{d\,P_1^2}\right)_{T_1} + \left(\frac{d^2 h_4}{d\,P_1^2}\right)_{T_1} - \left(\frac{d\,v_2}{d\,P_1}\right)_{T_1}\right]_{opt},$$

$$C_{opt} = P_1\left(\frac{1}{T_2}\right)_{opt}\left(\frac{d\,T_{3'}}{d\,P_1}\right)_{T_1}\left[\left(\frac{d\,h_1}{d\,P_1}\right)_{T_1} + \left(\frac{d\,h_4}{d\,P_1}\right)_{T_1} - v_2\right]_{opt}, \text{ and}$$

$$D_{opt} = P_1\left(\frac{T_{3'}}{T_2}\right)_{opt}\left(\frac{d\,T_2}{d\,P_1}\right)_{T_1}\left[\left(\frac{d\,h_1}{d\,P_1}\right)_{T_1} + \left(\frac{d\,h_4}{d\,P_1}\right)_{T_1} - v_2\right]_{opt}.$$

It is difficult to obtain precise values for $\left(\frac{d\,h_4}{d\,P_1}\right)_{T_1}$, $\left(\frac{d^2 h_4}{d\,P_1^2}\right)_{T_1}$, and $\left(\frac{d\,T_{3'}}{d\,P_1}\right)_{T_1}$ because neither h_4 nor $T_{3'}$ is an explicit function of P_1,

and no simple relationship between these properties exists. A brief examination will be made of the term C_{opt} which, in fact, is responsible for the discontinuities. The two derivatives $\left(\frac{d\,h_1}{d\,P_1}\right)_{T_1}$ and $\left(\frac{d\,h_4}{d\,P_1}\right)_{T_1}$ are quite small relative to the specific volume v_2, thus these three terms combine to form a negative quantity. The ratio P_1/T_2 is positive, while the derivative $\left(\frac{d\,T_{3'}}{d\,P_1}\right)_{T_1}$ is negative (the temperature $T_{3'}$ decreases with increasing pressure P_1). Thus the C_{opt} term provides a positive contribution to the slope equation.

Since $T_{3'}$ decreases as P_1 is increased, there is some pressure $P_{1(i)}$ at which the temperature $T_{3'}$ reaches the liquid temperature of the refrigerant. When this occurs, the derivative must go to zero. Hence the positive contribution is no longer available, causing the slope to change abruptly to some lesser value. The remaining charts do not exhibit this behavior because the temperature $T_{3'}$ does not reach the liquid temperature of the refrigerant for the stated conditions. Had this happened, a discontinuity would be present.

In a few instances two optimum pressures (i.e., two minimum points) were found for parahydrogen precooled to 77.36 K. The first minimum generally occurred in the low pressure region of two to ten atmospheres, while the second occurred in the high pressure region of 90 to 200 atmospheres. Figure 5 shows a sketch of a typical double minimum curve which appears to be inconsistent when it is recalled that the ideal gas calculations predicted only one minimum.

Because the isothermal compressor power W_c is calculated in the same way for either the ideal or the real gas, it is evident that this

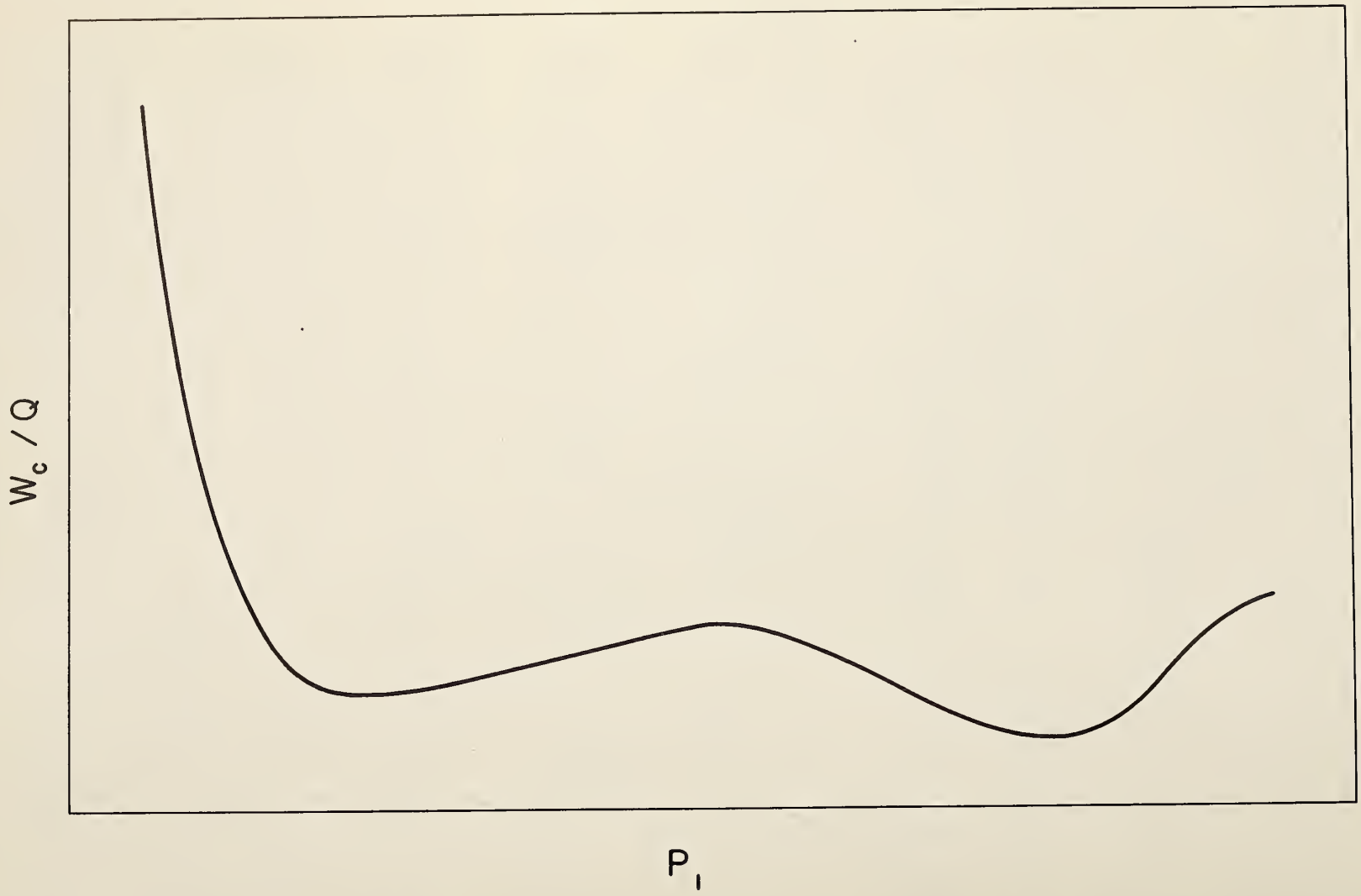

Figure 5. Schematic Diagram of the Brayton Refrigerator Performance Showing a Double Minimum Curve.

quantity is not responsible for the unusual behavior. The inconsistencies therefore must be attributed to the refrigeration load Q which is defined as

$$Q = W_e + m\,(h_5 - h_1) \tag{19}$$

for both cases. The expander power W_e changes with increasing pressure for the ideal gas, while the enthalpy difference remains constant at some fixed negative value. For the real gas, however, both terms change with increasing pressure. A typical plot of enthalpy difference as a function of high pressure for parahydrogen is shown in figure 6. The diagram shows that Δh_{1-5} is independent of pressure and temperature for the ideal gas, while it is dependent upon both the high pressure and the cycle inlet temperature T_1 for the real gas. The temperature T_{1-a} is less than T_{1-b} which is less than T_{1-c}; therefore, the real gas curves begin to flatten out somewhat and the enthalpy difference tends to approach a constant value at the higher cycle inlet temperature. Some of the isotherms reach a maximum value, at which point the derivative $\left(\frac{d\,h_1}{d\,P_1}\right)_{T_1}$ must go to zero. For this special condition, and this condition only, the Joule-Thomson coefficient $\left(\frac{d\,T_1}{d\,P_1}\right)_{h_1}$ will also be equal to zero. Therefore, the locus of all such maxima represent the well-known inversion curve.

If a refrigeration load Q for the ideal gas is recalculated using an enthalpy difference that varies in a manner similar to that of the T_{1-a} curve in figure 6, a revised figure of merit W_c/Q_{rev} will be obtained. Curves representing the original figure of merit W_c/Q_{orig} (solid line) and the revised figure of merit W_c/Q_{rev} (dashed line) are shown in figure 7.

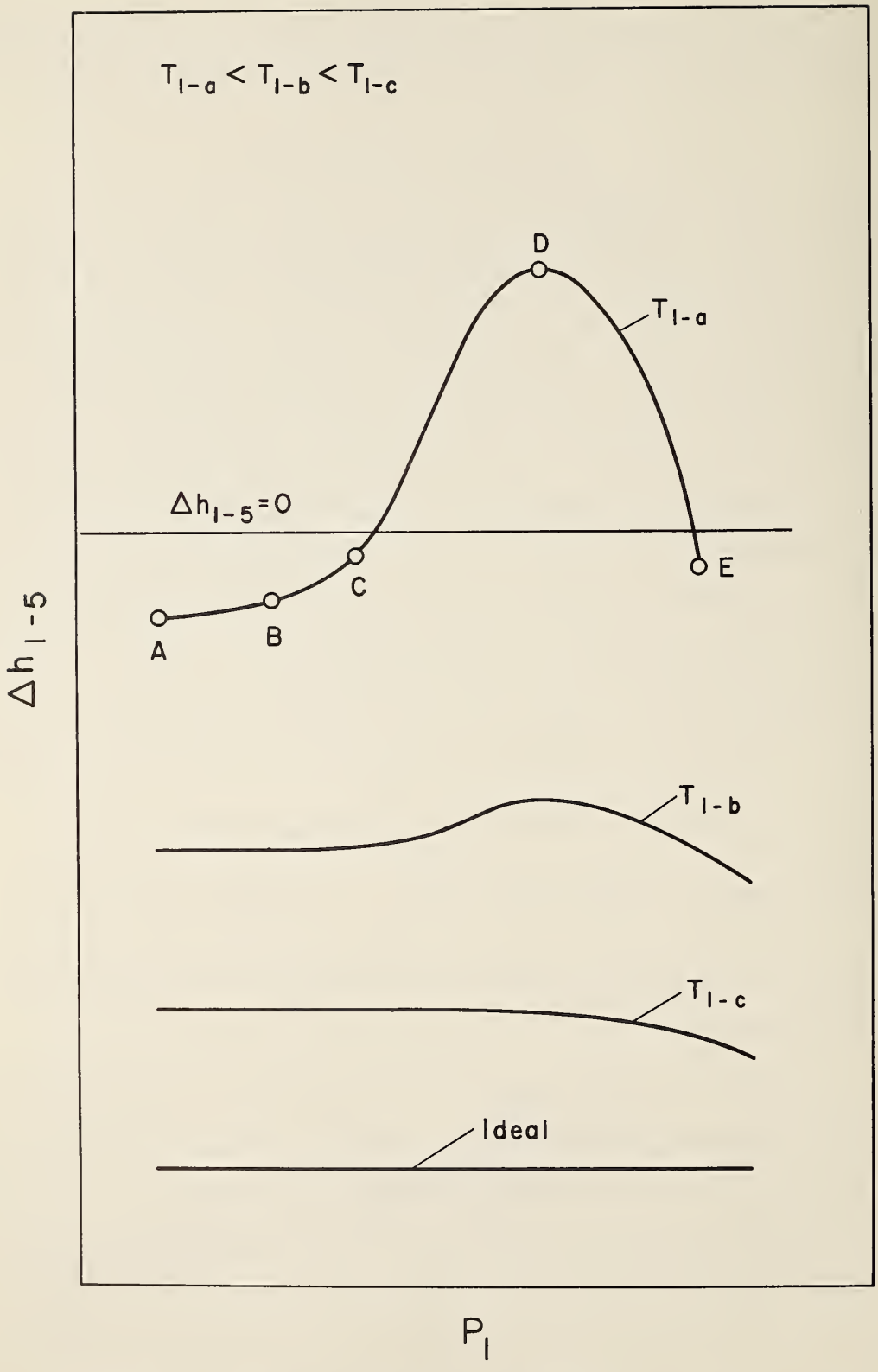

Figure 6. Schematic Diagram of Enthalpy Difference as a Function of High Pressure for Parahydrogen.

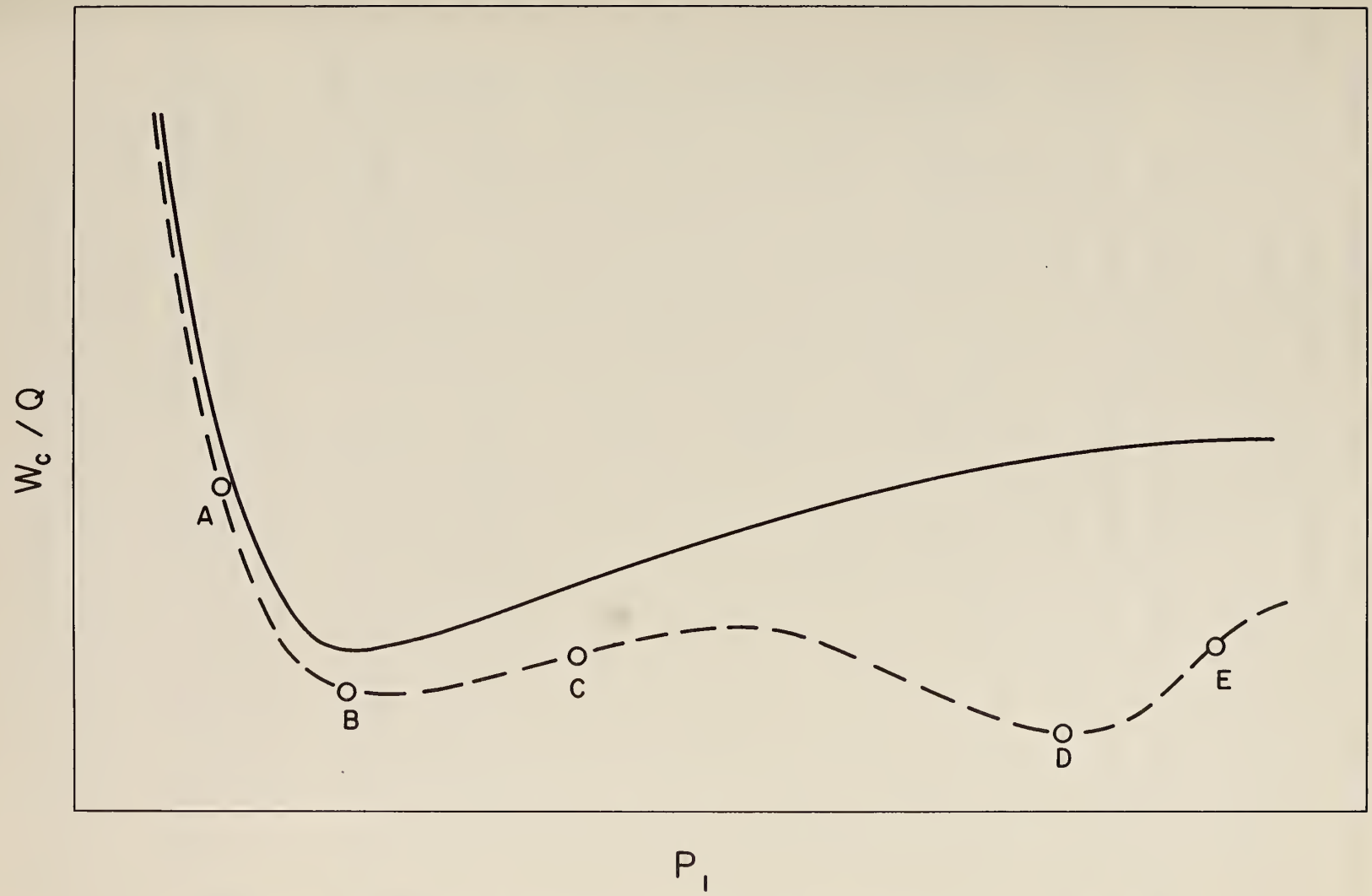

Figure 7. Schematic Diagram of Brayton Refrigerator Performance with an Ideal Gas as the Working Fluid - Single and Double Minimum Curves.

At low pressures (point A) the new enthalpy difference is fairly constant but slightly greater than the original value. Hence, the revised curve will lie slightly below the original curve. The minimum (point B) of the revised curve will occur in approximately the same general pressure region as that of the original, but it will be a lesser value.

As the pressure is increased beyond the minimum point, the new enthalpy difference becomes somewhat larger. Therefore, the magnitude of the revised W_c/Q_{rev} will be less than that of the original W_c/Q_{orig}, and the W_c/Q_{rev} curve should begin to rise (point C). As the pressure is increased further, the new enthalpy difference reaches its maximum value causing W_c/Q_{rev} to be considerably less than W_c/Q_{orig}. In this pressure region (point D) the revised W_c/Q_{rev} curve can be expected to have another minimum or, at the very least, an inflection point. As the pressure is increased further, the new enthalpy difference begins to decrease. In this region (point E) W_c/Q_{rev} increases gradually at first, and then as the magnitude of the new enthalpy difference approaches that of the original, it increases at a more rapid rate. Thus, for a cycle inlet temperature less than the maximum inversion temperature of the refrigerant, the J-T effect will force either a second minimum or an inflection point to occur on the figure of merit curve. The cycle inlet temperature of 300.0 K is above the maximum inversion temperature (about 208.0 K) for parahydrogen; therefore, no extreme deviation from the normal shape of the W_c/Q curve should be expected for this condition.

Cycle inlet temperatures of 300.0 and 77.36 K are above the maximum inversion temperature (approximately 55.0 K) for helium. Hence no unusual behavior is expected for the curves representing these conditions. On the other hand, the cycle inlet temperature of 20.27 K definitely is below the maximum inversion temperature, and although no double minima were observed for this condition, there was some

evidence of an inflection point. This appears to be reasonable because the maximum deviation of the enthalpy difference curves for helium precooled to 20.27 K are considerably less than those for parahydrogen precooled to 77.36 K.

For the few cases where double minima did occur, the first was always selected as the optimum operating condition because it was felt that the second occurred at a pressure too high to be practicable.

Some of the charts for parahydrogen and all of those for nitrogen show expansion engine exhaust temperatures that are the fluid saturation temperatures at the low pressure. This means that a portion of the refrigerant may change phase from gas to liquid in the expander. In many units, not designed for this condition, the presence of liquid will cause a drop in efficiency; however, the operation of "wet" expansion engines is becoming more common. While the problems encountered are not insurmountable, it is most important for the designer to be aware of the situation so that an allowance can be made for the liquid and for the possibility that a lower efficiency must be tolerated.

The flow data (i.e., T_3 as a function of T_4 and F/Q) for 1.2 atmospheres showed close agreement with that for 1.0 atmosphere, with differences in T_3 of about 0.01 K and 0.5 K at the high and low ends of the T_3 range respectively. Since these differences are negligible and unreadable on the charts, only the 1.0 atmosphere data are included.

The performance charts may be used in combination to determine the operating parameters, including the optimum pressure, for a given refrigeration requirement. Consider the following conditions:

Refrigerant	=	helium	,
Q	=	100 W	,
$\eta_{c\ \text{isothermal}}$	=	60%	,
$\eta_{e\ \text{isentropic}}$	=	70%	,
T_1	=	300 K	,
T_4	=	30 K	,
T_5	=	296 K	,
P_2	=	$0.9\ P_1$	,
P_3	=	$1.2\ P_5$	,
P_4	=	$1.2\ P_5$	, and
P_5	=	1.0 atm	.

Figure 44 shows that the optimum operating high pressure P_1 is 11 atm for which T_3 and W_c/Q are 21 K and 32 watts/watt respectively. The isothermal compressor efficiency must be considered, and this increases W_c/Q to 53.3 watts/watt for the 60 percent efficient compressor. Thus a 5.33 kW compressor is needed to provide the required amount of refrigeration. As indicated, the chart accounts for pressure changes of 10 and 20 percent in the high and low pressure streams of the heat exchanger respectively. These losses result in pressures of 9.9 atm for P_2 and 1.2 atm for P_3 and P_4.

Flow rate information is given in figure 74. For an evaporator inlet temperature T_3 of 21 K and an evaporator outlet temperature T_4 of 30 K the flow per unit of refrigeration F/Q is 250 scfm/kW. Thus for a refrigeration load Q of 100 watts, the flow is 25 scfm.

The expander performance may be determined from figure 70. For a high pressure P_1 of 11 atm and an evaporator inlet temperature T_3 of 21 K, the expander output power per unit flow W_e/F and the

expander inlet temperature are 6 watts/scfm and ~ 35 K respectively. Thus, for a flow of 25 scfm, the expander output power is 150 watts.

The various refrigeration parameters found from the graphs will then be

T_2	=	35 K	,
T_3	=	21 K	,
P_1	=	11 atm	,
P_2	=	9.9 atm	,
P_3	=	1.2 atm	,
P_4	=	1.2 atm	,
$W_{c\ isothermal}$	=	5.33 kW	,
$W_{e\ isentropic}$	=	150 W	,
F	=	25 scfm	and
Q	=	100 W	.

In order to illustrate the effect of component efficiencies on the performance of the cycle, consider decreasing ΔT_{1-5} (i.e., increasing T_5) while holding η_e and T_1 constant. The engine inlet temperature T_2, and thus the evaporator inlet temperature T_3, will decrease. For the same refrigeration capability, Q, the mass flow decreases therefore, the figure of merit W_c/Q will be smaller. The cycle, however, will not be operating at the optimum high pressure which will have a new, somewhat lower value.

Increasing the isentropic efficiency of the expander η_e, while holding ΔT_{1-5} and T_1 constant, produces an increase in the expander power output. For the same refrigeration capability, Q, the mass flow required decreases because of this additional power output and the value of W_c/Q becomes smaller. Again the high pressure P_1 can be reduced to achieve optimum operating conditions.

If component efficiencies could be slightly upgraded, considerable improvement in cycle performance would be obtained. For example, consider the following design requirements. The refrigerant is helium, T_4 is 20 K, T_1 is 300 K, ΔT_{1-5} is 6 K, η_e is 50 percent, η_c is 60 percent, and the pressure drop in the heat exchanger is 10 and 20 percent, respectively, in the high and low pressure streams. Figure 45 gives a value of 185 watts/watt for W_c/Q and an optimum pressure of 28 atm for a 100 percent efficient isothermal compressor. The 60 percent efficient compressor increases that value to about 310 watts/watt.

If the component efficiencies could be improved to the following values

$$\Delta T_{1-5} = 4 \text{ K} ,$$
$$\eta_e = 70\% , \text{ and}$$
$$\eta_c = 70\%$$

the figure of merit W_c/Q will be approximately 80 watts/watt for the 70 percent efficient compressor which is nearly a 75 percent reduction. In addition, the optimum high pressure will be about 15 atm which amounts to about a 50% reduction.

11. Conclusions

The proper choice of a low temperature refrigeration cycle to meet a given set of duty requirements rests on a balance between economic and technical requirements. Present applications for such refrigerators are so varied that it is impossible to make definite statements about the "best" cycle for general use. It is, however, possible to discuss the advantages and disadvantages of a particular cycle.

The modified Brayton refrigeration cycle has basic advantages which warrant its consideration when choosing a cryogenic refrigerator. The system is relatively simple, requiring only a compressor, an expansion engine, and a heat exchanger as its main components. Compared to cycles using Joule-Thomson expansion valves which produce cooling isothermally only at the liquid temperatures of the refrigerant, the modified Brayton cycle permits a large selection of refrigeration temperatures. However, unless specific design allowances have been made, difficulty could be encountered in attempting to cool at liquid temperatures with the Brayton cycle because of the gas to liquid phase change which would occur in the expansion engine.

The optimum high pressures for helium and parahydrogen are not excessive so the problems of designing expansion engines for large pressure ratios may be eased. While computing the optimum pressures, it was evident that the minima in the performance curves were quite wide, so it would be possible to operate the refrigerator at pressures lower than the optimum without suffering a severe loss of efficiency.

The Brayton cycle refrigerator is capable of reaching potentially high thermal efficiencies with reasonable improvements in present heat exchangers, expanders, and compressors, and competitive performance can be obtained with present components. However, calculations show that utilizing reheat expansion stages may increase the available refrigeration by 10 to 20 percent with no change in compressor capacity or input power requirements. Two-stage reheat involves expanding the high pressure gas not to the low pressure, but to some intermediate pressure. The cold gas passes through the first portion of the load exchanger which is now in two sections, where it is warmed to the expander inlet temperature as it absorbs energy from the refrigeration

load. After the final expansion to the low pressure, the fluid enters the second section of the load heat exchanger. Additional expansion stages and heat exchanger sections may be added if warranted. In addition to improved performance, reheat reduces the temperature rise in the load heat exchanger appreciably and tends to a more uniform heat sink temperature.

Precooling helium to 77.36 K produces little if any advantage at the same ΔT_{1-5}. Precooling to 20.27 K, however, results in a pronounced reduction of the figure of merit at the expense of an increase in the optimum operating pressure. Precooling parahydrogen to 77.36 K definitely decreases both the figure of merit and the optimum operating pressure. The benefit to be derived by precooling either refrigerant to 65.0 rather than 77.36 K is negligible.

If the heat exchanger efficiency can be improved, both the optimum operating pressure and the figure of merit will be reduced. In addition, these values can also be decreased through the use of a more efficient expander. On the other hand, if a lower refrigeration temperature is required, the compressor power will be increased.

Any heat leak to the low temperature region of the refrigerator will decrease the amount of useful refrigeration. Thus the calculated performance is better than can be realized in practice. The magnitude of the heat leak depends upon the size and geometry of the low temperature enclosure and is especially critical in small capacity refrigerators.

12. References

Bernatowicz, D. T. (1963), NASA Solar Brayton-cycle Studies, Symposium on Solar Dynamic Systems, Interagency Advanced Power Group, Washington, D. C.

Glassman, A. J., R. P. Krebs, and T. A. Fox (1965), Brayton-cycle Nuclear Space Power Systems and their Heat Transfer Components, American Institute of Chemical Engineers 61, No. 57, 306-314.

Glassman, A. J. and W. L. Stewart (1964), Thermodynamic Characteristics of Brayton-cycles for Space Power, J. Spacecraft 1, No. 1, 25-64.

Harrach, W. G. and R. T. Caldwell (1963), System Optimization of Brayton-cycle Space Power Plants, ASME Winter Annual Meeting, Philadelphia, Pennsylvania.

Mann, D. B. (1962), The Thermodynamic Properties of Helium from 3 to 300°K between 0.5 and 100 Atmospheres, NBS Technical Note No. 154, National Bureau of Standards, Boulder, Colorado.

Roder, H. M. and R. D. Goodwin (1961), Provisional Thermodynamic Functions for Parahydrogen, NBS Technical Note No. 130, National Bureau of Standards, Boulder, Colorado.

Schultz, R. L. and W. E. Melber (1964), Brayton-cycle Radioisotope Space Power System, SAE National Aeronautical Space Engineering and Manufacturing Meeting, Los Angeles, California.

Strobridge, T. R. (1962), The Thermodynamic Properties of Nitrogen from 64 to 300°K between 0.1 and 200 Atmospheres, NBS Technical Note No. 129, National Bureau of Standards, Boulder, Colorado.

13. Appendix

The development of (13) proceeds in the following manner. A series of initial cycle calculations were performed using the basic equation (12)

$$\frac{W_c}{Q} = - \frac{RT_a \, \ell n \left(\frac{P_1}{P_5}\right)}{\eta_c \, M(h_4 - h_3)} \quad .$$

Again the output data were plotted as a function of high pressure for several values of evaporator outlet temperature, and as expected, these curves also contained minimum points. Therefore, it was again necessary to derive a suitable means of determining their value.

Differentiating (12) with respect to pressure P_1, and setting the derivative equal to zero, yields

$$(h_4 - h_3) \frac{1}{P_1} + \left[\frac{d\, h_3}{d\, P_1}\right]_{T_1} \ell n \left(\frac{P_1}{P_5}\right) = 0 \quad , \tag{20}$$

where P_1 now represents the optimum operating pressure.

Because the enthalpy h_3 is not an explicit function of the pressure P_1, the derivative $(dh_3/dP_1)_{T_1}$ can not be evaluated directly; hence, an equivalent relationship must be found.

Taking an energy balance around the heat exchanger (see figure 1) gives

$$h_2 = h_1 - h_5 + h_4 \quad . \tag{21}$$

Differentiating (21) with respect to pressure P_1 yields

$$\left[\frac{d\,h_2}{d\,P_1}\right]_{T_1} = \left[\frac{d\,h_1}{d\,P_1}\right]_{T_1} \tag{22}$$

or

$$\left[\frac{d\,h_2}{d\,h_1}\right]_{h_4 h_5} = 1 \quad . \tag{23}$$

The isentropic efficiency of an expander is given by (14) as

$$\eta_e = \frac{h_2 - h_3}{h_2 - h_{3'}}$$

Solving for h_3 and differentiating with respect to P_1 yields

$$\left[\frac{d\,h_3}{d\,P_1}\right]_{T_1} = \eta_e\left[\frac{d\,h_{3'}}{d\,P_1}\right]_{T_1} + (1 - \eta_e)\left[\frac{d\,h_2}{d\,P_1}\right]_{T_1} \quad . \tag{24}$$

Substituting (22) into (24) and (24) into (20) gives

$$(h_4 - h_3)\frac{1}{P_1} + \left[\eta_e\left(\frac{d\,h_{3'}}{d\,P_1}\right)_{T_1} + (1 - \eta_e)\left(\frac{d\,h_1}{d\,P_1}\right)_{T_1}\right]$$

$$x\,\ell n\left(\frac{P_1}{P_5}\right) = 0 \quad . \tag{25}$$

Because $h_{3'}$ is not an explicit function of P_1, the derivative $(dh_{3'}/dP_1)_{T_1}$ can not be readily obtained; therefore, some relationship between these two properties remains to be determined. The following functions are known:

$$h_1 = f(P_1, T_1) \tag{26}$$

where P_1 is an independent variable, and T_1 is a constant;

$$h_2 = g(h_1, h_4, h_5), \tag{27}$$

where h_1 is a dependent variable, and h_4 and h_5 are constants;

$$s_2 = j(h_2, P_2), \tag{28}$$

where h_2 is a dependent variable, and P_2 equals P_1, an independent variable; and

$$h_{3'} = k(s_2, P_3), \tag{29}$$

where s_2 is a dependent variable, and P_3 is a constant.

Differentiating the above four equations, yields

$$d h_1 = \left(\frac{\partial h_1}{\partial P_1}\right)_{T_1} d P_1 \quad , \tag{30}$$

$$d h_2 = \left(\frac{\partial h_2}{\partial h_1}\right)_{h_4 h_5} d h_1 \quad , \tag{31}$$

$$d s_2 = \left(\frac{\partial s_2}{\partial h_2}\right)_{P_2} d h_2 + \left(\frac{\partial s_2}{\partial P_2}\right)_{h_2} d P_2 \quad , \text{ and} \tag{32}$$

$$d h_{3'} = \left(\frac{\partial h_{3'}}{\partial s_2}\right)_{P_3} d s_2 \tag{33}$$

respectively. Substituting (30), (31), and (32) into (33) produces the expression

$$d h_3 = \left(\frac{\partial h_{3'}}{\partial s_2}\right)_{P_3}$$

$$x \left[\left(\frac{\partial s_2}{\partial h_2}\right)_{P_2} \left(\frac{\partial h_2}{\partial h_1}\right)_{h_4 h_5} \left(\frac{\partial h_1}{\partial P_1}\right)_{T_1} d P_1 + \left(\frac{\partial s_2}{\partial P_2}\right)_{h_2} d P_2 \right] . \quad (34)$$

Since the pressure at station 2 of figure 1 is the same as that at station 1, $d P_2$ must equal $d P_1$. Thus (34) becomes

$$\frac{d h_{3'}}{d P_1} = \left(\frac{\partial h_{3'}}{\partial s_2}\right)_{P_3}$$

$$x \left[\left(\frac{\partial s_2}{\partial h_2}\right)_{P_2} \left(\frac{\partial h_2}{\partial h_1}\right)_{h_4 h_5} \left(\frac{\partial h_1}{\partial P_1}\right)_{T_1} + \left(\frac{\partial s}{\partial P_2}\right)_{h_2} \right] . \quad (35)$$

From basic thermodynamics it is known that

$$dh = Tds + vdP.$$

When the pressure is held constant,

$$\left(\frac{\partial h}{\partial s}\right)_P = T \quad (36)$$

and when the enthalpy is held constant,

$$\left(\frac{\partial s}{\partial P}\right)_h = - \frac{v}{T} \quad . \quad (37)$$

If the specific volume-density relationship is considered, (37) becomes

$$\left(\frac{\partial s}{\partial P}\right)_h = -\frac{1}{\rho T} \quad . \tag{38}$$

Inserting the proper subindices and substituting (23), (36), and (38) into (35) yields

$$\left(\frac{d h_{3'}}{d P_1}\right)_{T_1} = \frac{T_{3'}}{T_2} \left[\left(\frac{d h_1}{d P_1}\right)_{T_1} - \frac{1}{\rho_2}\right] . \tag{39}$$

Finally, substituting (39) into (25), rearranging, and inserting the proper conversion factors, produces

$$(h_4 - h_3) + \left(\frac{101.32779}{M}\right)\left(P_1 \ln \frac{P_1}{P_5}\right)$$

$$\times \left[\left(1 - \eta_e + \frac{\eta_e T_{3'}}{T_2}\right)\left(\frac{d h_1}{d P_1}\right)_{T_1} - \frac{\eta_e T_{3'}}{\rho_2 T_2}\right] = 0 \quad , \tag{40}$$

where the enthalpy h_1 is an explicit function of pressure P_1, and therefore the derivative $(d h_1/d P_1)_{T_1}$ can be readily evaluated.

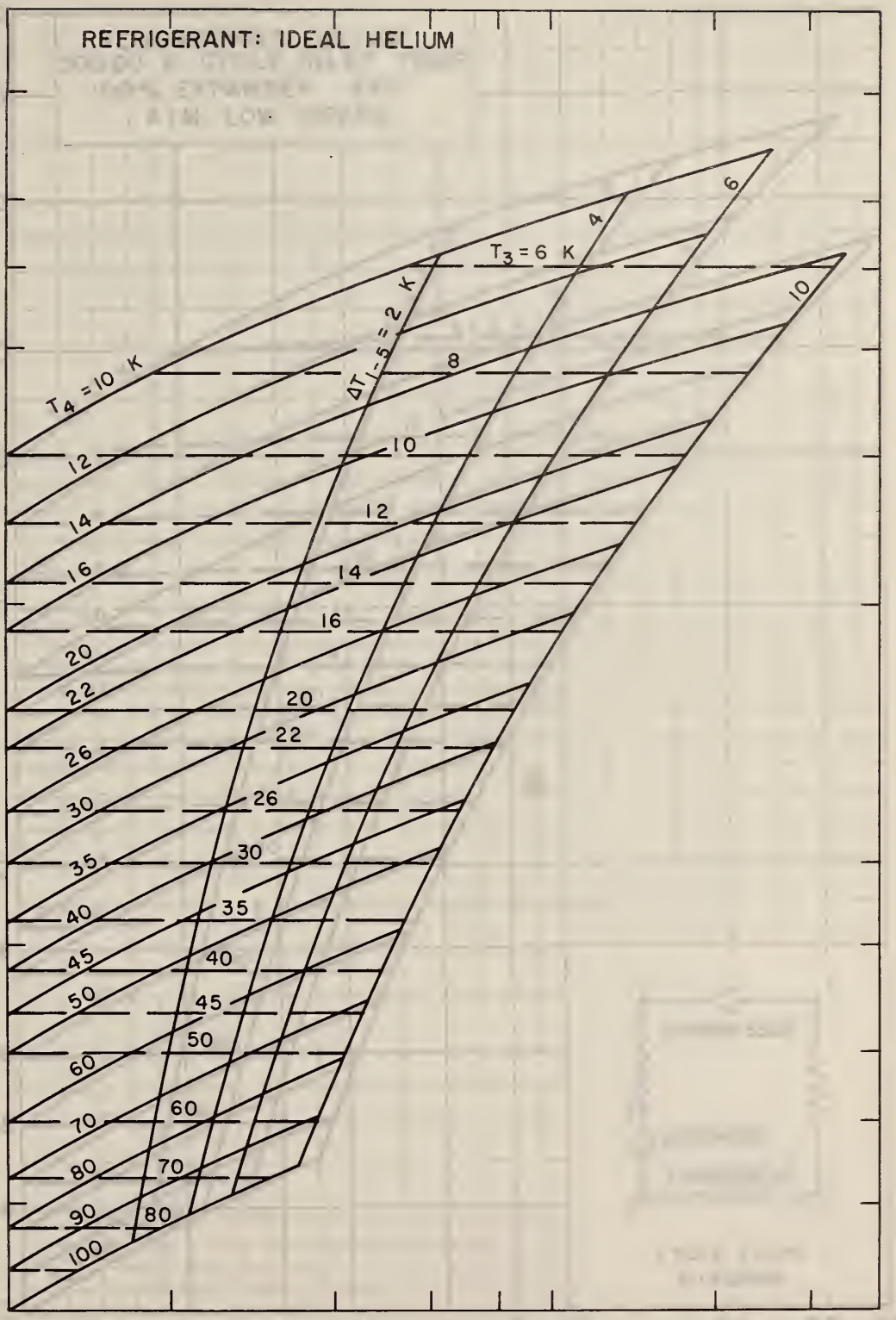

Figure 8 Overlay

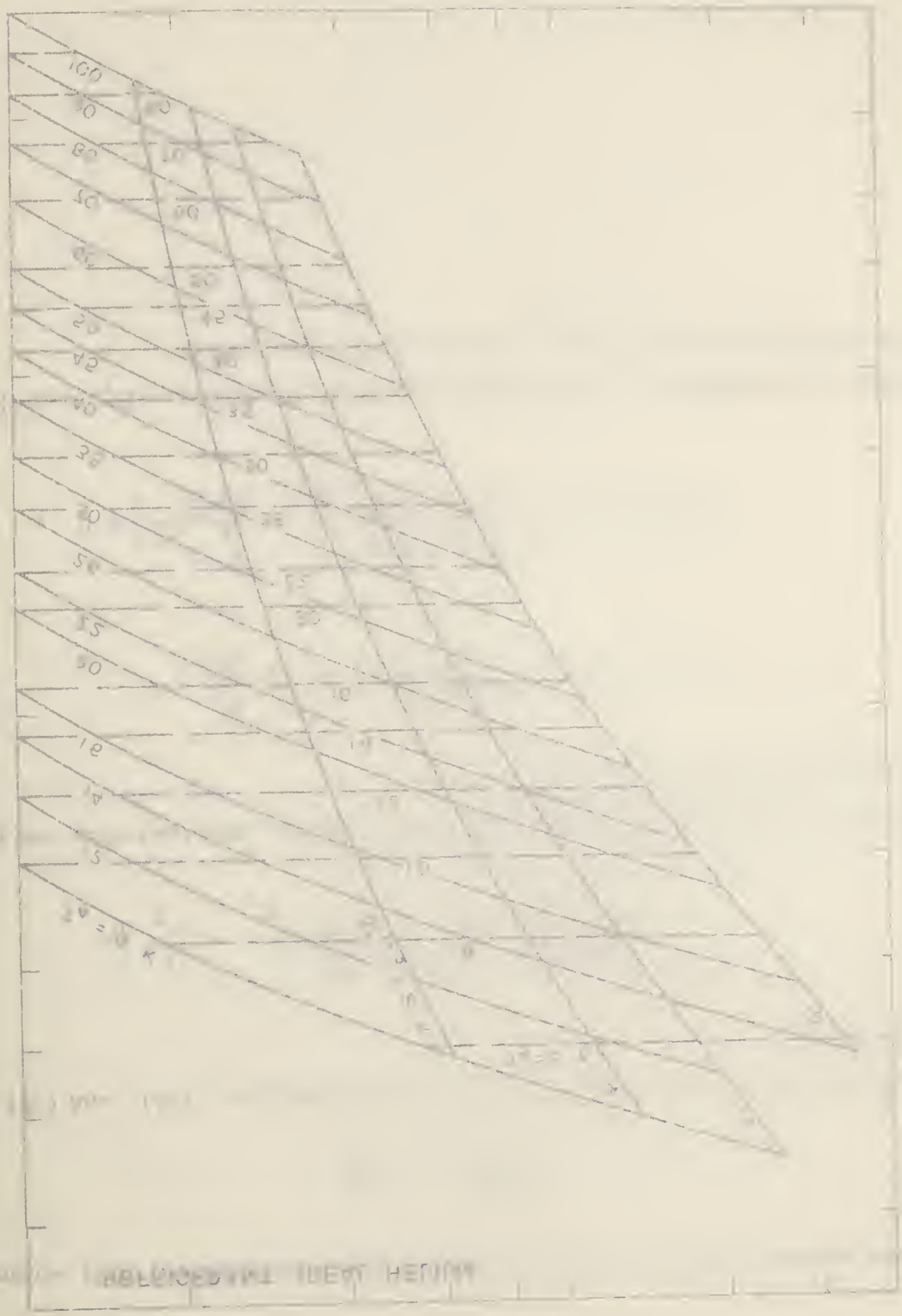

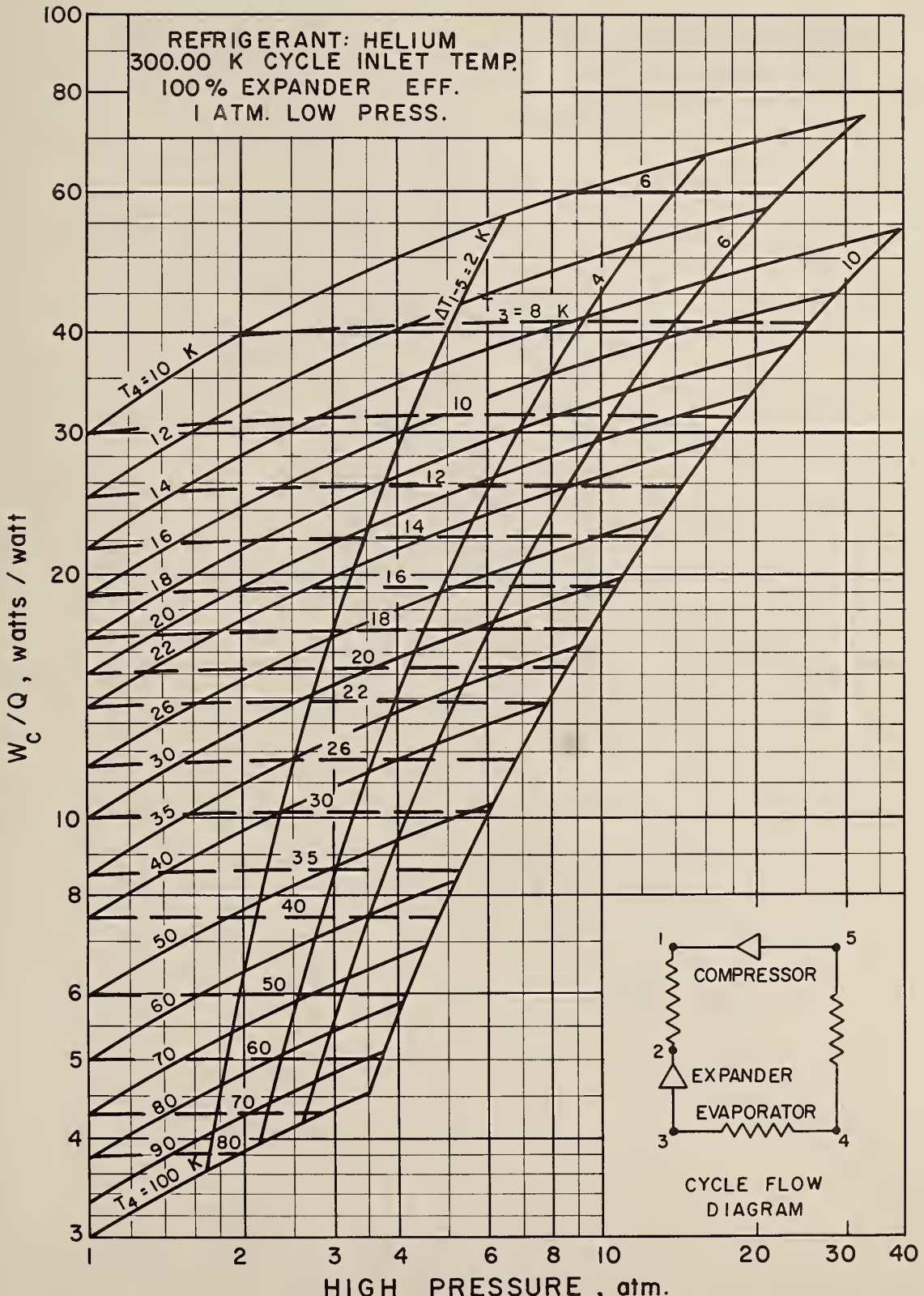

Figure 8. Brayton Refrigerator Performance - Helium Refrigerant - 300 K Cycle Inlet Temperature - 100% Expander Efficiency - No Pressure Drop.

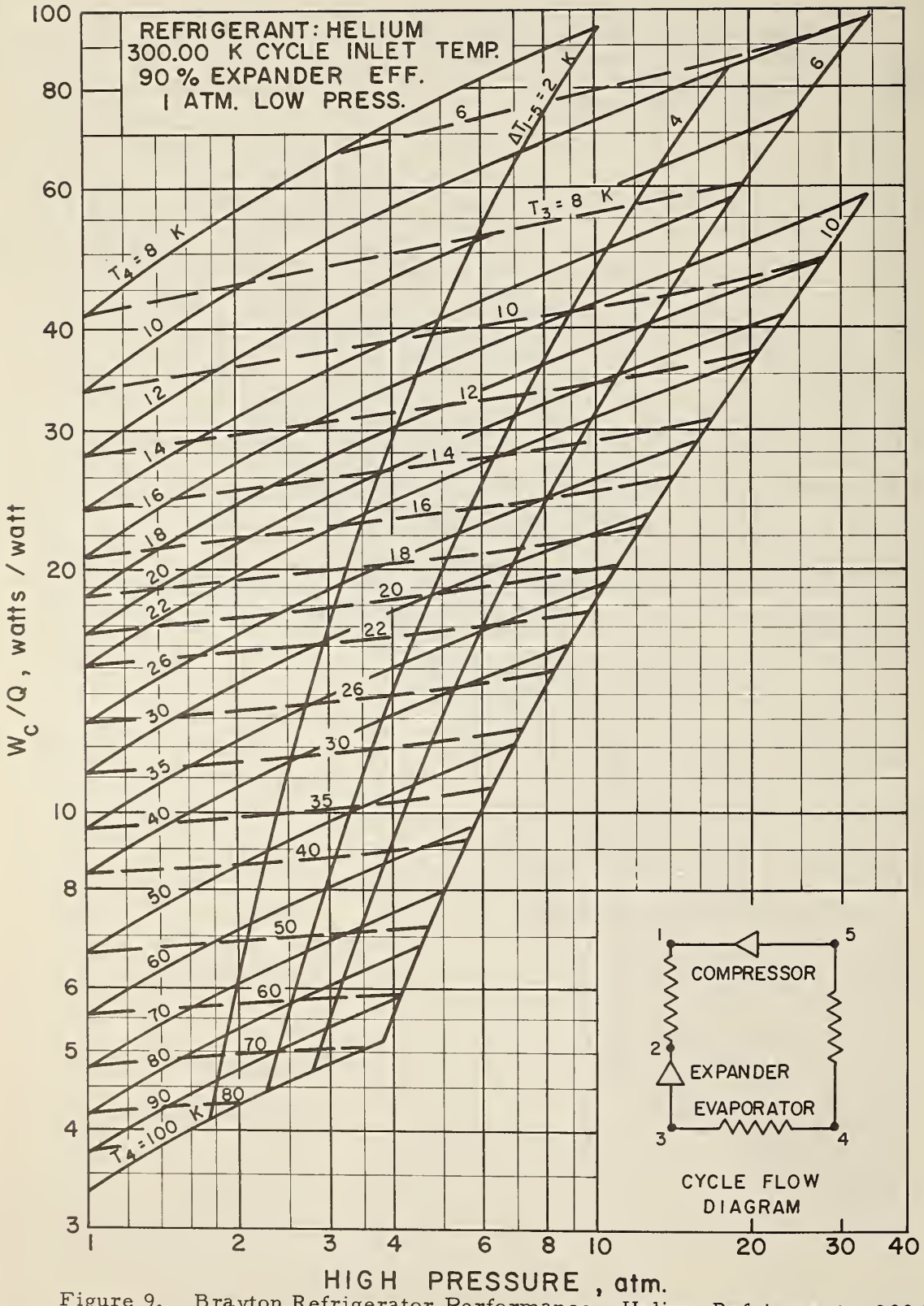

Figure 9. Brayton Refrigerator Performance - Helium Refrigerant - 300 K Cycle Inlet Temperature - 90% Expander Efficiency - No Pressure Drop.

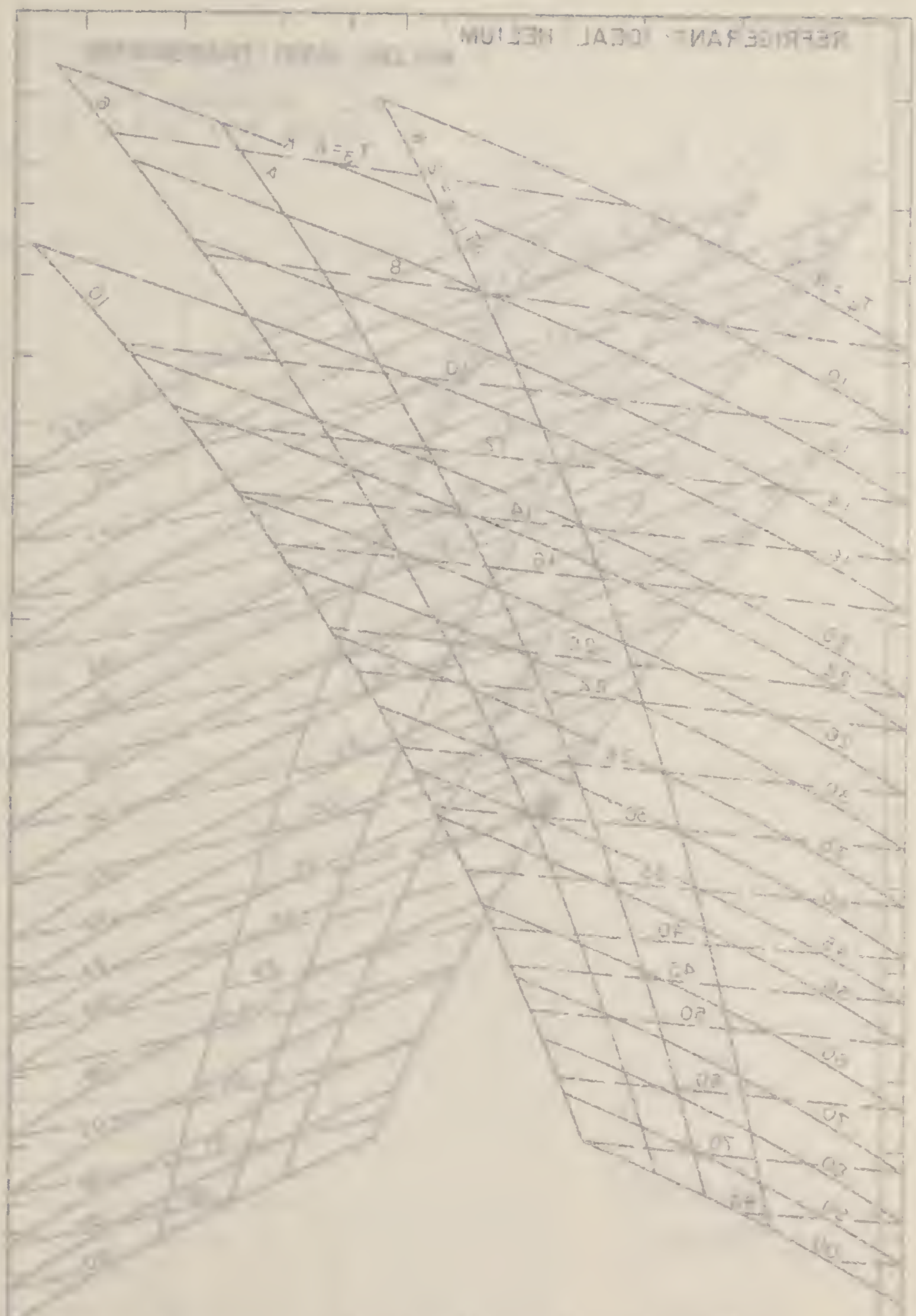

Figure 9 Overlay

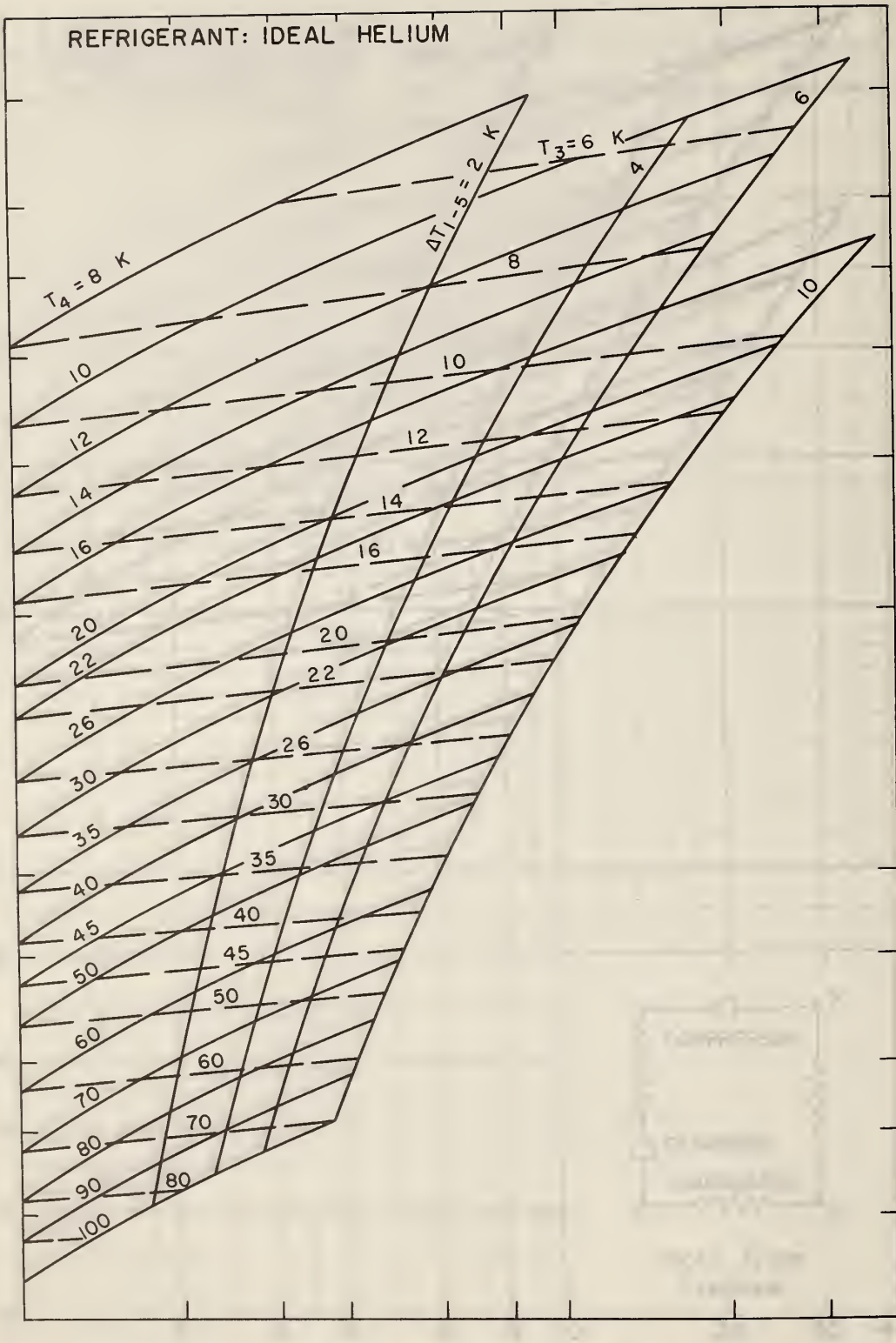

Figure 9 Overlay

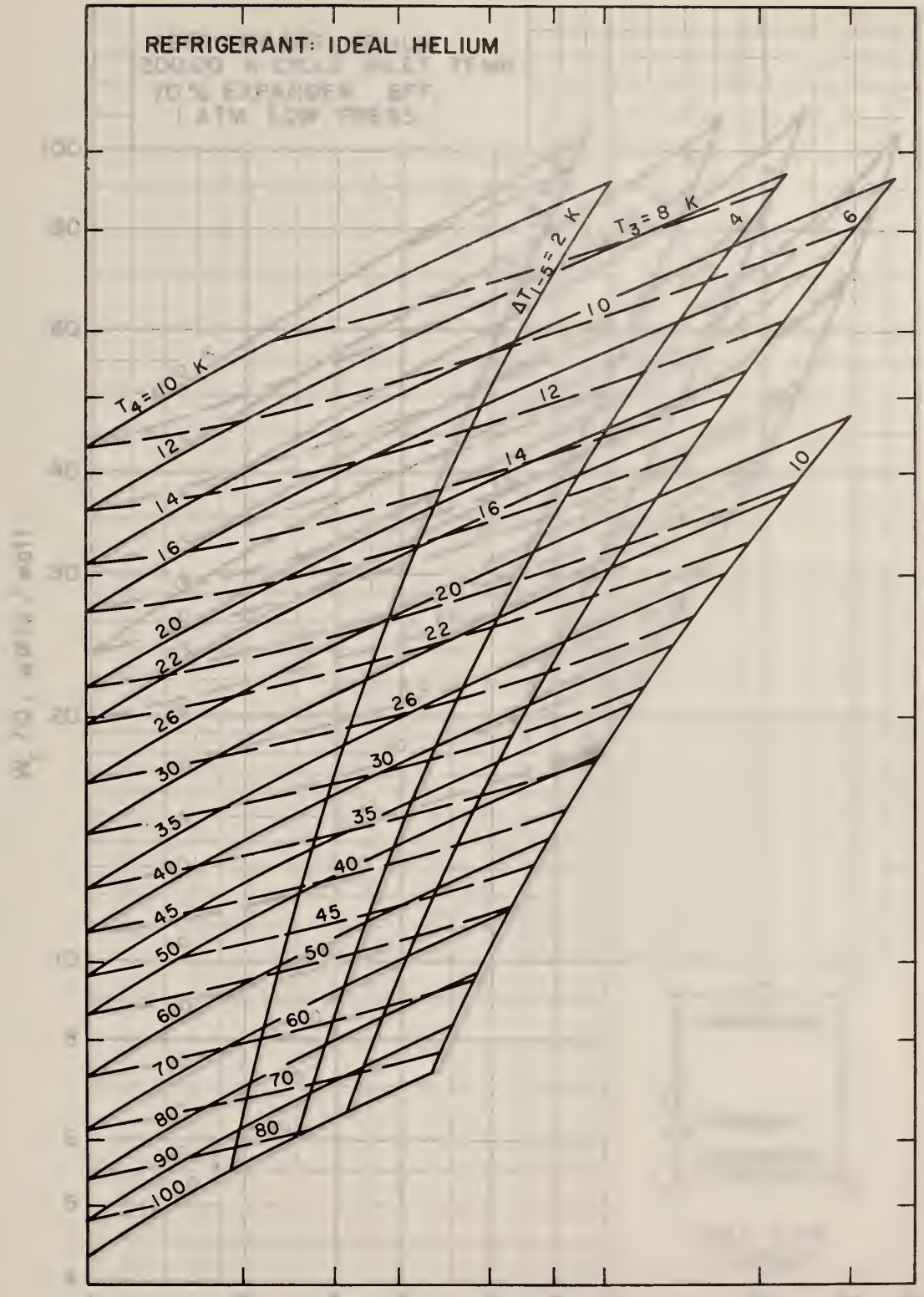

Figure 10 Overlay

Figure 10 Overlay

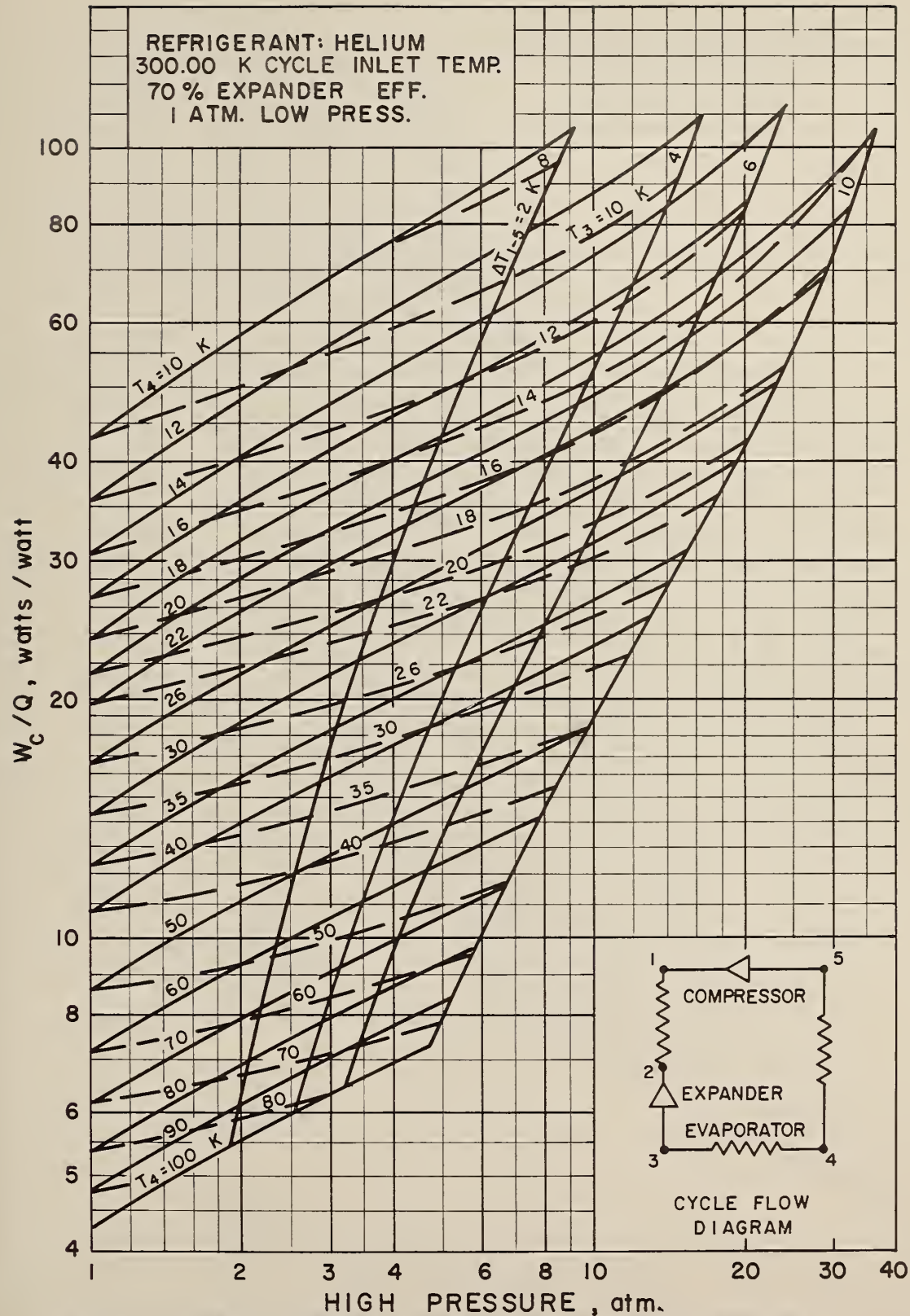

Figure 10. Brayton Refrigerator Performance - Helium Refrigerant - 300 K Cycle Inlet Temperature - 70% Expander Efficiency - No Pressure Drop.

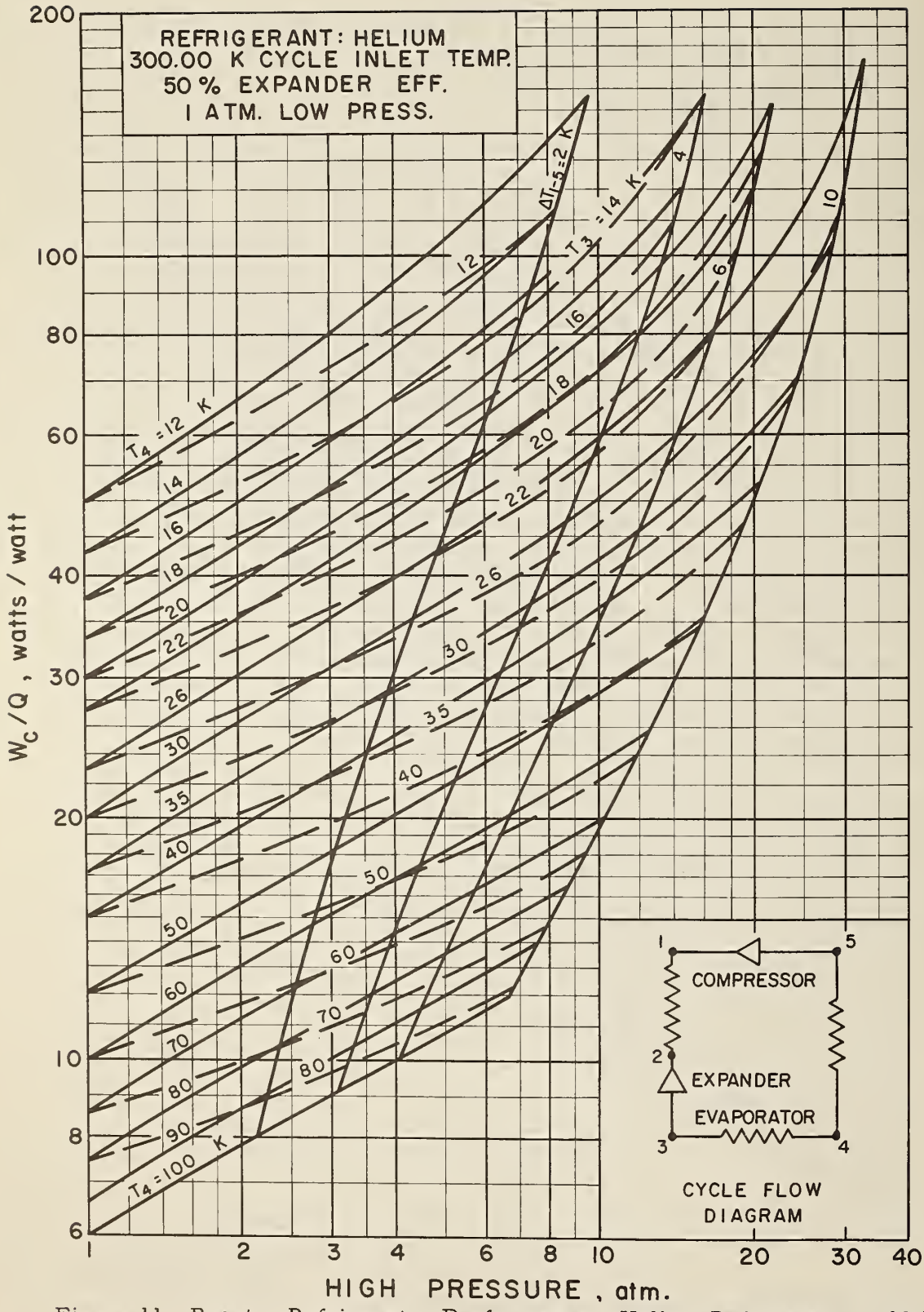

Figure 11. Brayton Refrigerator Performance - Helium Refrigerant - 300 K Cycle Inlet Temperature - 50% Expander Efficiency - No Pressure Drop.

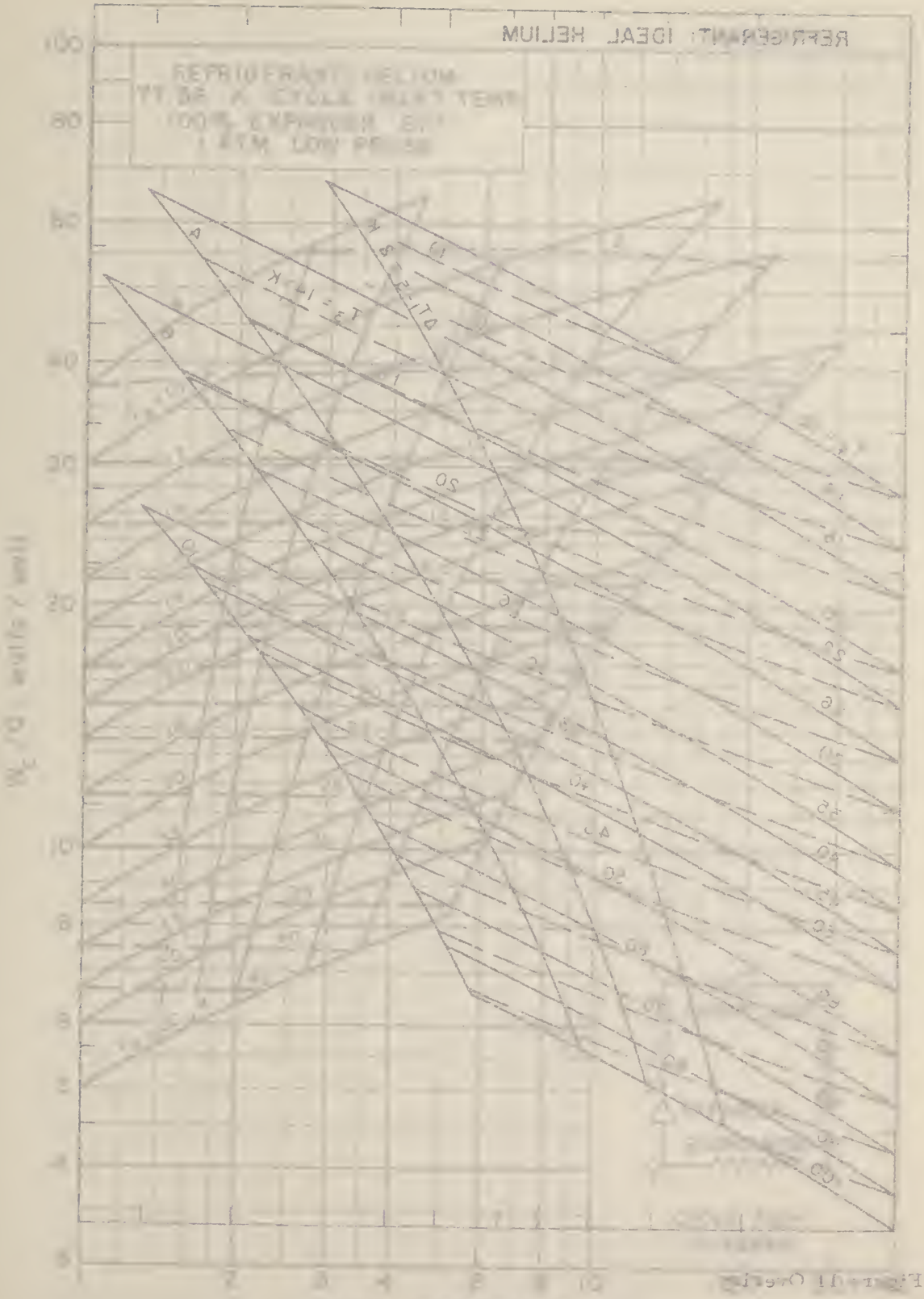
REFRIGERANT: IDEAL HELIUM
REFRIGERANT: HELIUM
HIGH PRESSURE, atm.

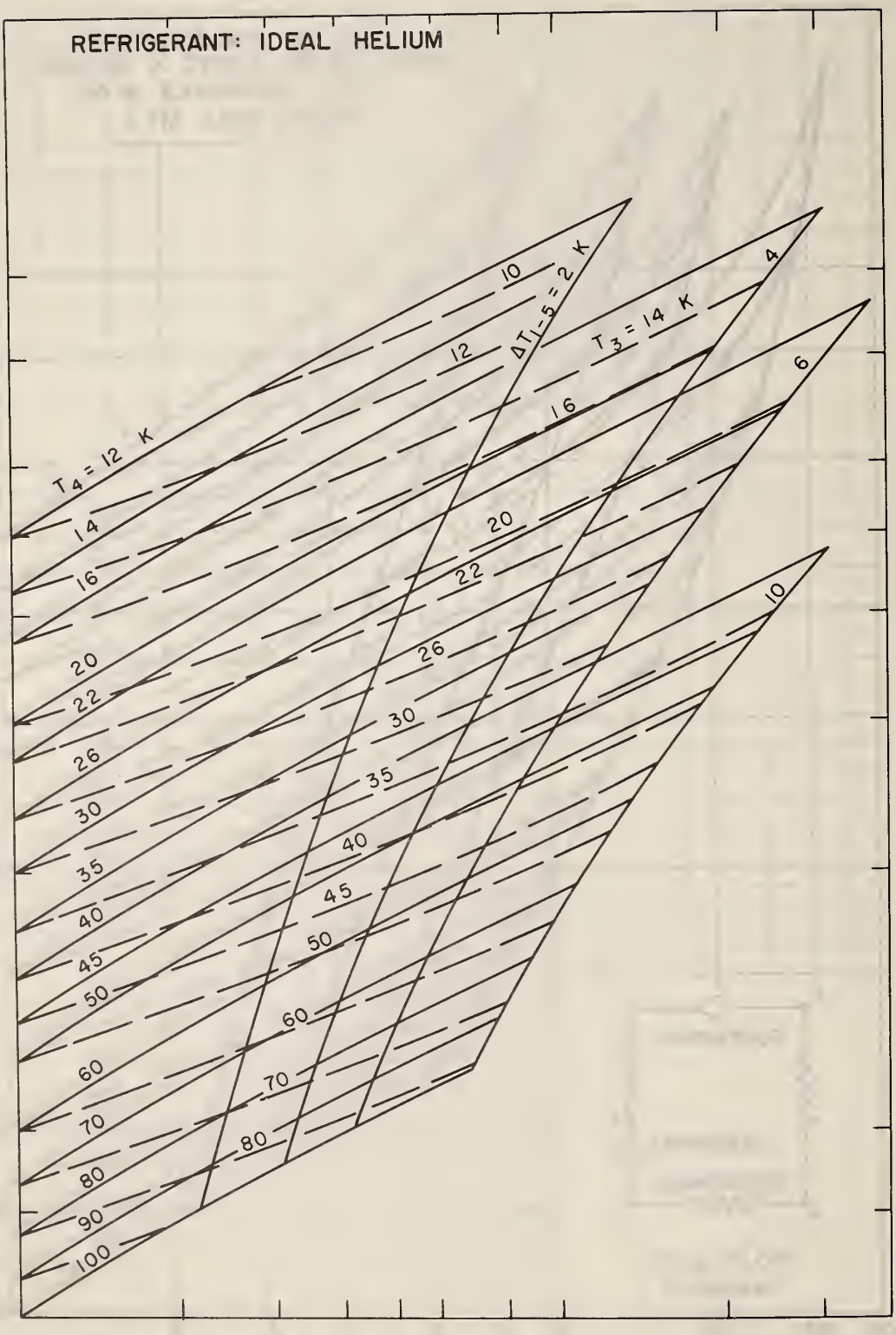

Figure 11 Overlay

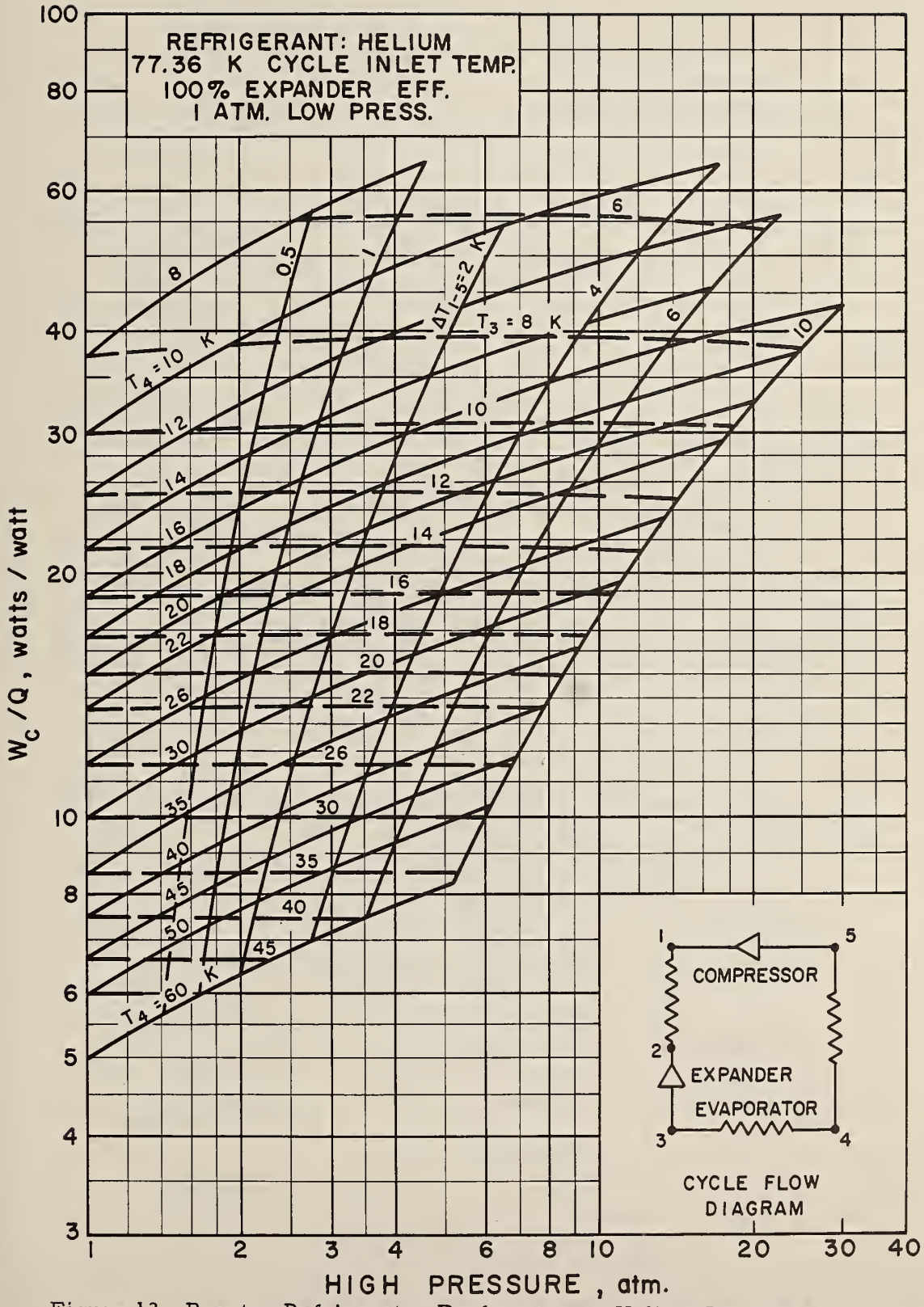

Figure 12. Brayton Refrigerator Performance - Helium Refrigerant - 77.36 K Cycle Inlet Temperature - 100% Expander Efficiency - No Pressure Drop.

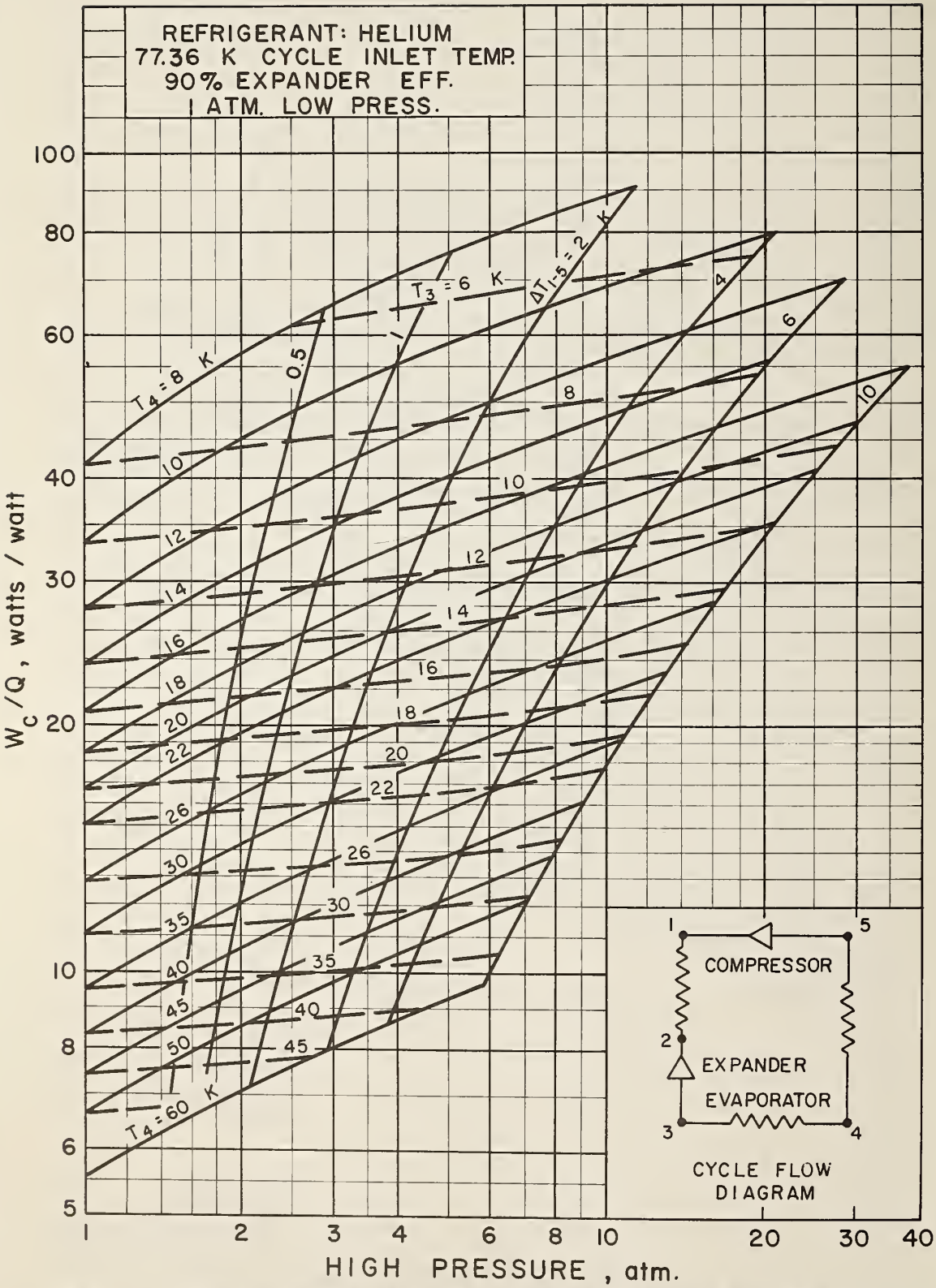

Figure 13. Brayton Refrigerator Performance - Helium Refrigerant - 77.36 K Cycle Inlet Temperature - 90% Expander Efficiency - No Pressure Drop.

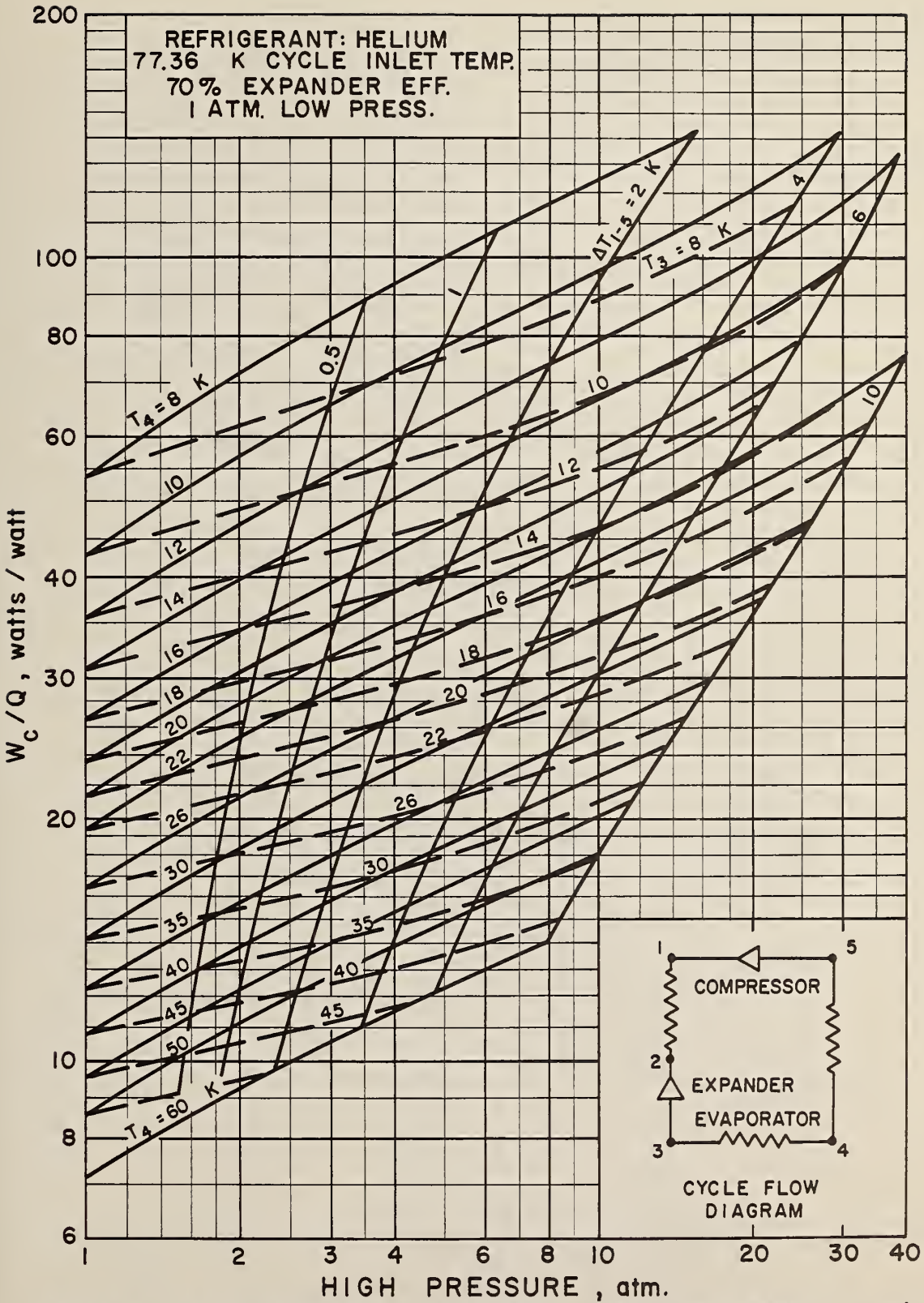

Figure 14. Brayton Refrigerator Performance - Helium Refrigerant - 77.36 K Cycle Inlet Temperature - 70% Expander Efficiency - No Pressure Drop.

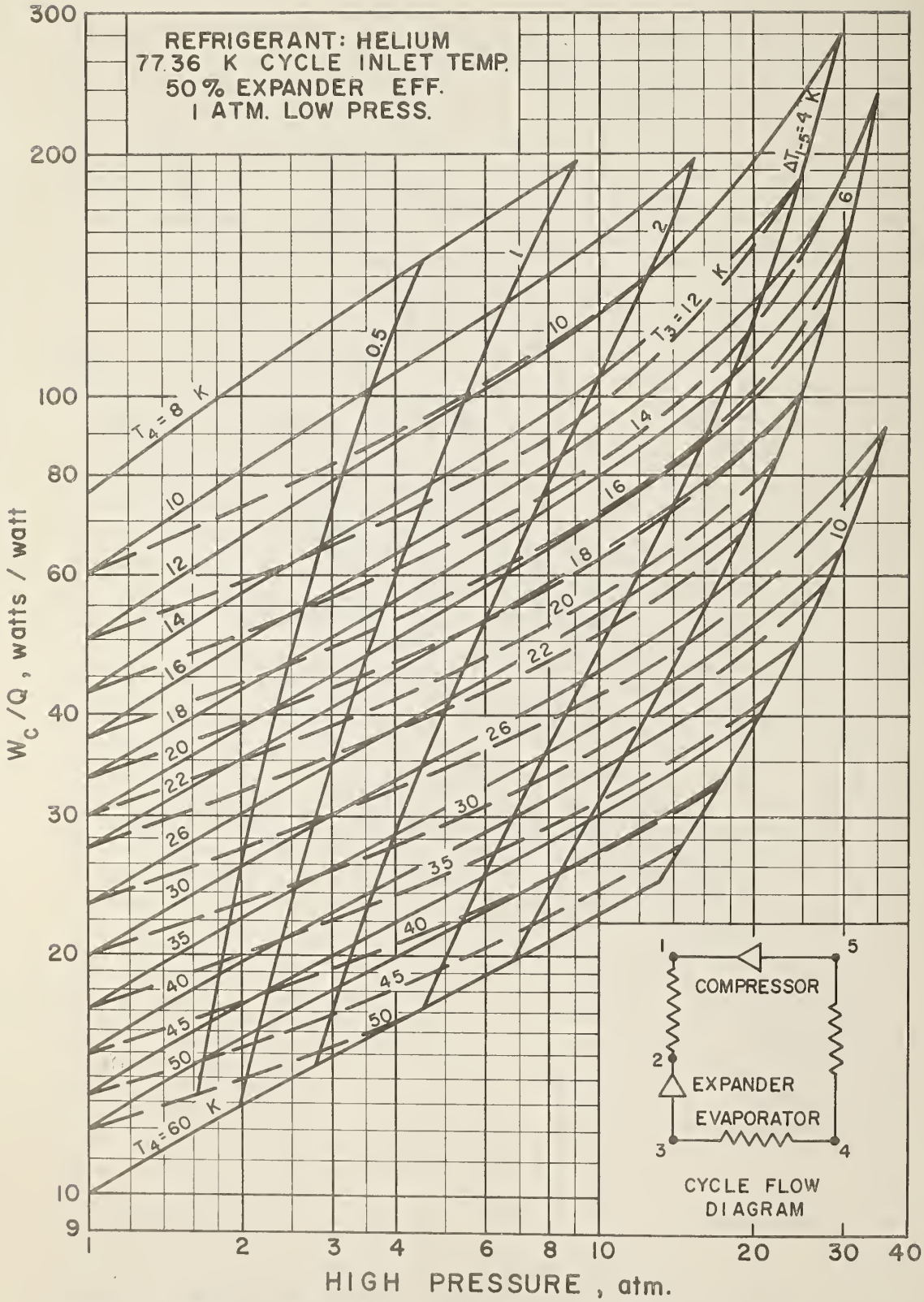

Figure 15. Brayton Refrigerator Performance - Helium Refrigerant - 77.36 K Cycle Inlet Temperature - 50% Expander Efficiency - No Pressure Drop.

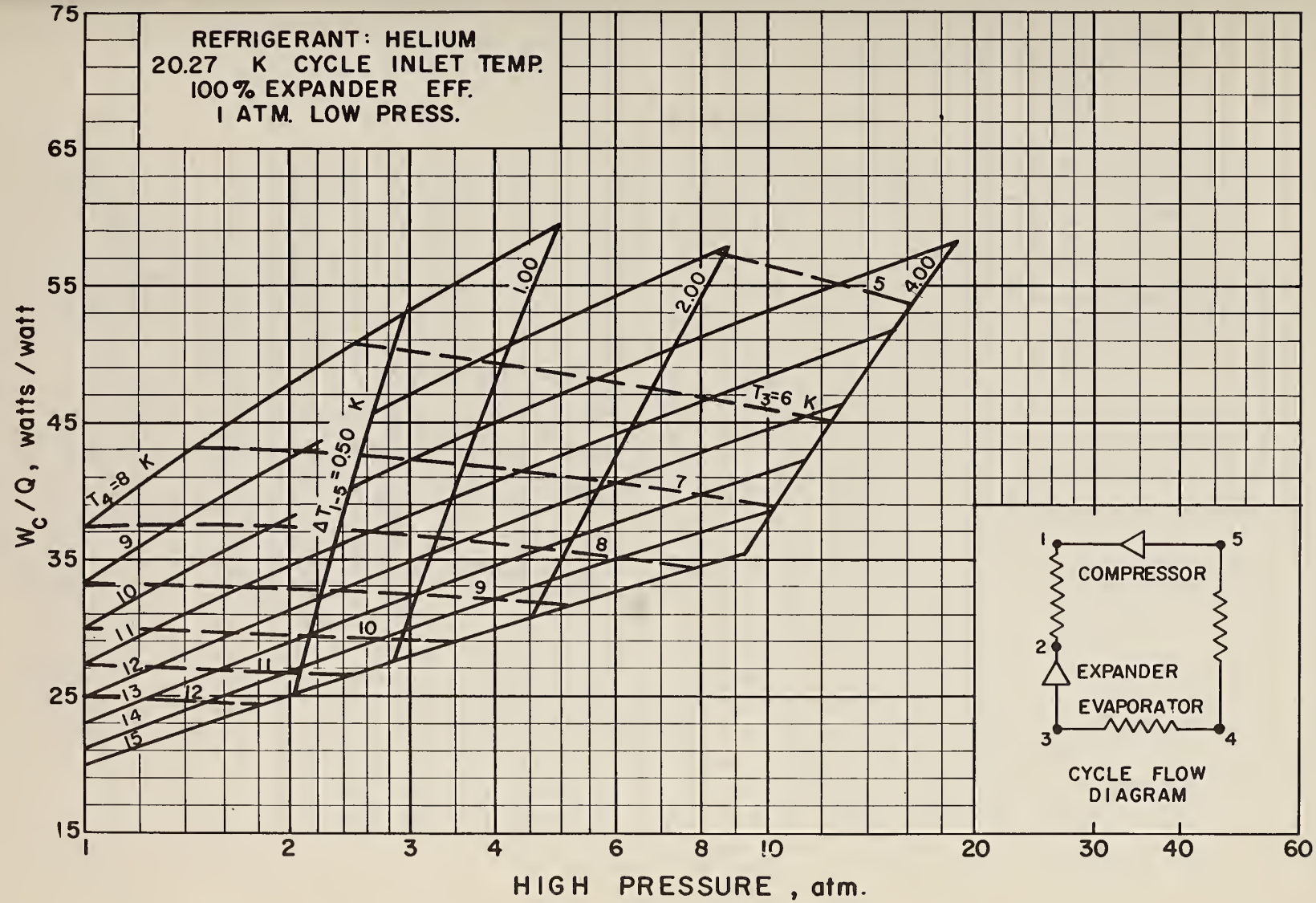

Figure 16. Brayton Refrigerator Performance - Helium Refrigerant - 20.27 K Cycle Inlet Temperature - 100% Expander Efficiency - No Pressure Drop.

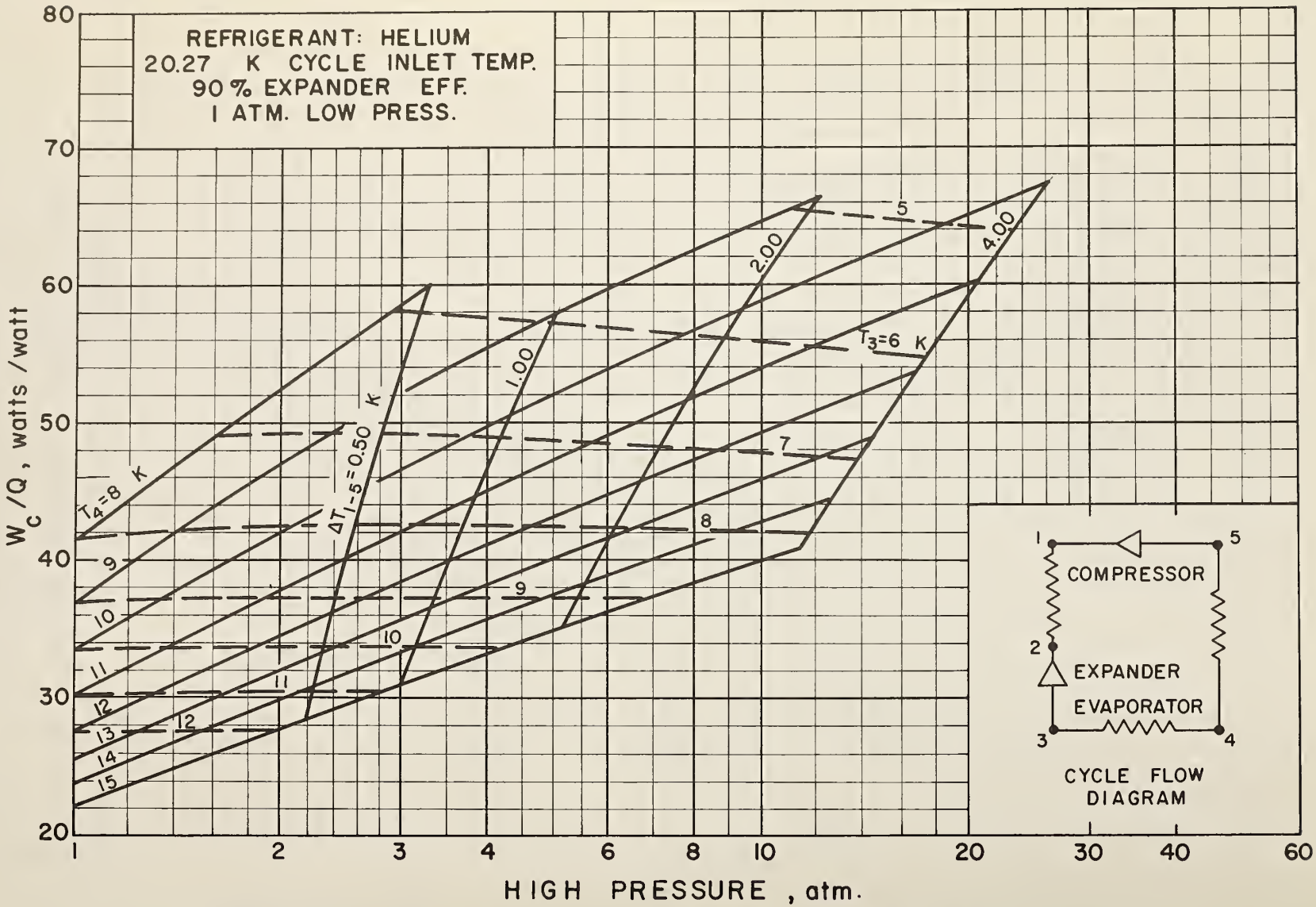

Figure 17. Brayton Refrigerator Performance - Helium Refrigerant - 20.27 K Cycle Inlet Temperature - 90% Expander Efficiency - No Pressure Drop.

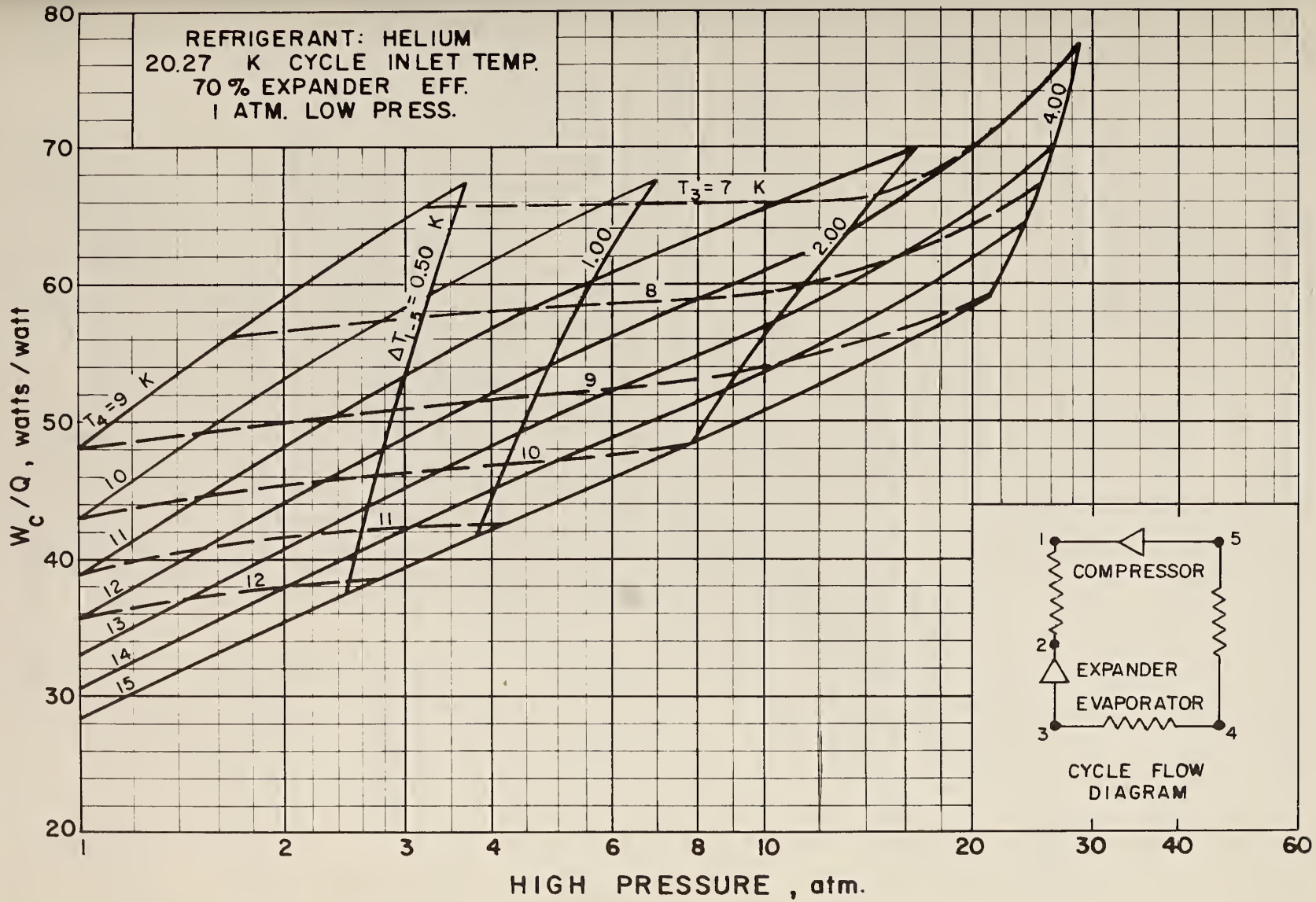

Figure 18. Brayton Refrigerator Performance - Helium Refrigerant - 20.27 K Cycle Inlet Temperature - 70% Expander Efficiency - No Pressure Drop.

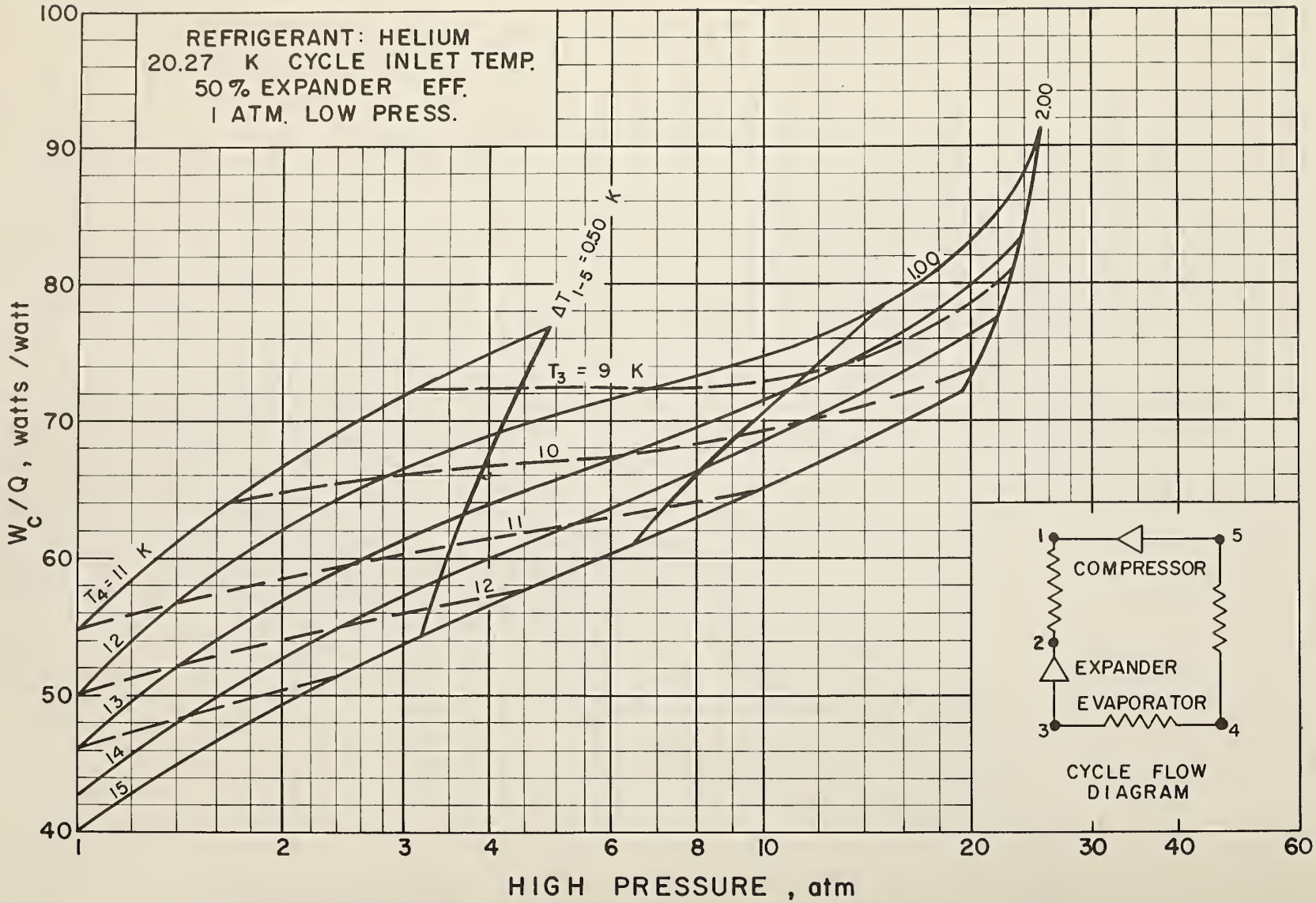

Figure 19. Brayton Refrigerator Performance - Helium Refrigerant - 20.27 K Cycle Inlet Temperature - 50% Expander Efficiency - No Pressure Drop.

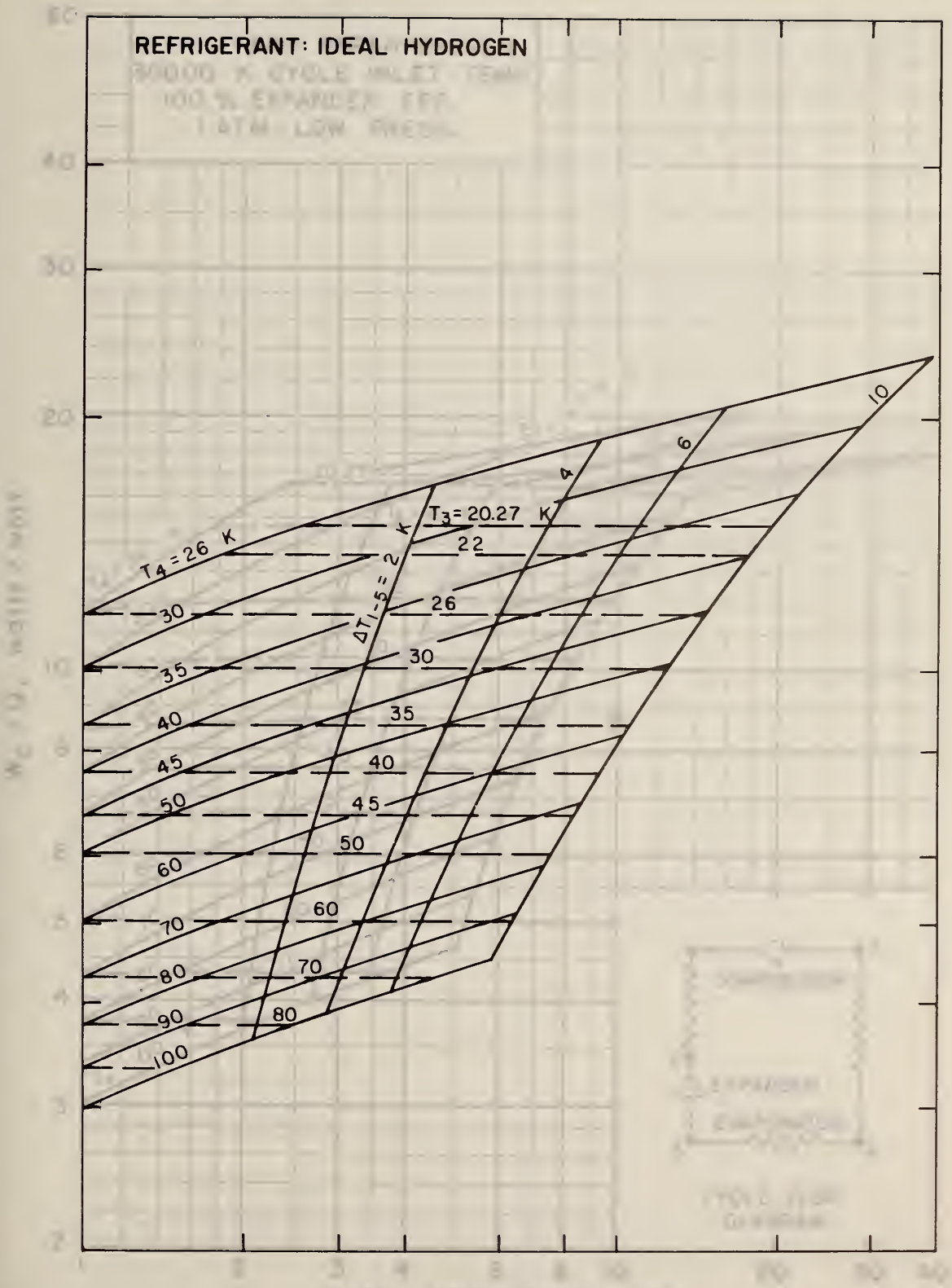

Figure 20 Overlay

Figure 20 Overlay

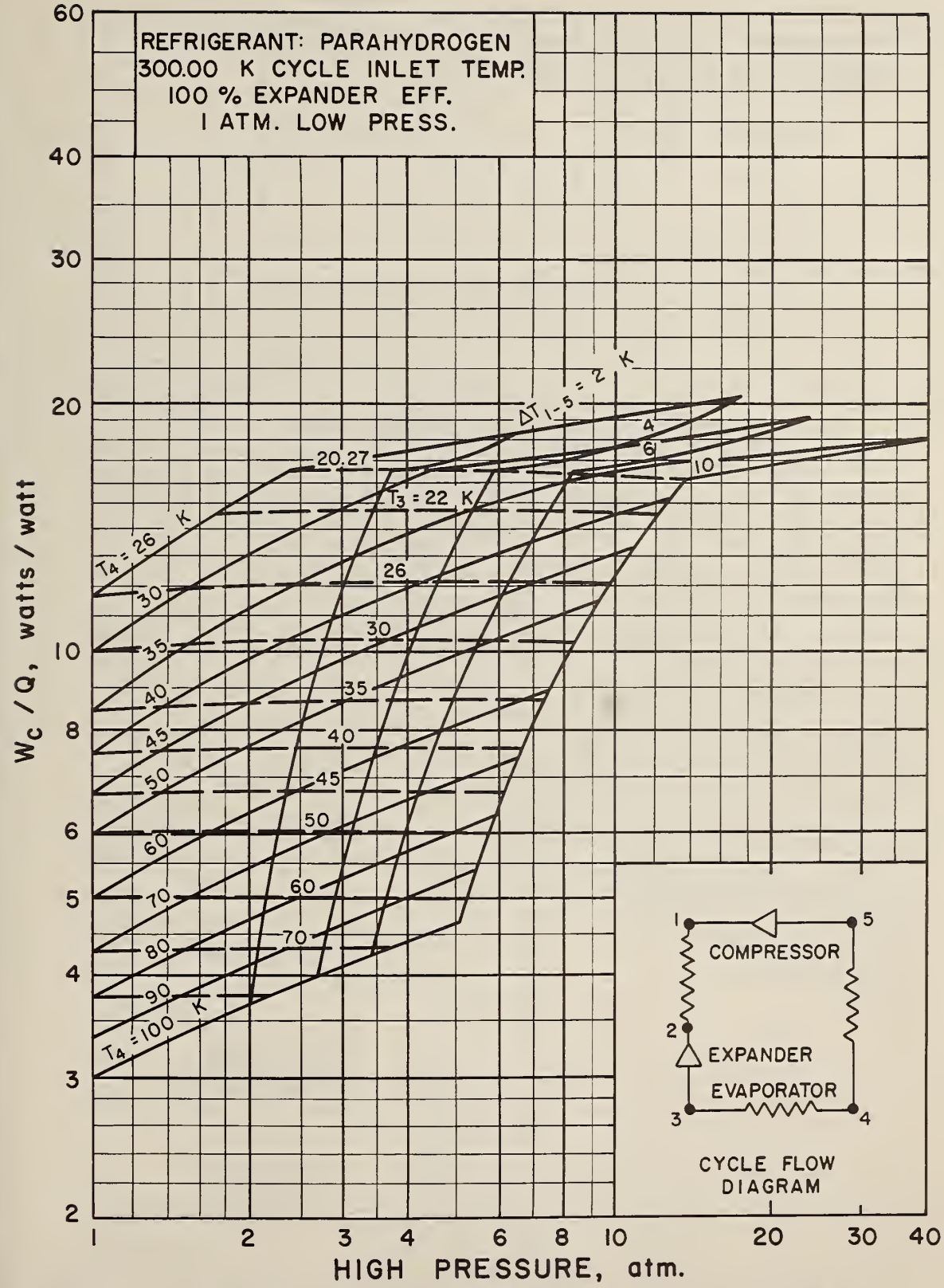

Figure 20. Brayton Refrigerator Performance - Parahydrogen Refrigerant - 300 K Cycle Inlet Temperature - 100% Expander Efficiency - No Pressure Drop.

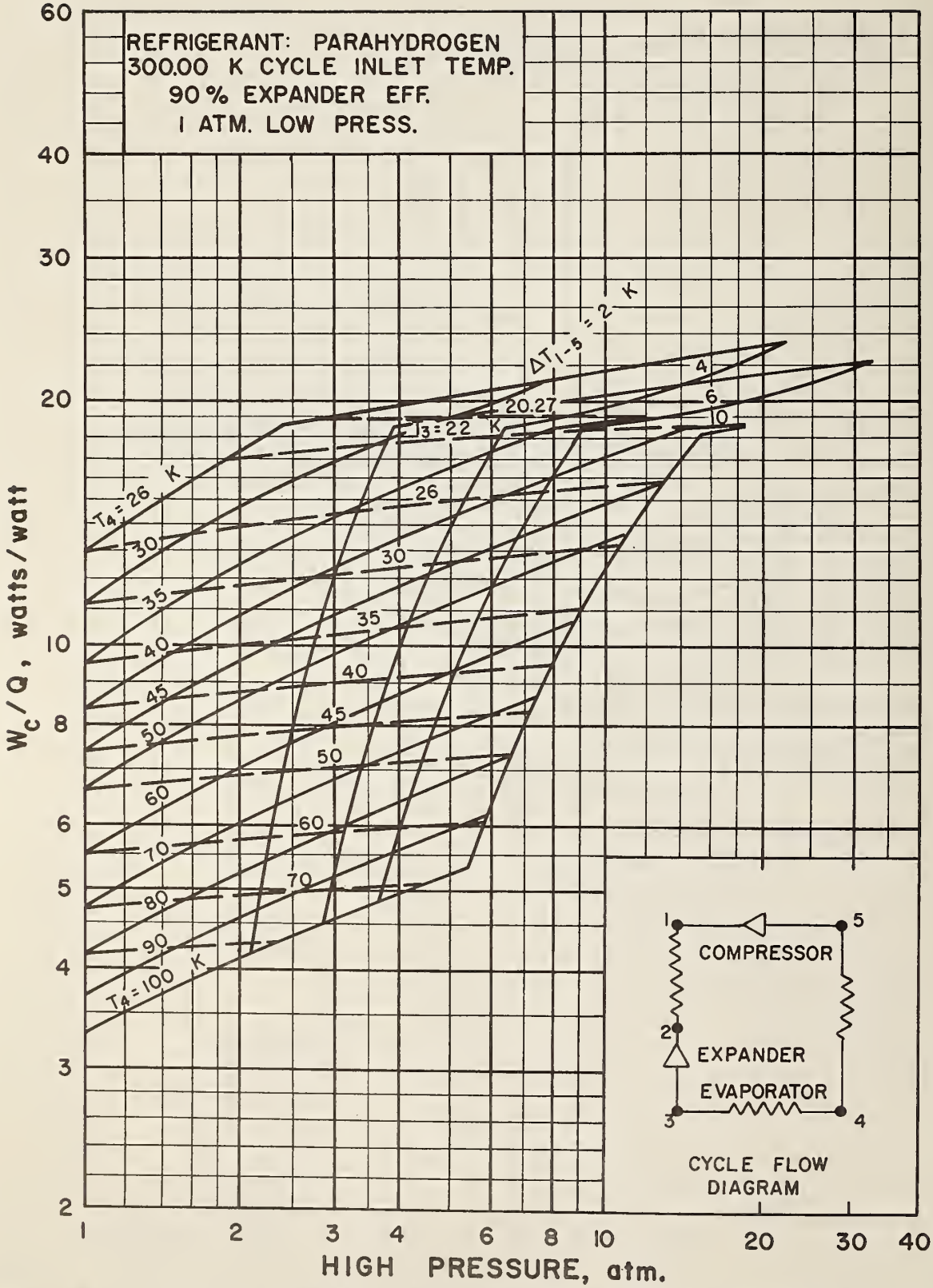

Figure 21. Brayton Refrigerator Performance - Parahydrogen Refrigerant - 300 K Cycle Inlet Temperature - 90% Expander Efficiency - No Pressure Drop.

REFRIGERANT: IDEAL HYDROGEN
$T_3 = 20.27$ K
$T_4 = 25$ K
22
25
30
35
40
45
50
55
60
70
80
90
100

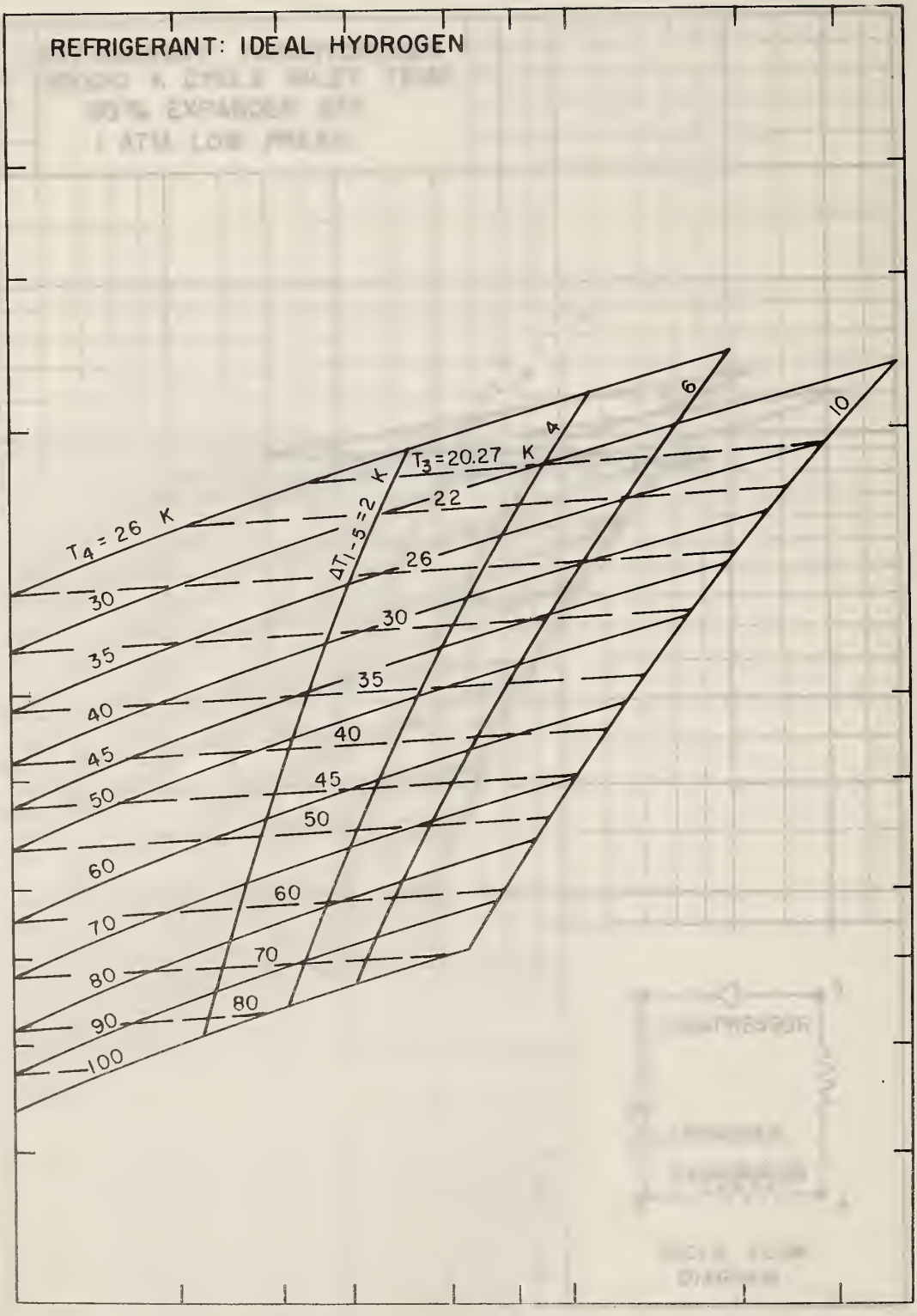

Figure 21 Overlay

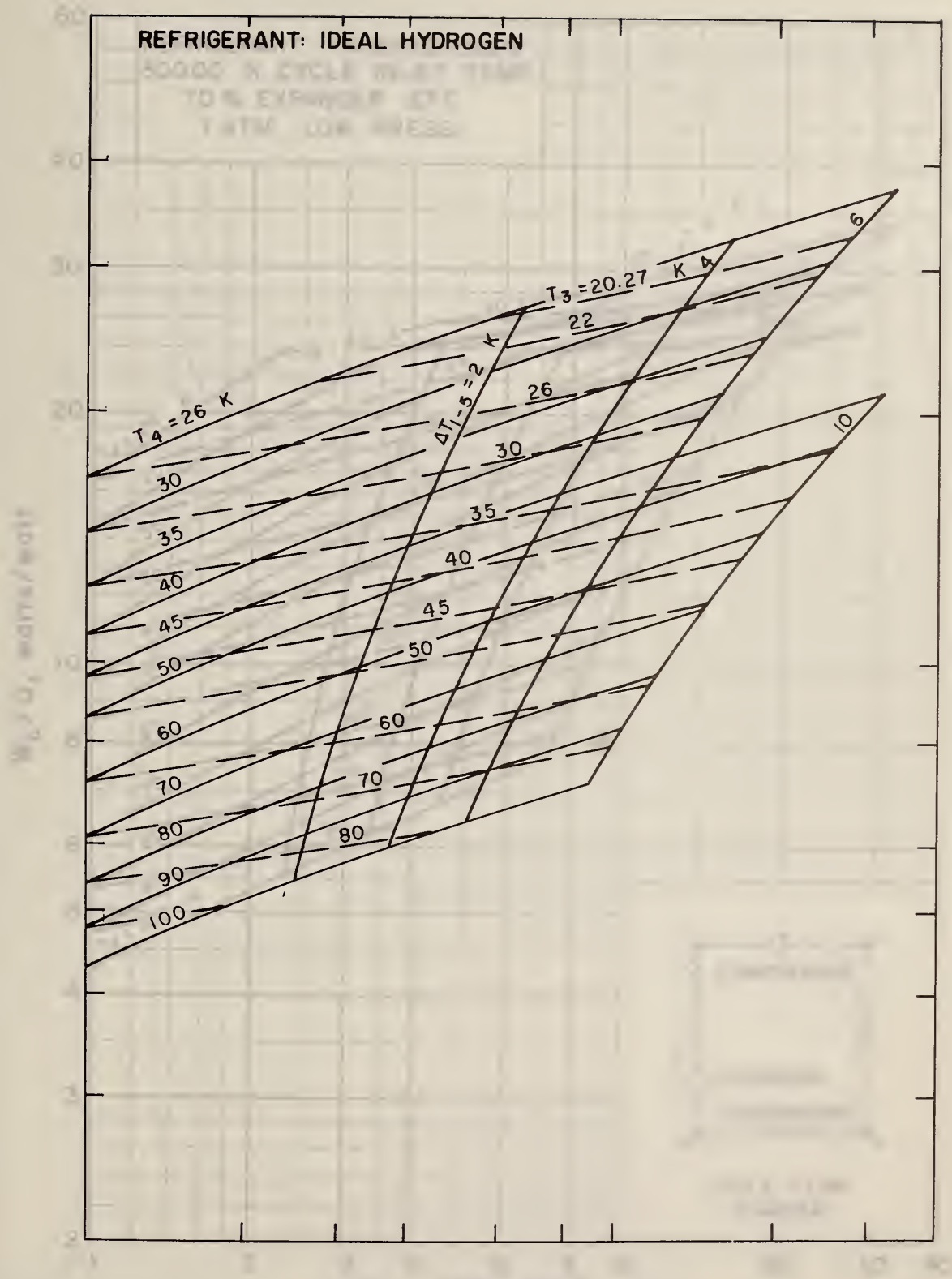

Figure 22 Overlay

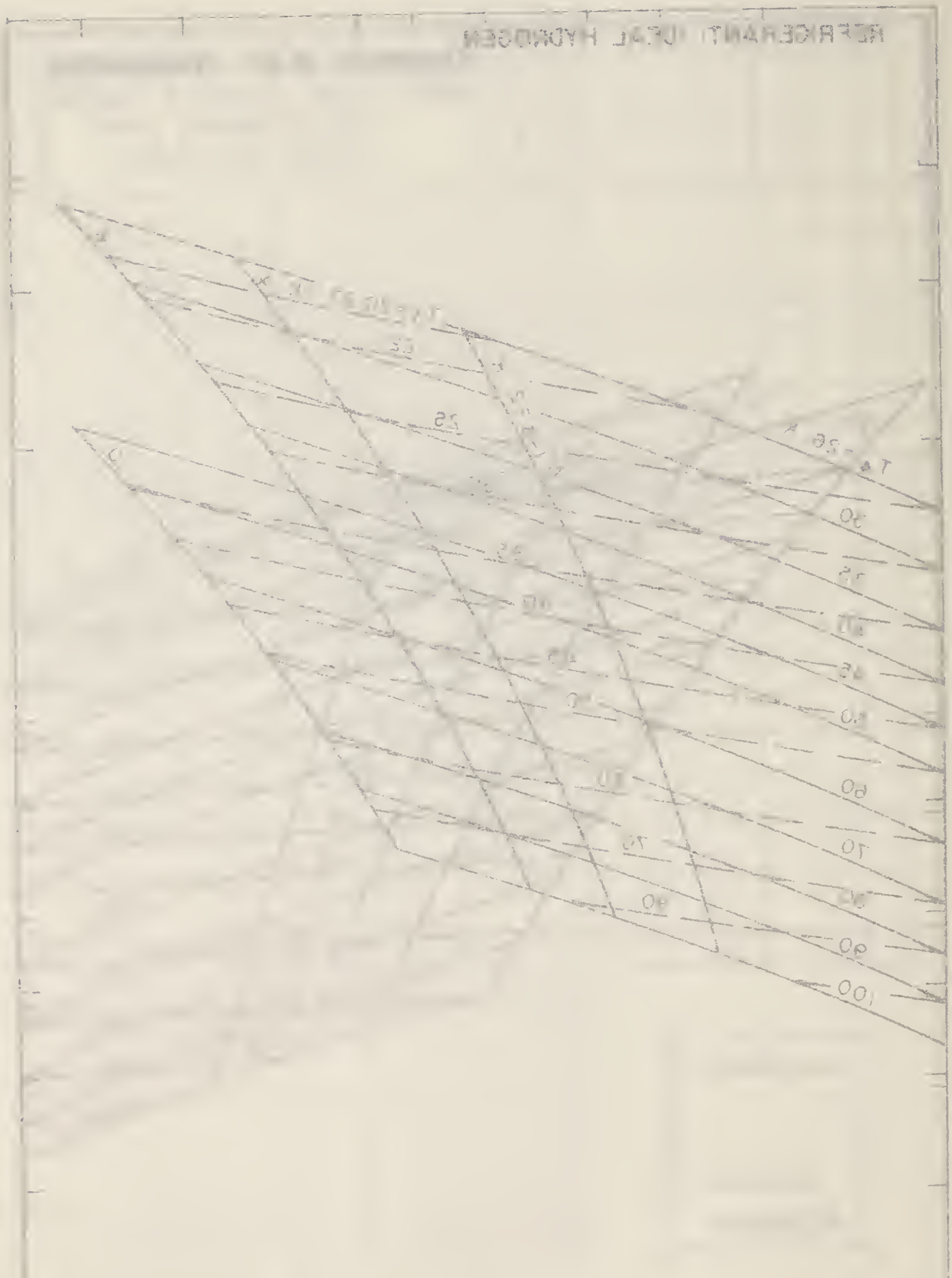

Figure 22 Overlay

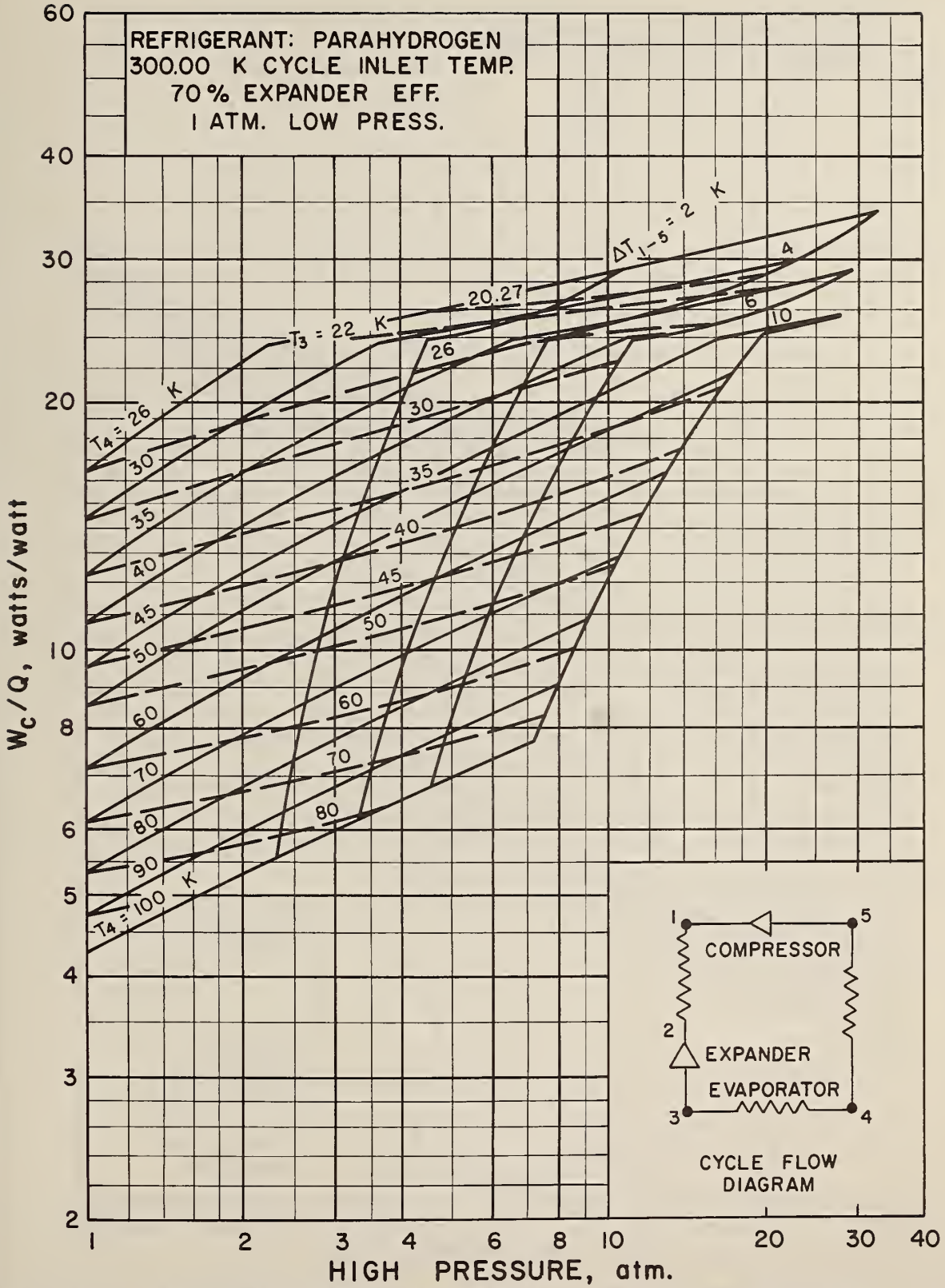

Figure 22. Brayton Refrigerator Performance - Parahydrogen Refrigerant - 300 K Cycle Inlet Temperature - 70% Expander Efficiency - No Pressure Drop.

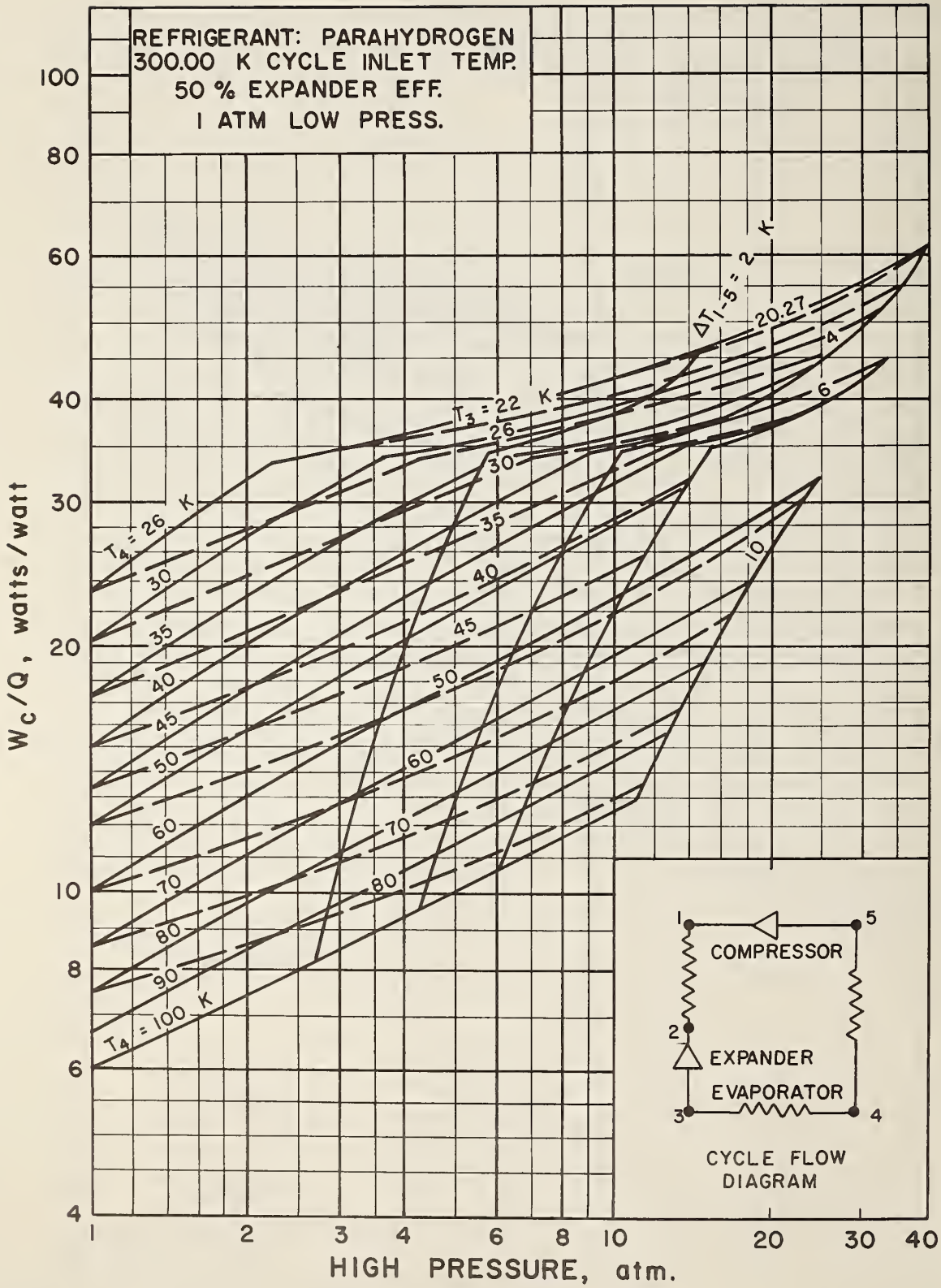

Figure 23. Brayton Refrigerator Performance - Parahydrogen Refrigerant - 300 K Cycle Inlet Temperature - 50% Expander Efficiency - No Pressure Drop.

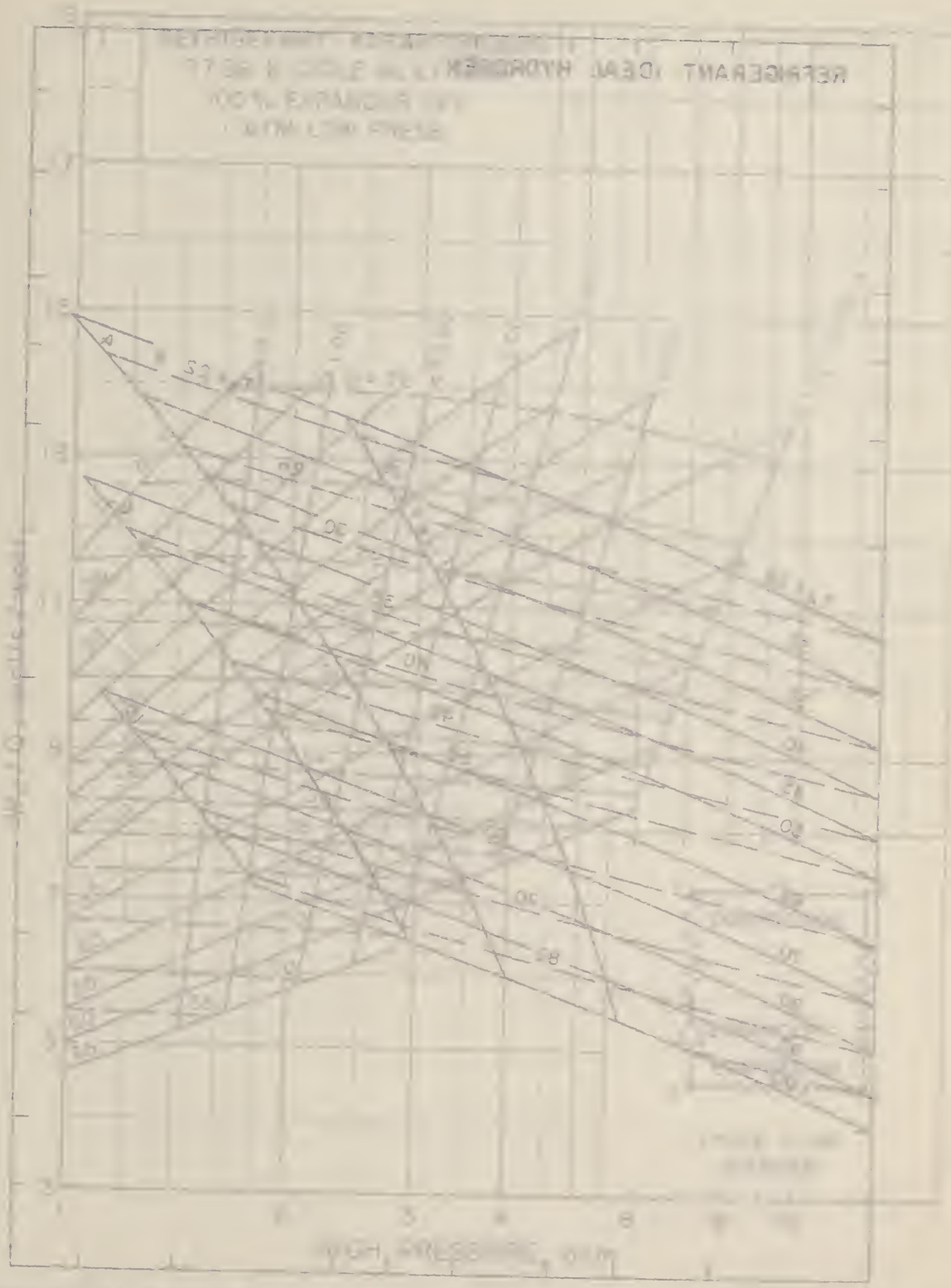

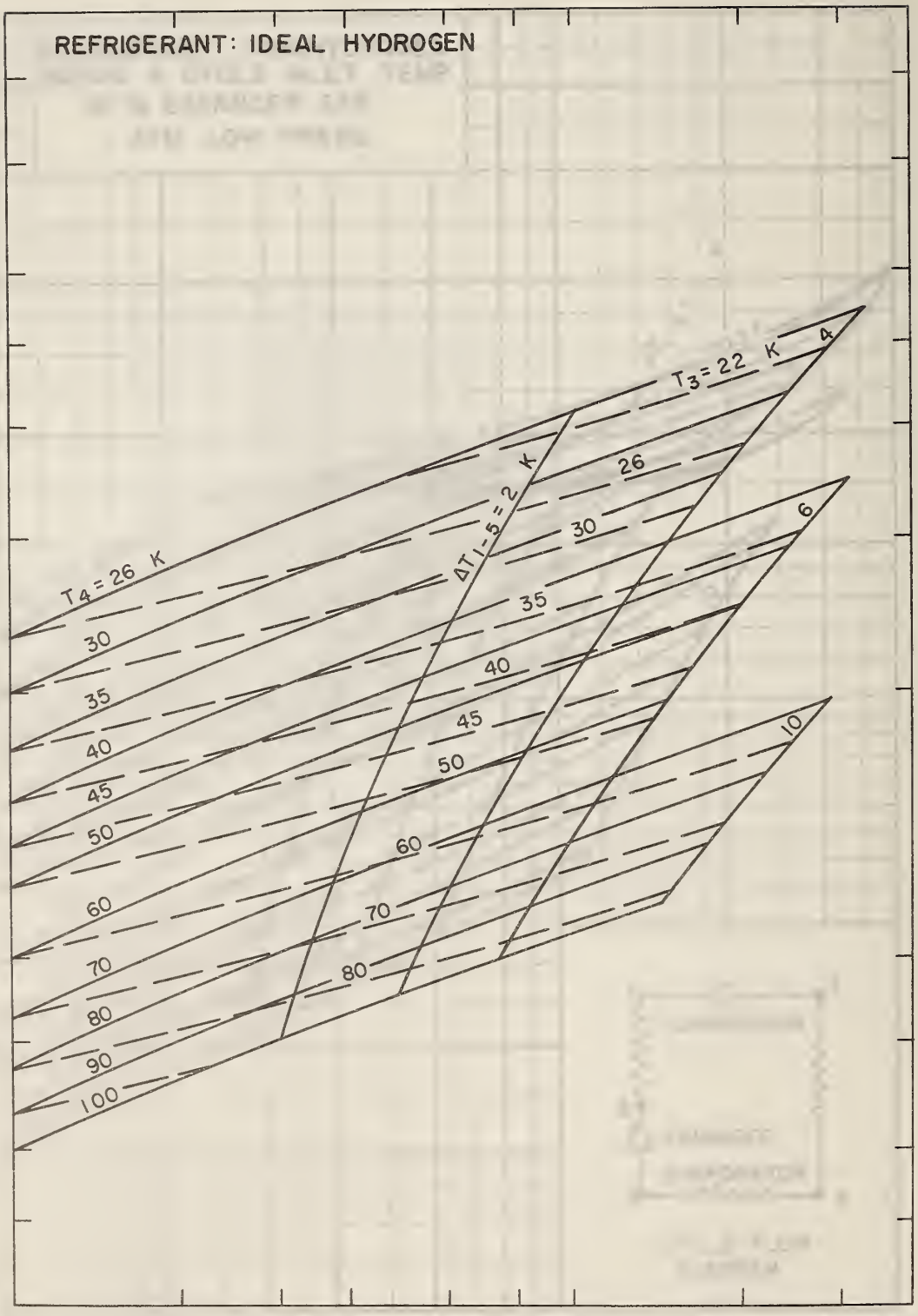

Figure 23 Overlay

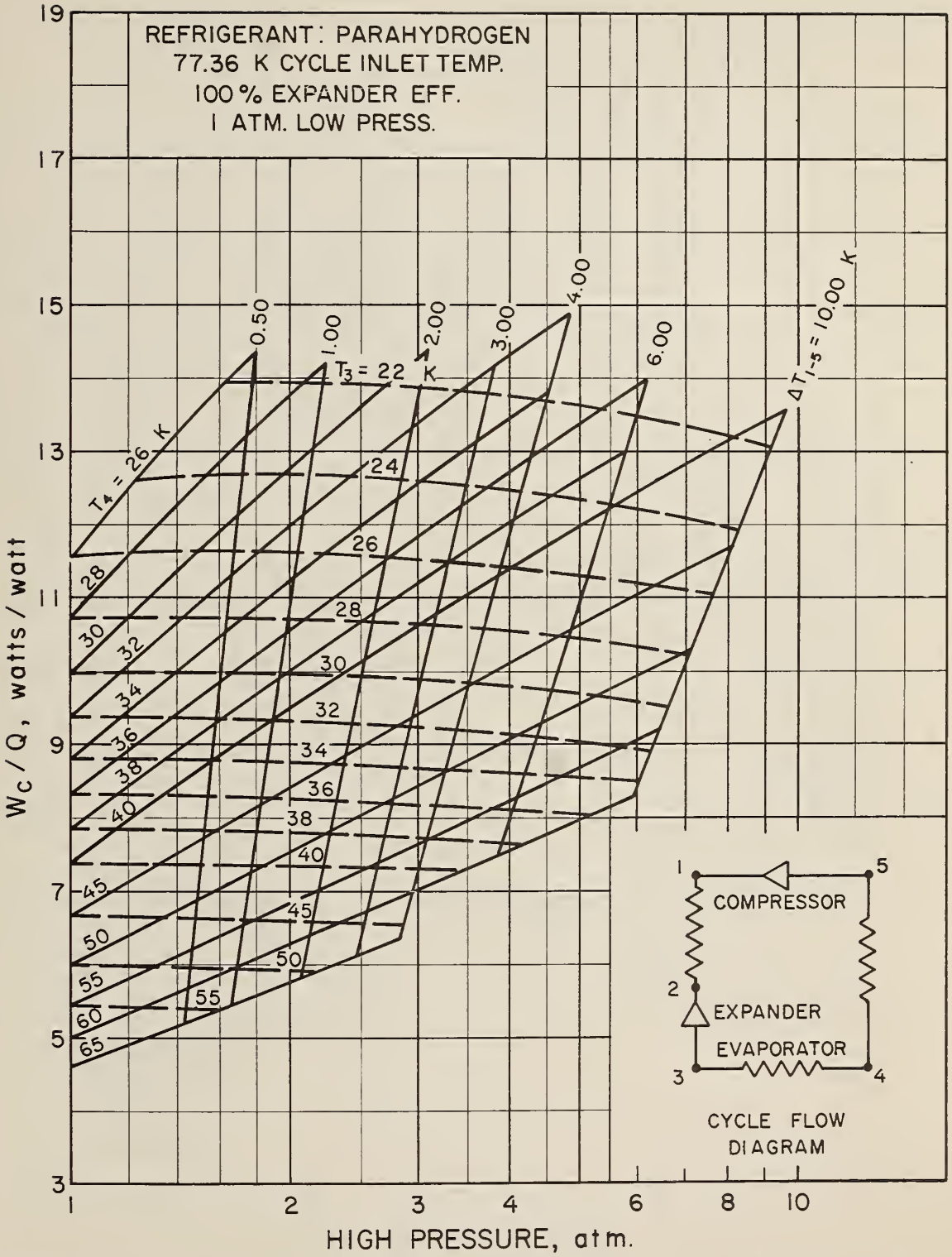

Figure 24. Brayton Refrigerator Performance - Parahydrogen Refrigerant - 77.36 K Cycle Inlet Temperature - 100% Expander Efficiency - No Pressure Drop.

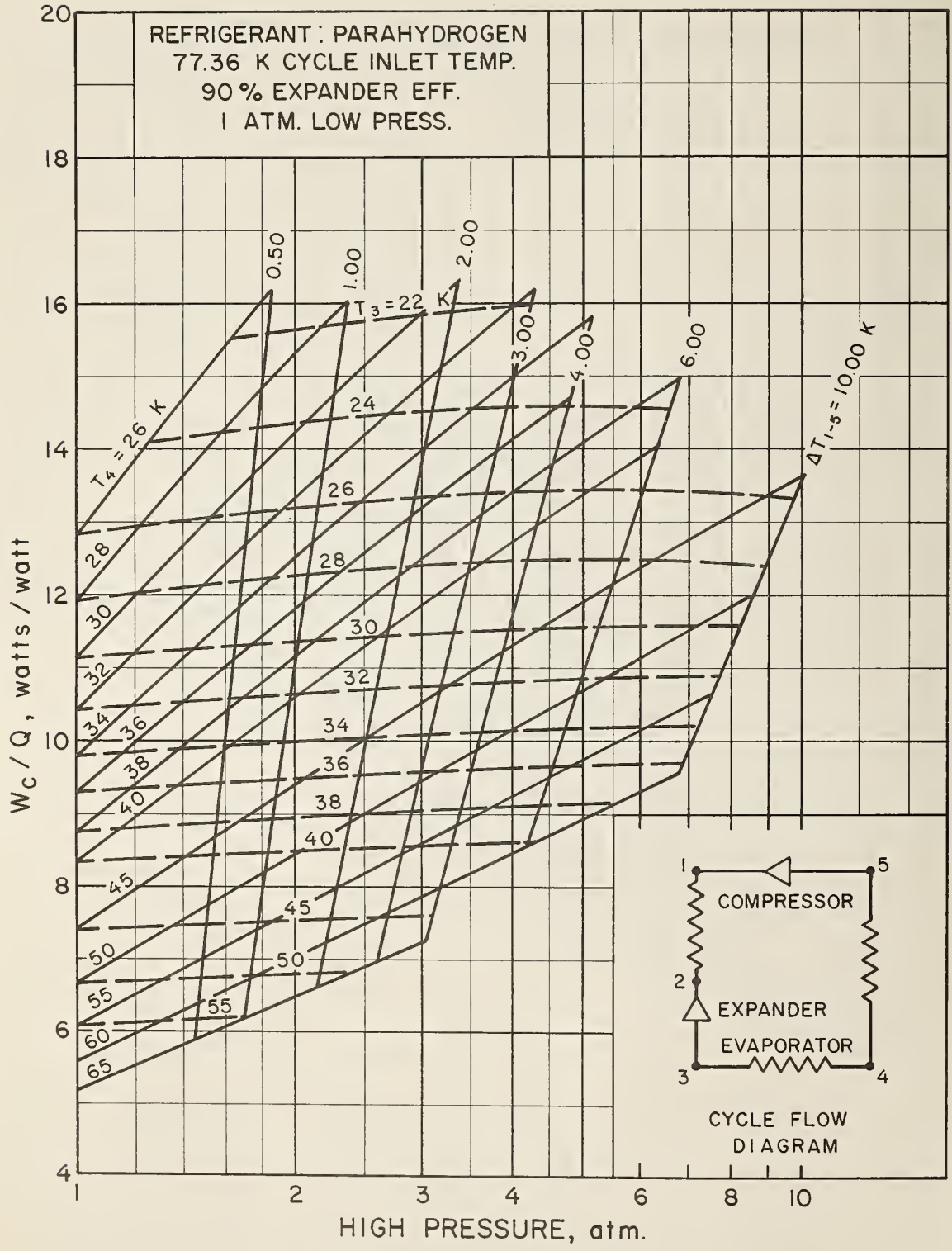

Figure 25. Brayton Refrigerator Performance - Parahydrogen Refrigerant - 77.36 K Cycle Inlet Temperature - 90% Expander Efficiency - No Pressure Drop.

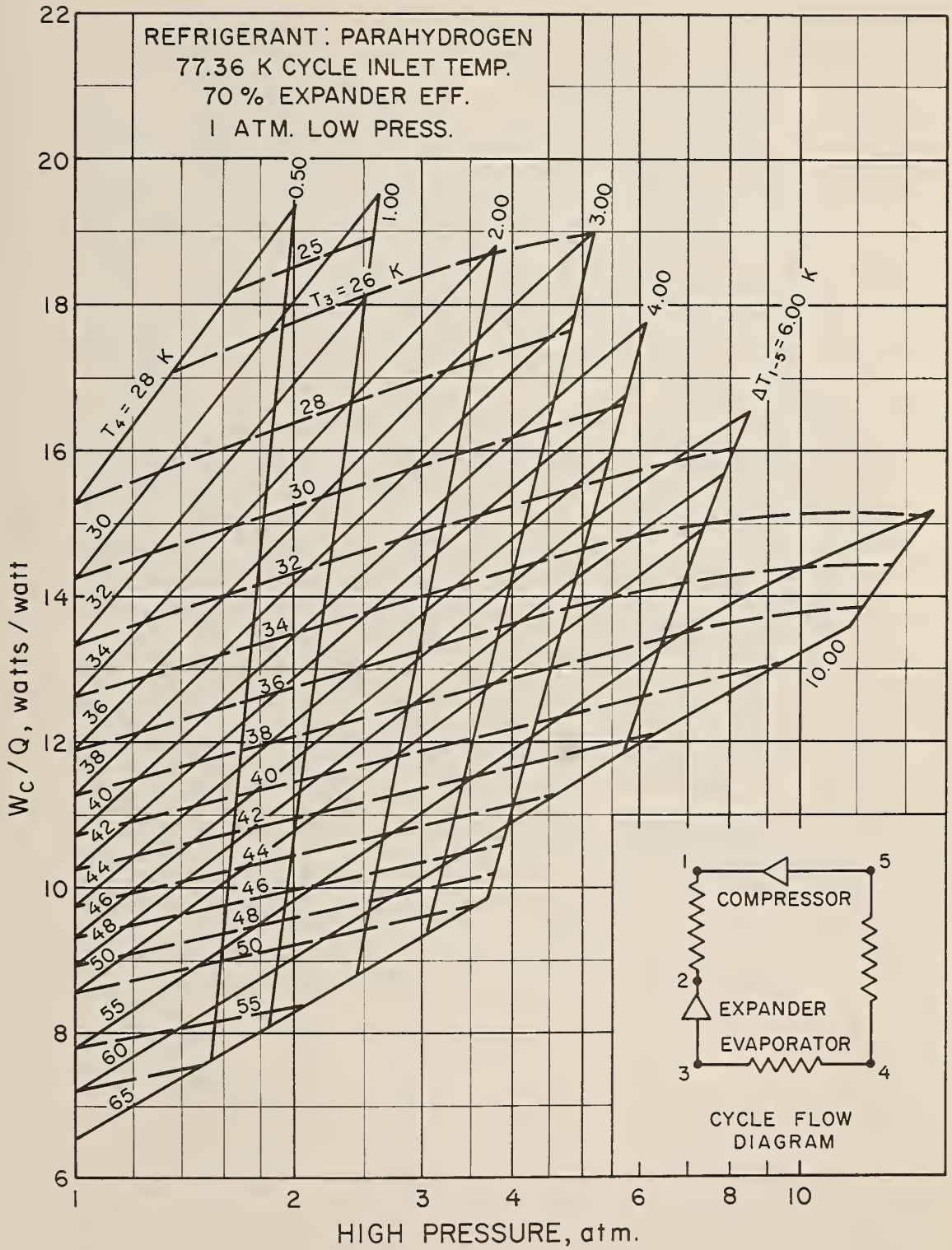

Figure 26. Brayton Refrigerator Performance - Parahydrogen Refrigerant - 77.36 K Cycle Inlet Temperature - 70% Expander Efficiency - No Pressure Drop.

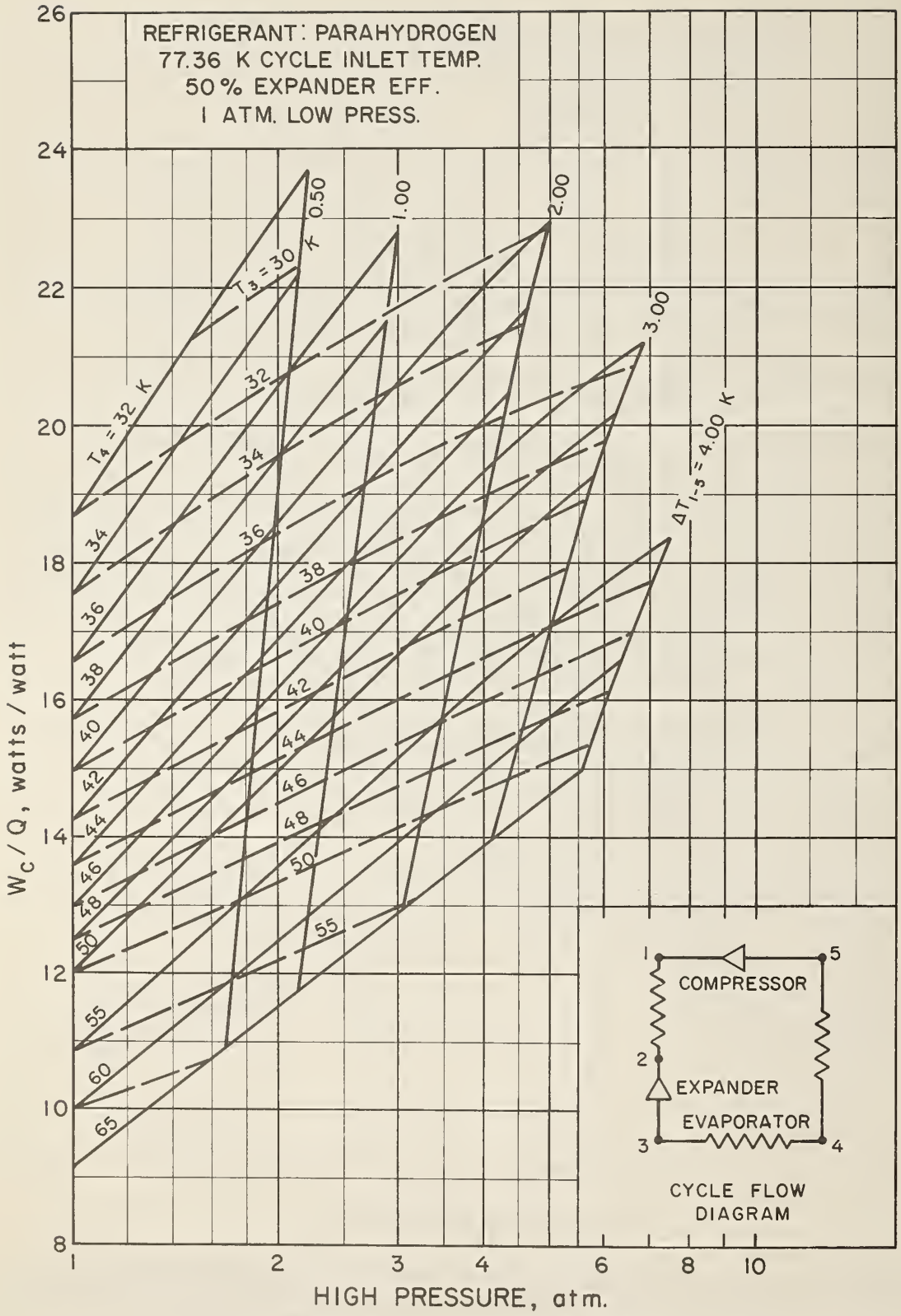

Figure 27. Brayton Refrigerator Performance - Parahydrogen Refrigerant - 77.36 K Cycle Inlet Temperature - 50% Expander Efficiency - No Pressure Drop.

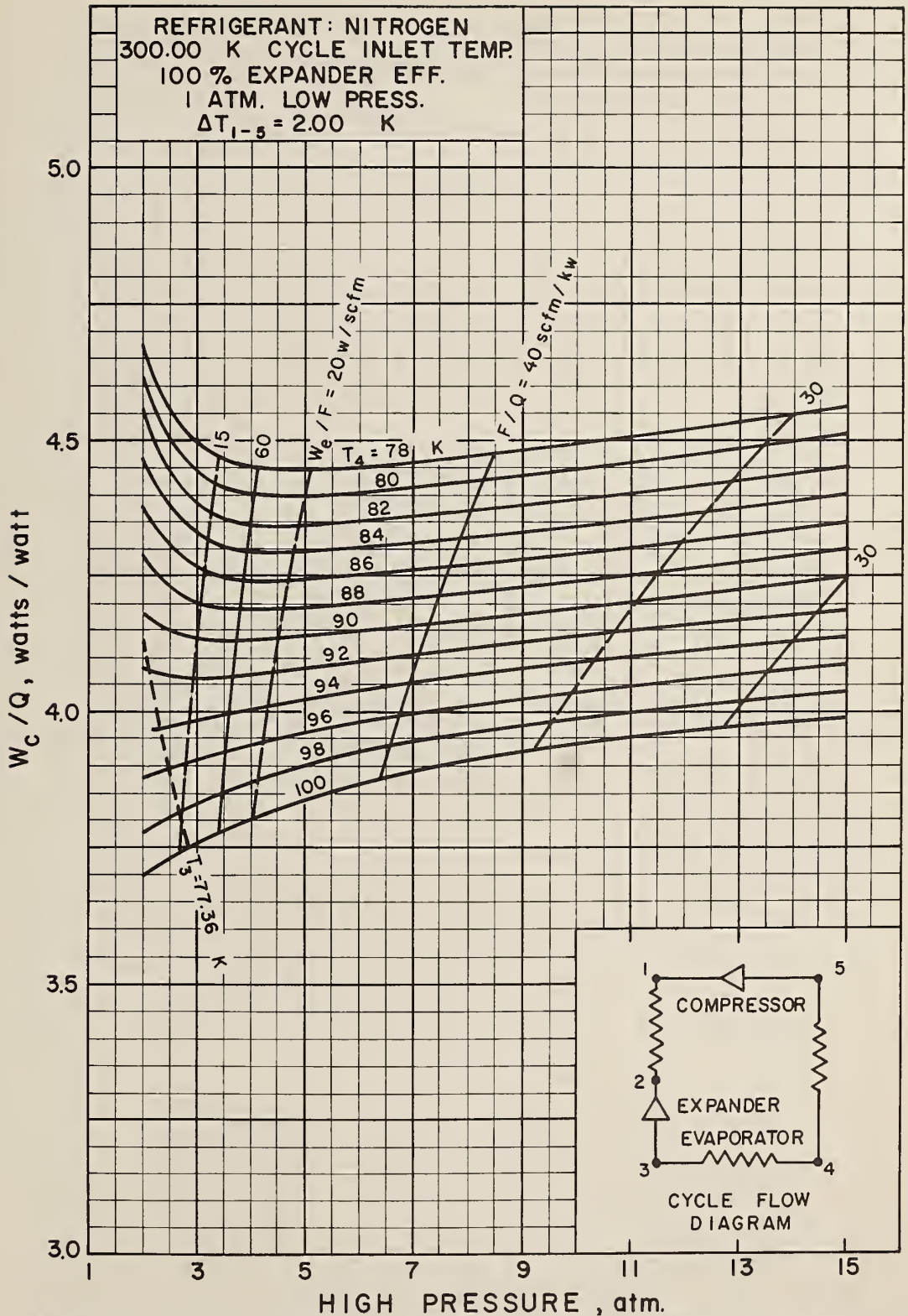

Figure 28. Brayton Refrigerator Performance - Nitrogen Refrigerant - 300 K Cycle Inlet Temperature - 100% Expander Efficiency - 2 K Heat Exchanger Temperature Difference - No Pressure Drop.

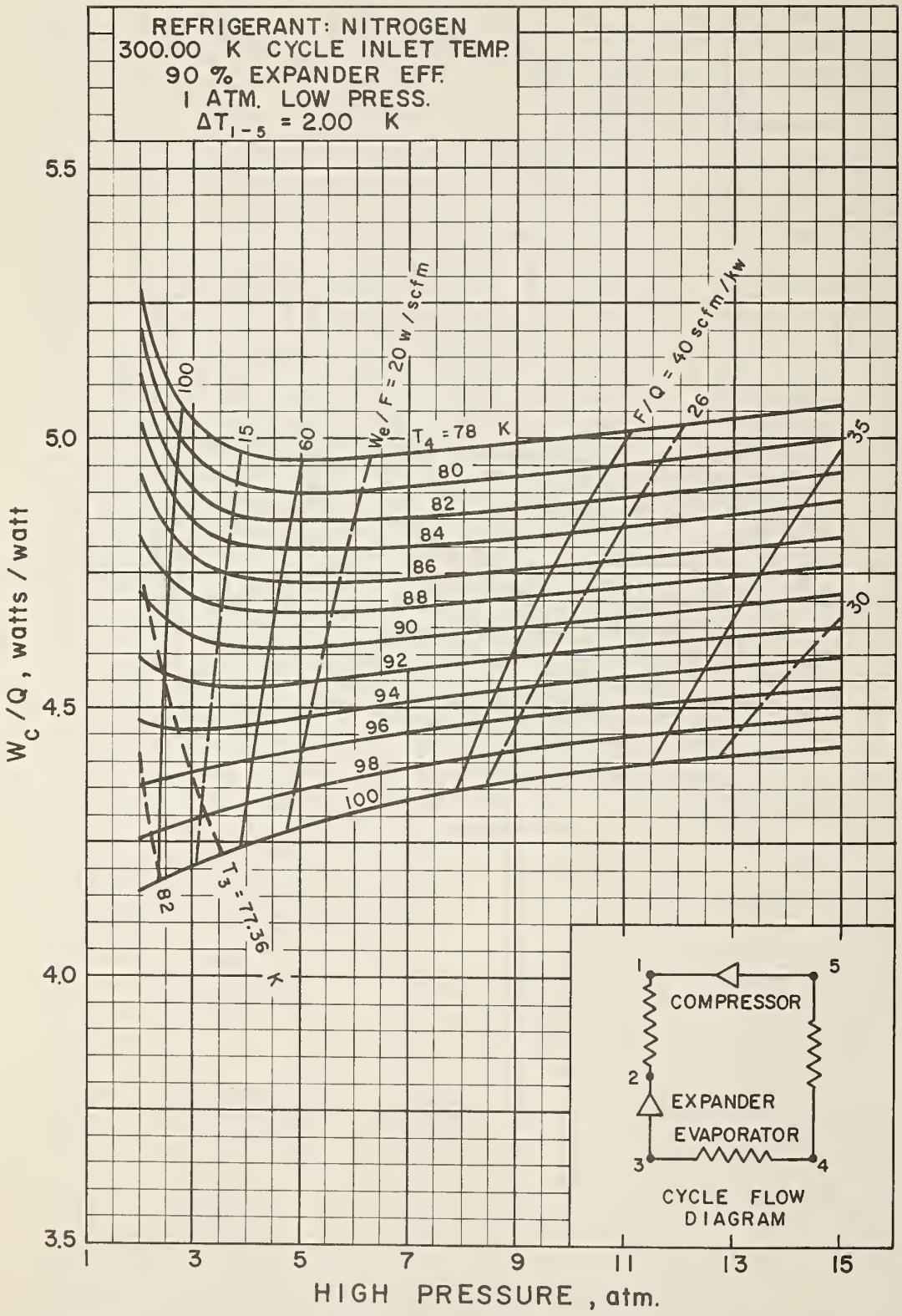

Figure 29. Brayton Refrigerator Performance - Nitrogen Refrigerant - 300 K Cycle Inlet Temperature - 90% Expander Efficiency - 2 K Heat Exchanger Temperature Difference - No Pressure Drop.

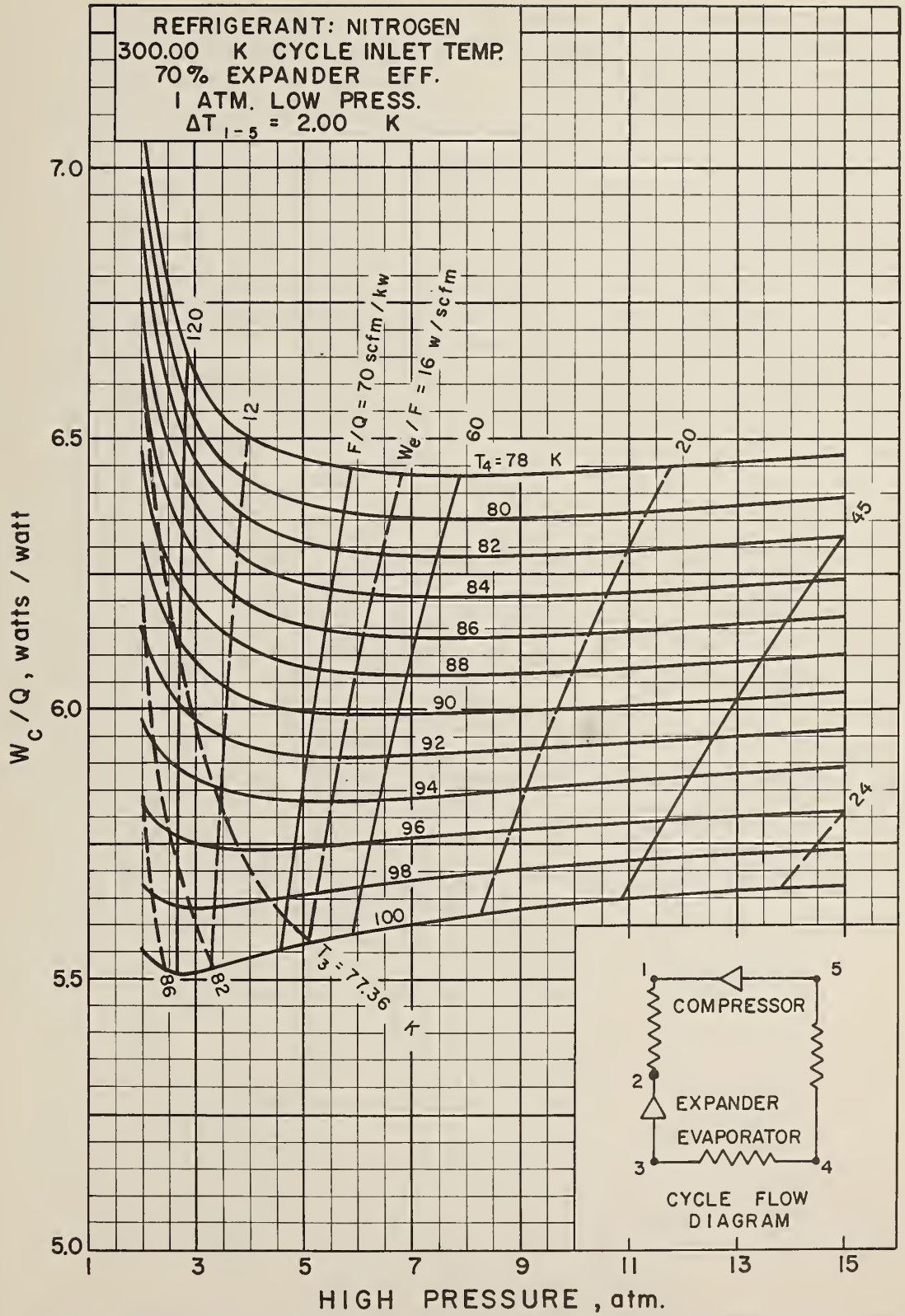

Figure 30. Brayton Refrigerator Performance - Nitrogen Refrigerant - 300 K Cycle Inlet Temperature - 70% Expander Efficiency - 2 K Heat Exchanger Temperature Difference - No Pressure Drop.

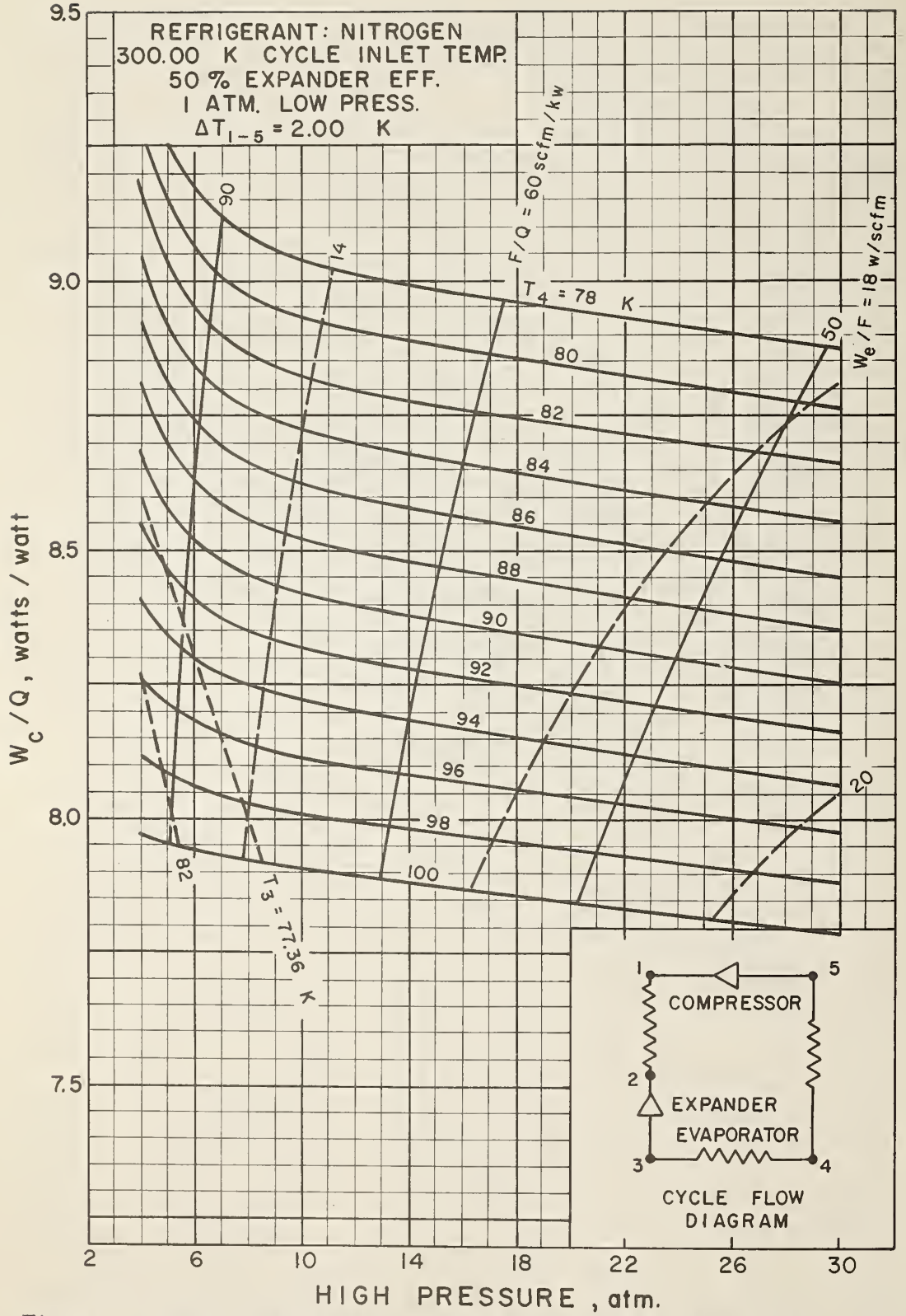

Figure 31. Brayton Refrigerator Performance - Nitrogen Refrigerant - 300 K Cycle Inlet Temperature - 50% Expander Efficiency - 2 K Heat Exchanger Temperature Difference - No Pressure Drop.

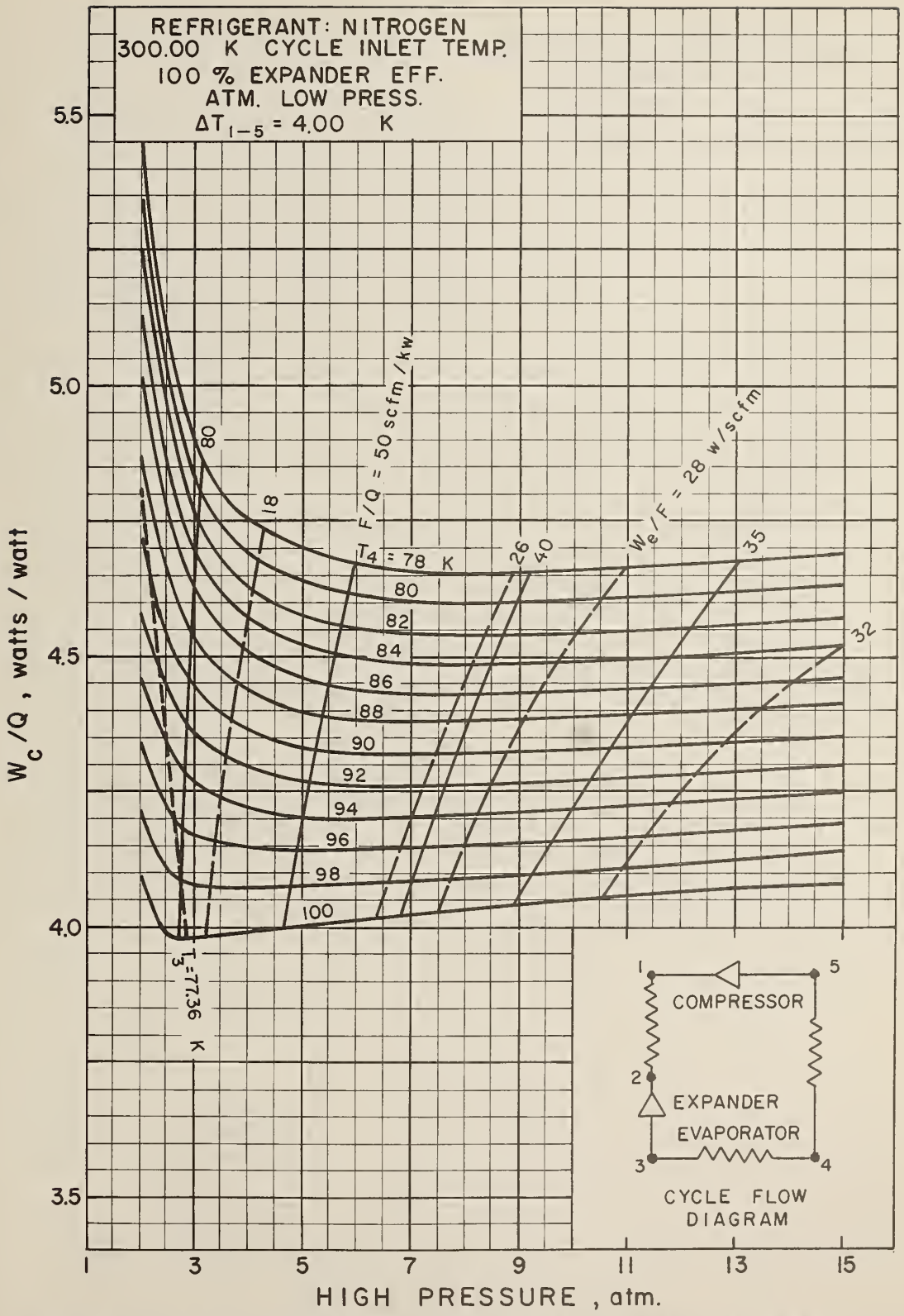

Figure 32. Brayton Refrigerator Performance - Nitrogen Refrigerant - 300 K Cycle Inlet Temperature - 100% Expander Efficiency - 4 K Heat Exchanger Temperature Difference - No Pressure Drop.

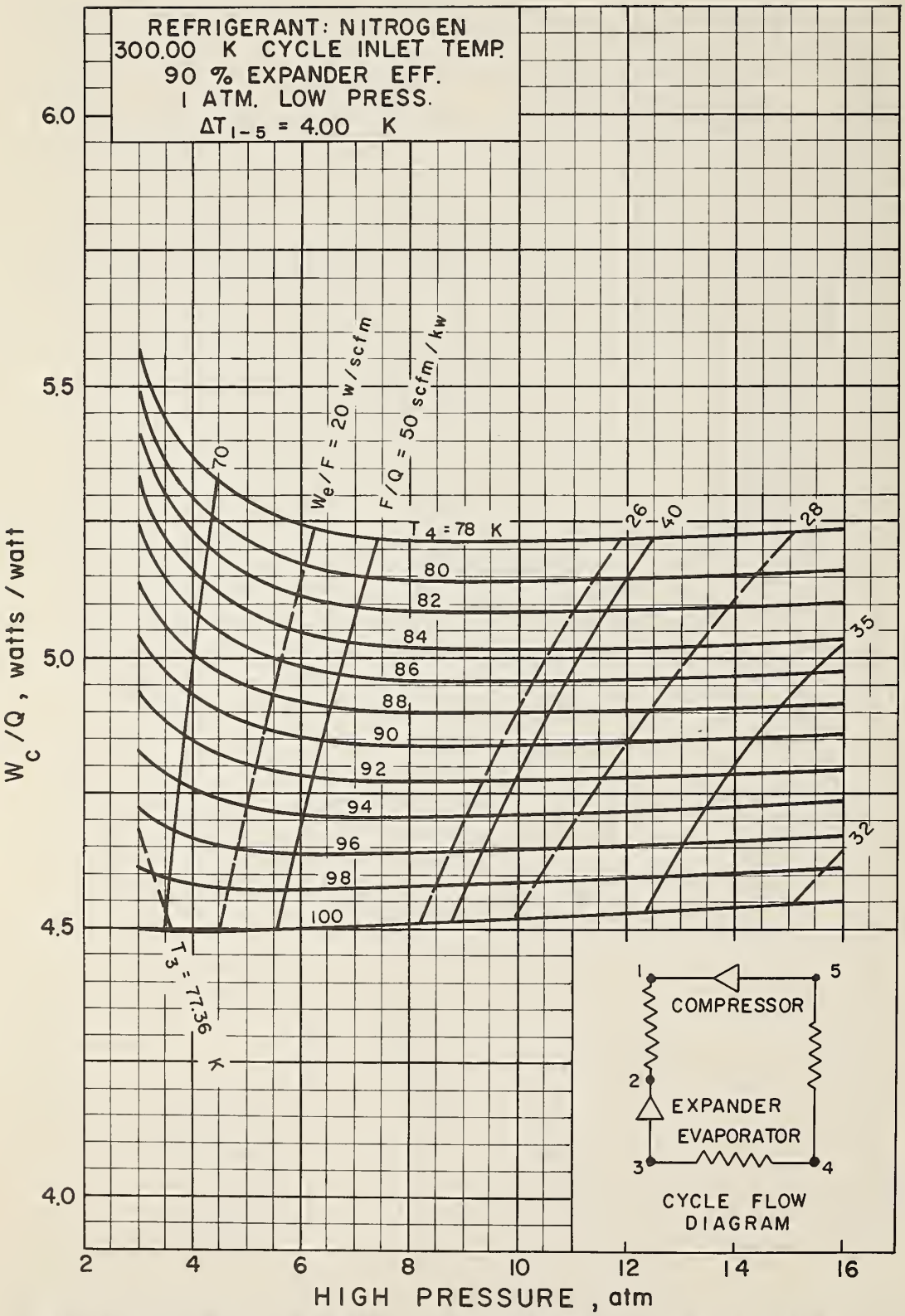

Figure 33. Brayton Refrigerator Performance - Nitrogen Refrigerant - 300 K Cycle Inlet Temperature - 90% Expander Efficiency - 4 K Heat Exchanger Temperature Difference - No Pressure Drop.

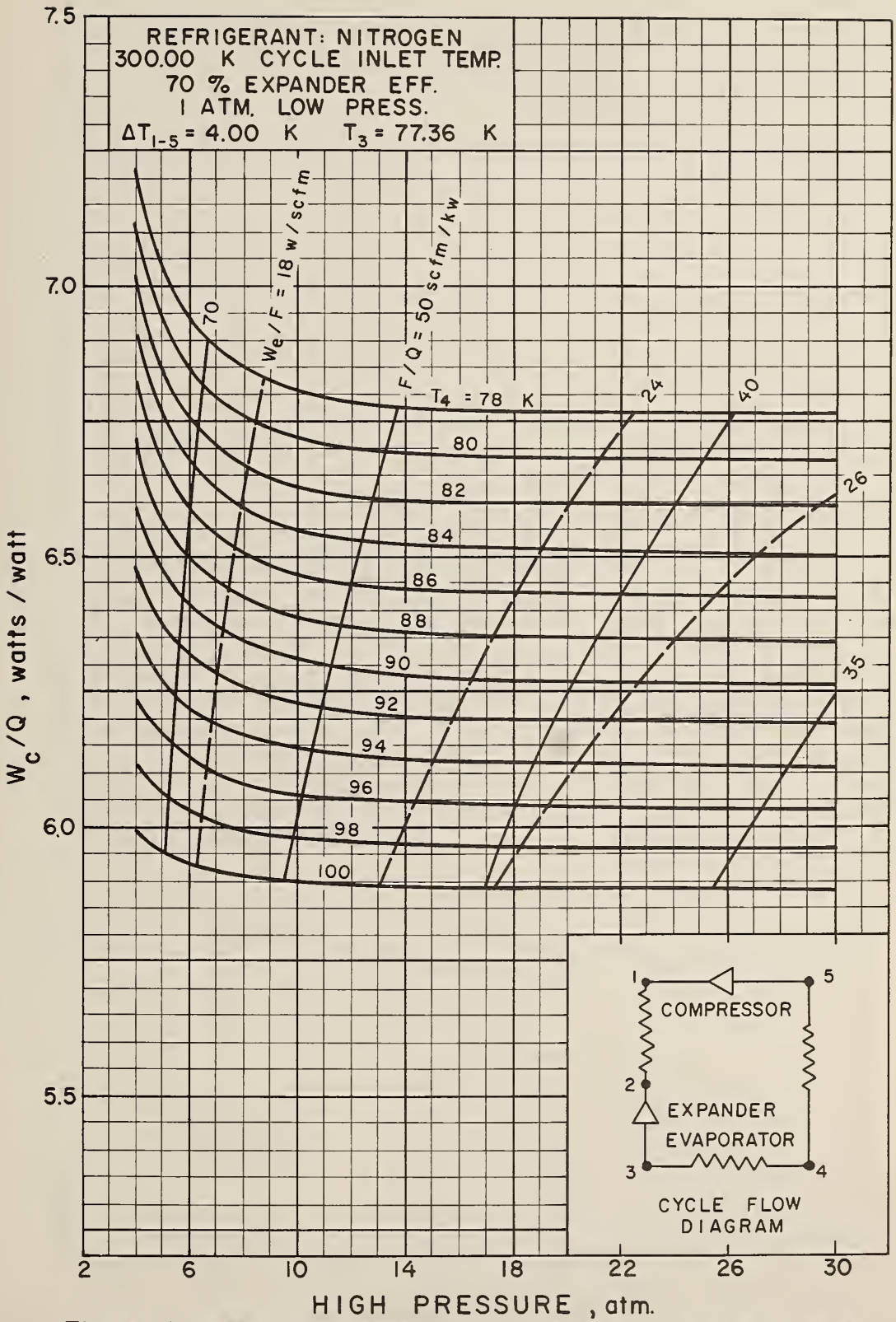

Figure 34. Brayton Refrigerator Performance - Nitrogen Refrigerant - 300 K Cycle Inlet Temperature - 70% Expander Efficiency - 4 K Heat Exchanger Temperature Difference - No Pressure Drop.

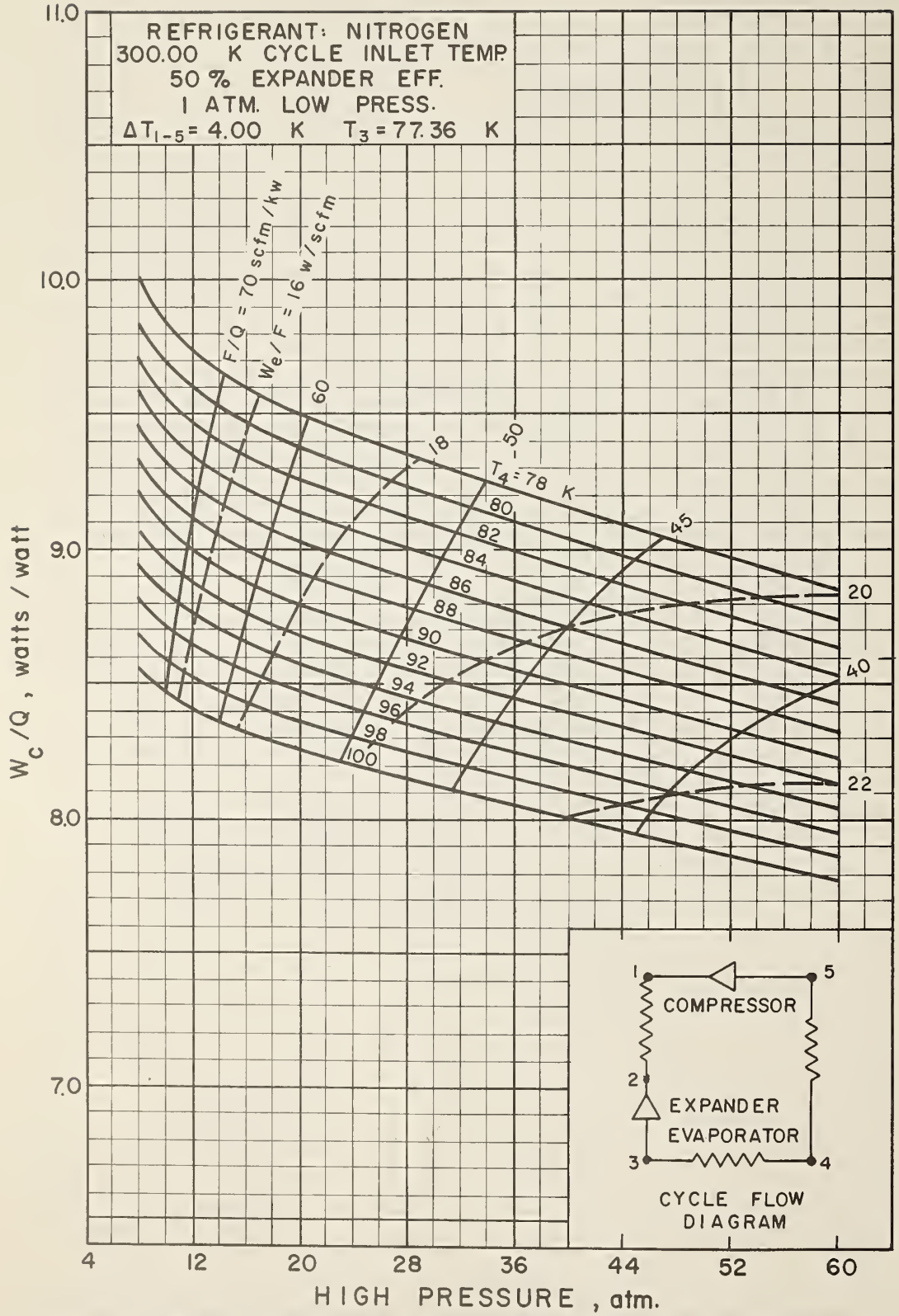

Figure 35. Brayton Refrigerator Performance - Nitrogen Refrigerant - 300 K Cycle Inlet Temperature - 50% Expander Efficiency - 4 K Heat Exchanger Temperature Difference - No Pressure Drop.

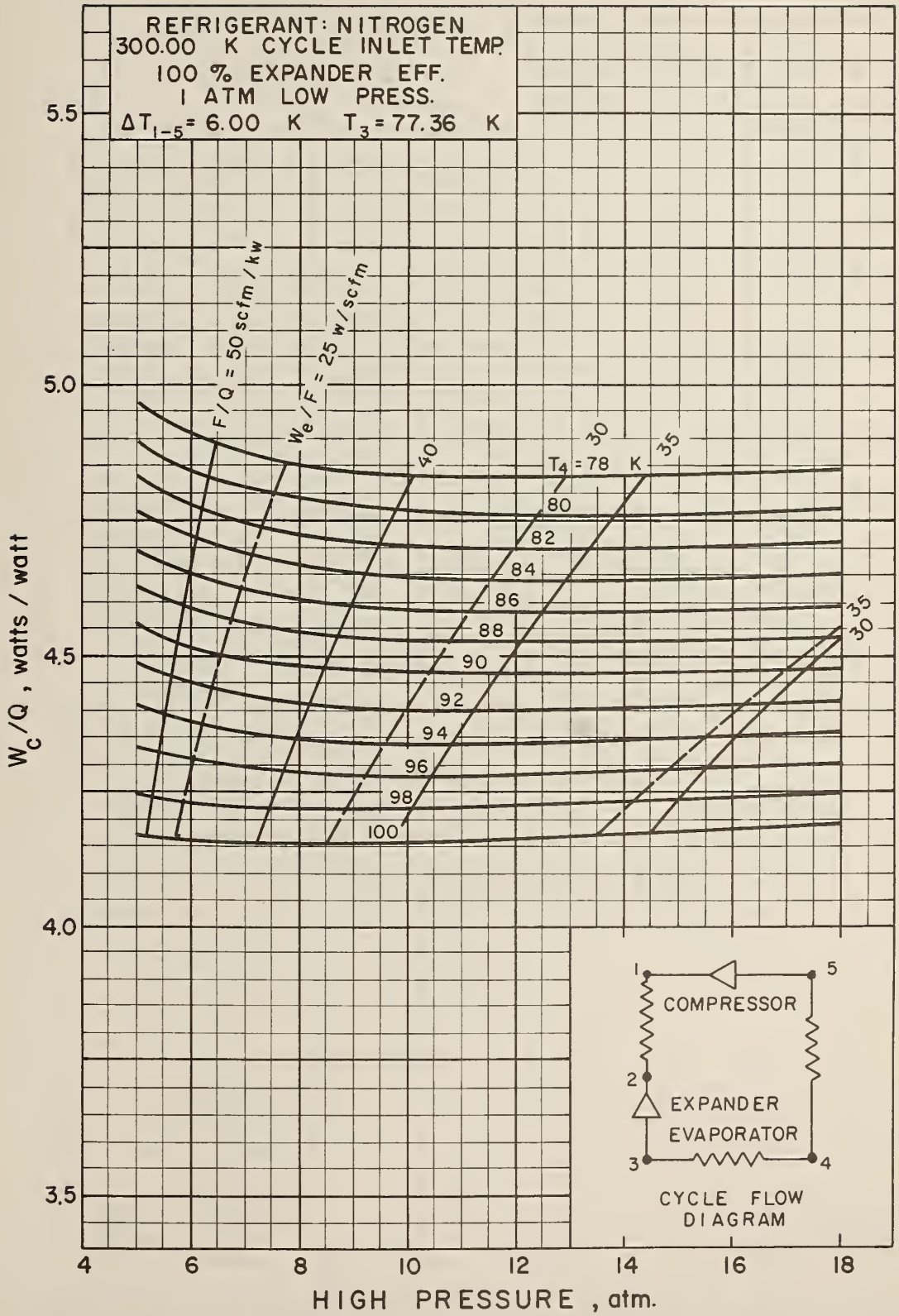

Figure 36. Brayton Refrigerator Performance - Nitrogen Refrigerant - 300 K Cycle Inlet Temperature - 100% Expander Efficiency - 6 K Heat Exchanger Temperature Difference - No Pressure Drop.

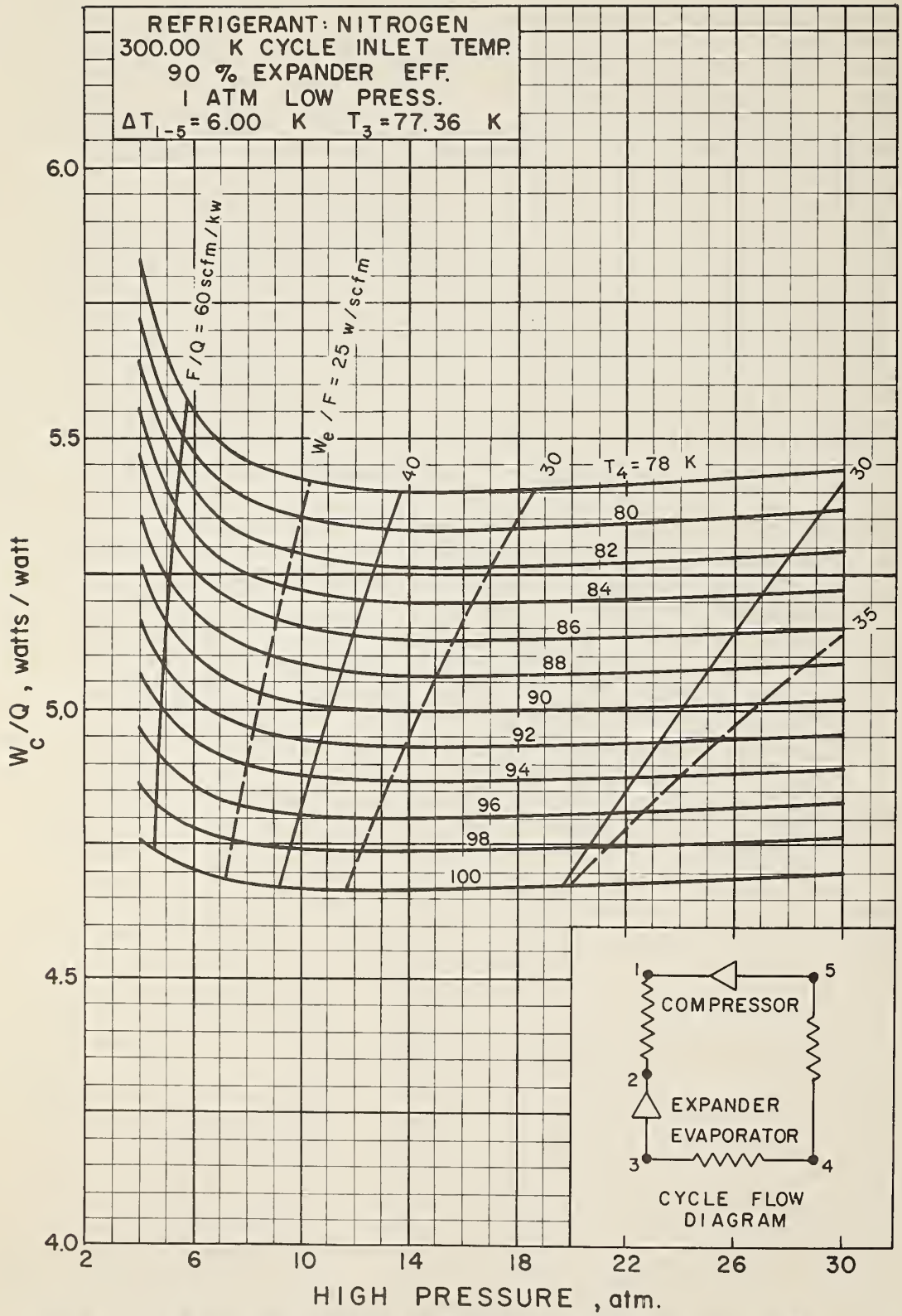

Figure 37. Brayton Refrigerator Performance - Nitrogen Refrigerant - 300 K Cycle Inlet Temperature - 90% Expander Efficiency - 6 K Heat Exchanger Temperature Difference - No Pressure Drop.

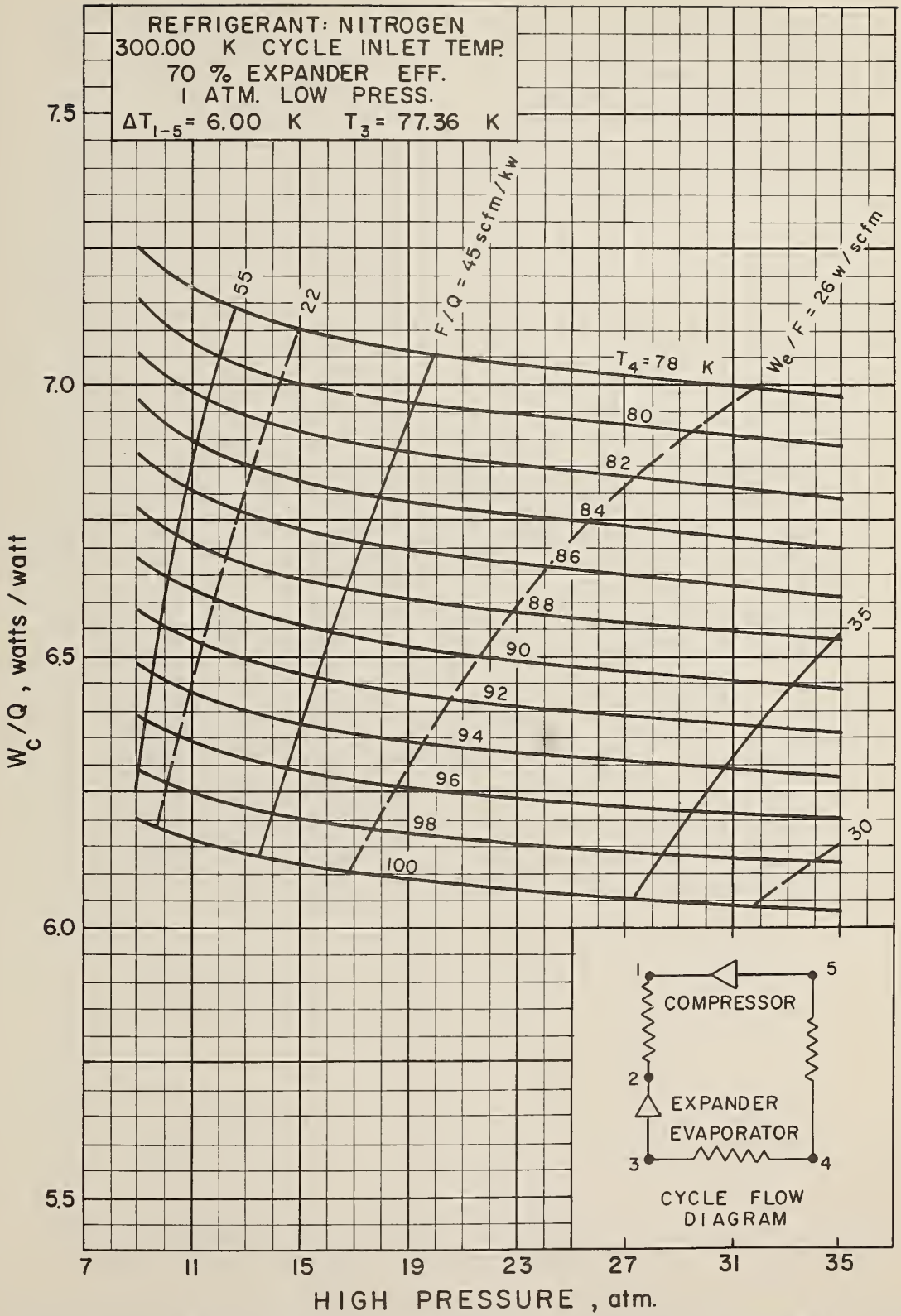

Figure 38. Brayton Refrigerator Performance - Nitrogen Refrigerant - 300 K Cycle Inlet Temperature - 70% Expander Efficiency - 6 K Heat Exchanger Temperature Difference - No Pressure Drop.

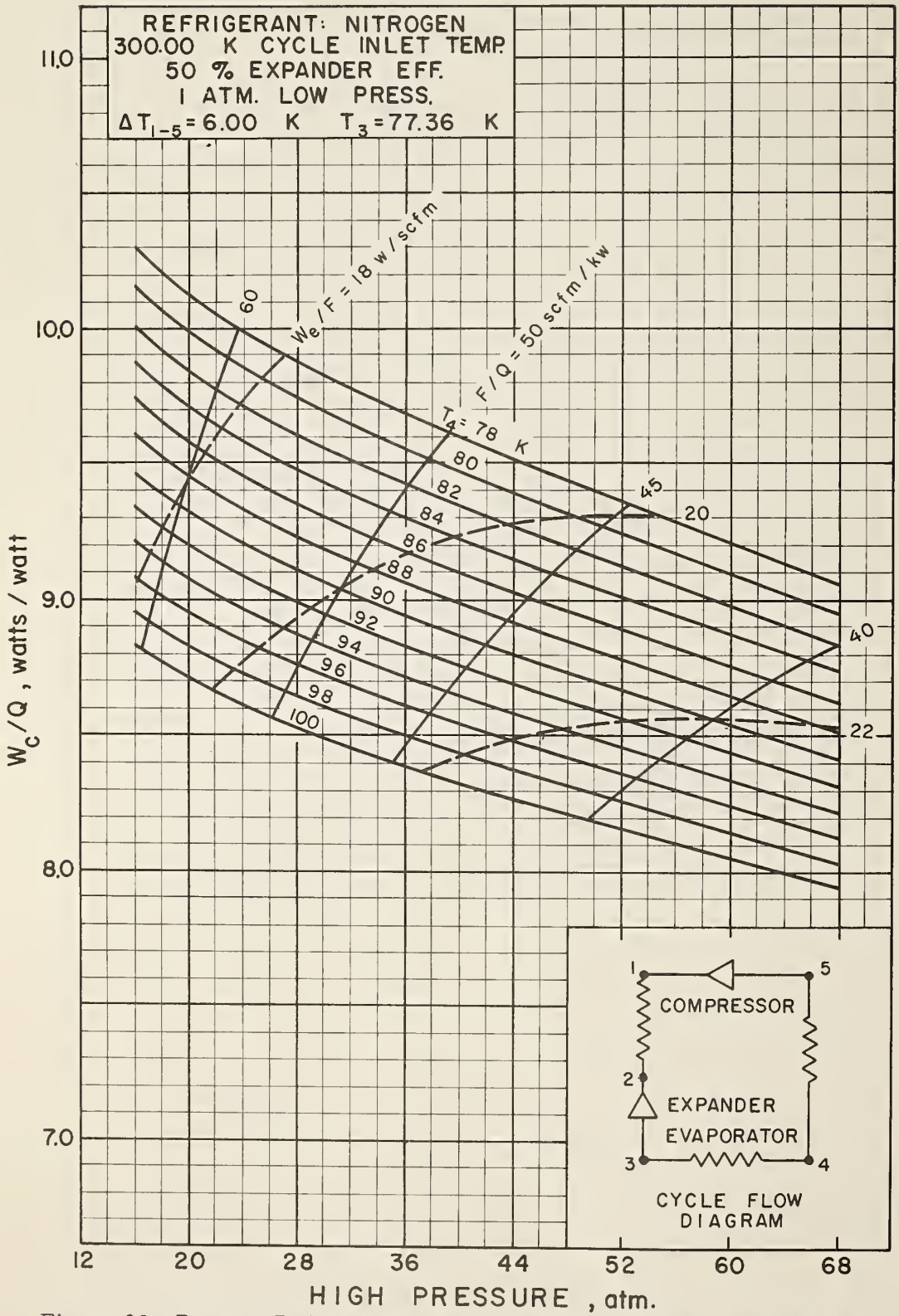

Figure 39. Brayton Refrigerator Performance - Nitrogen Refrigerant - 300 K Cycle Inlet Temperature - 50% Expander Efficiency - 6 K Heat Exchanger Temperature Difference - No Pressure Drop.

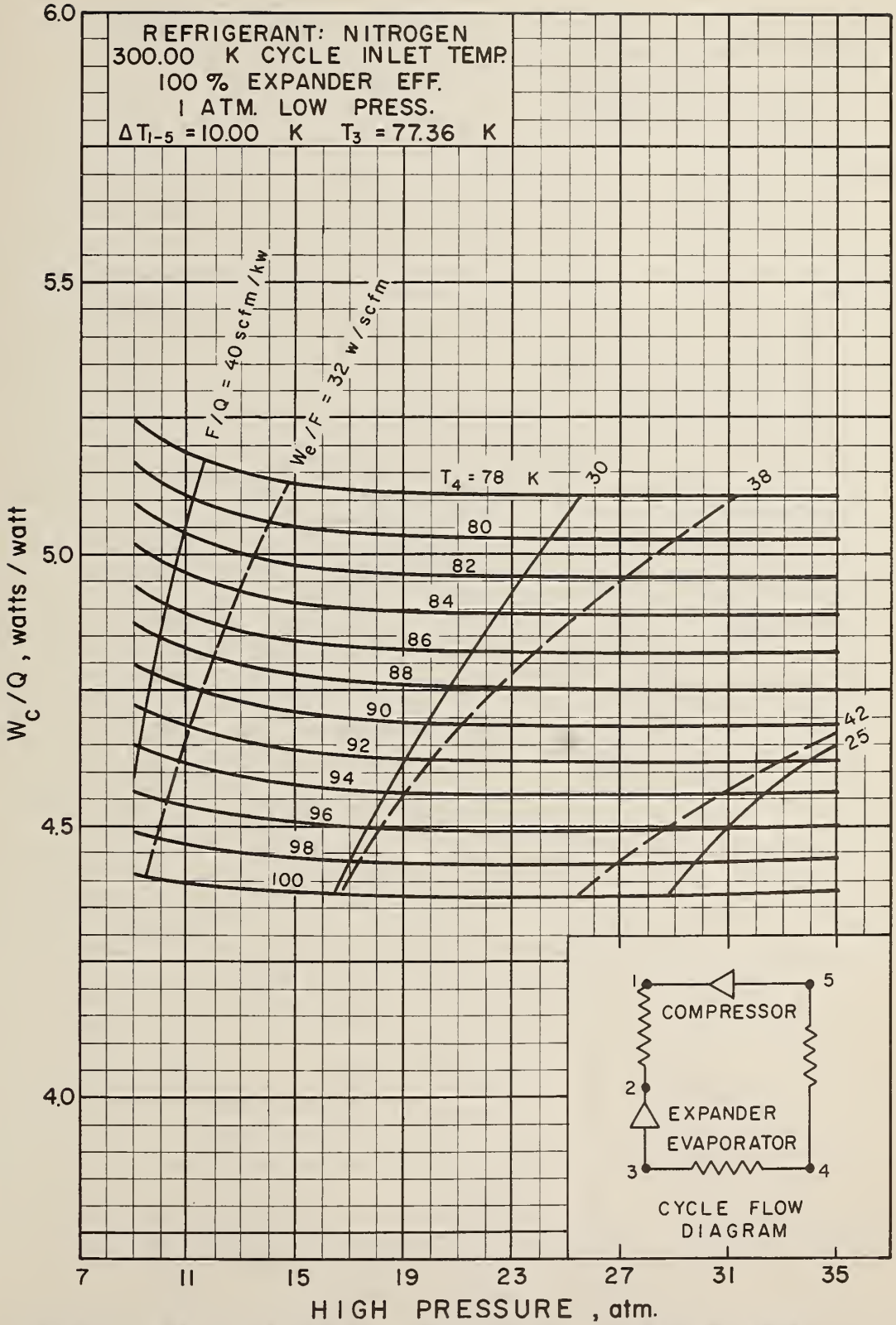

Figure 40. Brayton Refrigerator Performance - Nitrogen Refrigerant - 300 K Cycle Inlet Temperature - 100% Expander Efficiency - 10 K Heat Exchanger Temperature Difference - No Pressure Drop.

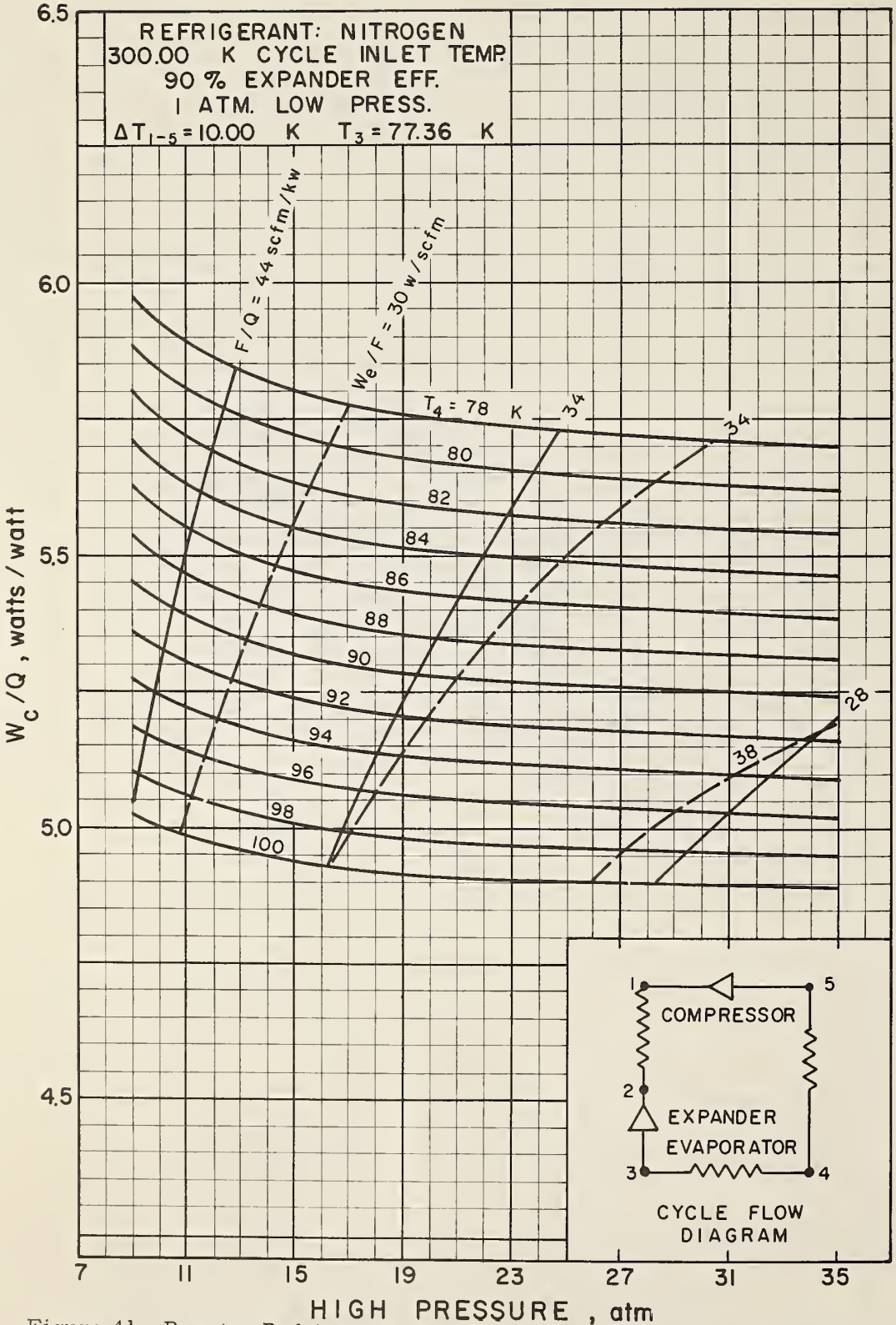

Figure 41. Brayton Refrigerator Performance - Nitrogen Refrigerant - 300 K Cycle Inlet Temperature - 90% Expander Efficiency - 10 K Heat Exchanger Temperature Difference - No Pressure Drop.

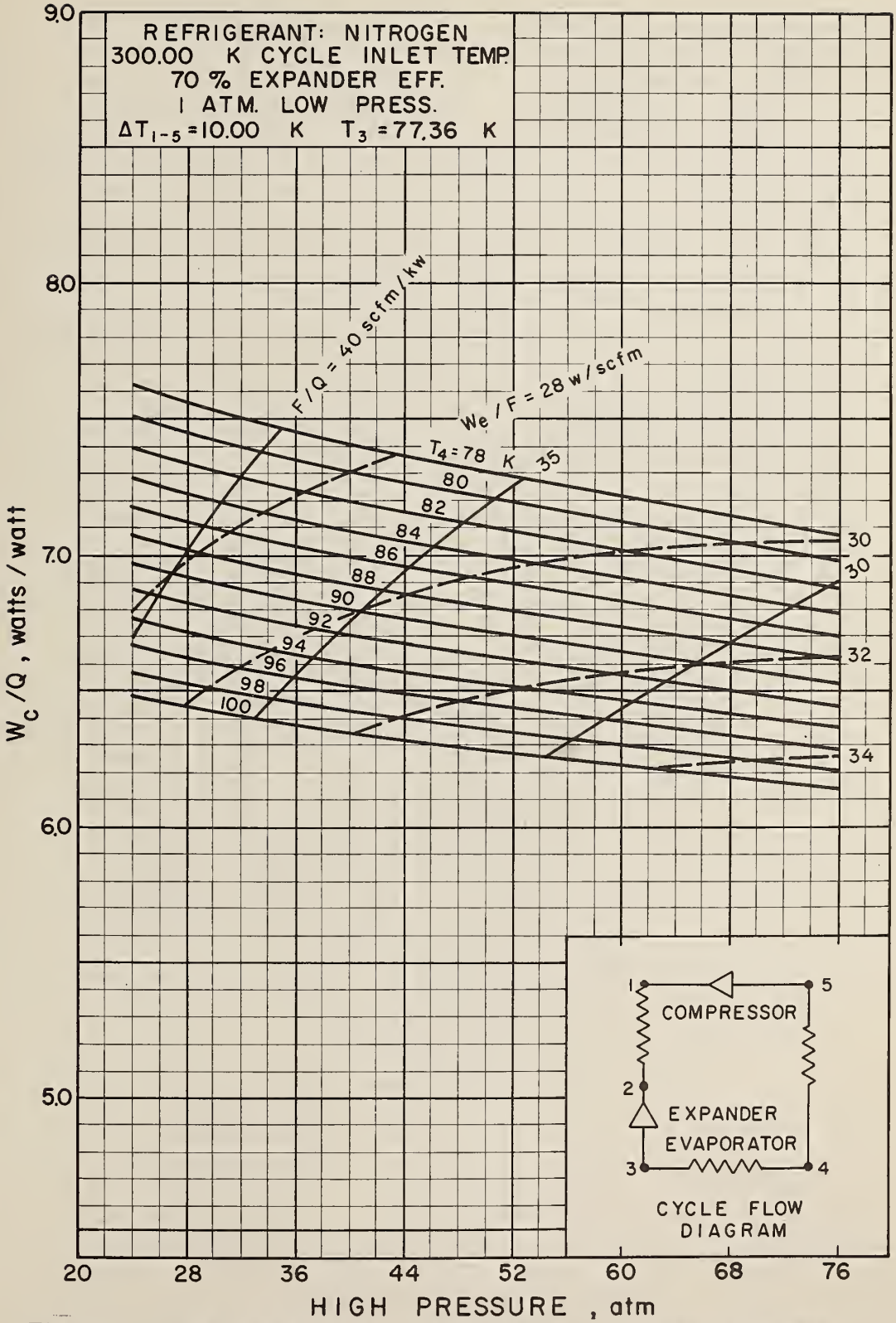

Figure 42. Brayton Refrigerator Performance - Nitrogen Refrigerant - 300 K Cycle Inlet Temperature - 70% Expander Efficiency - 10 K Heat Exchanger Temperature Difference - No Pressure Drop.

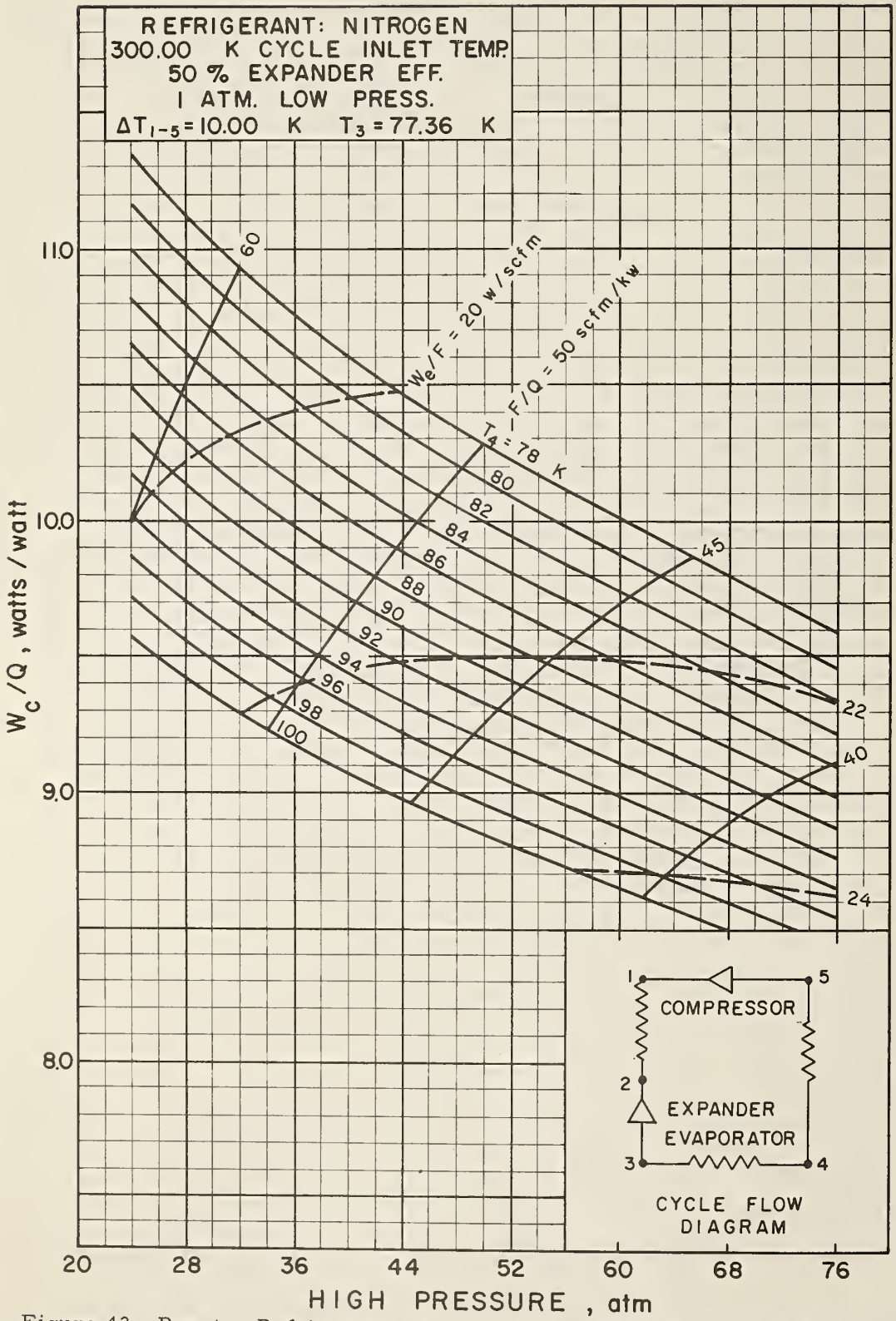

Figure 43. Brayton Refrigerator Performance - Nitrogen Refrigerant - 300 K Cycle Inlet Temperature - 50% Expander Efficiency - 10 K Heat Exchanger Temperature Difference - No Pressure Drop.

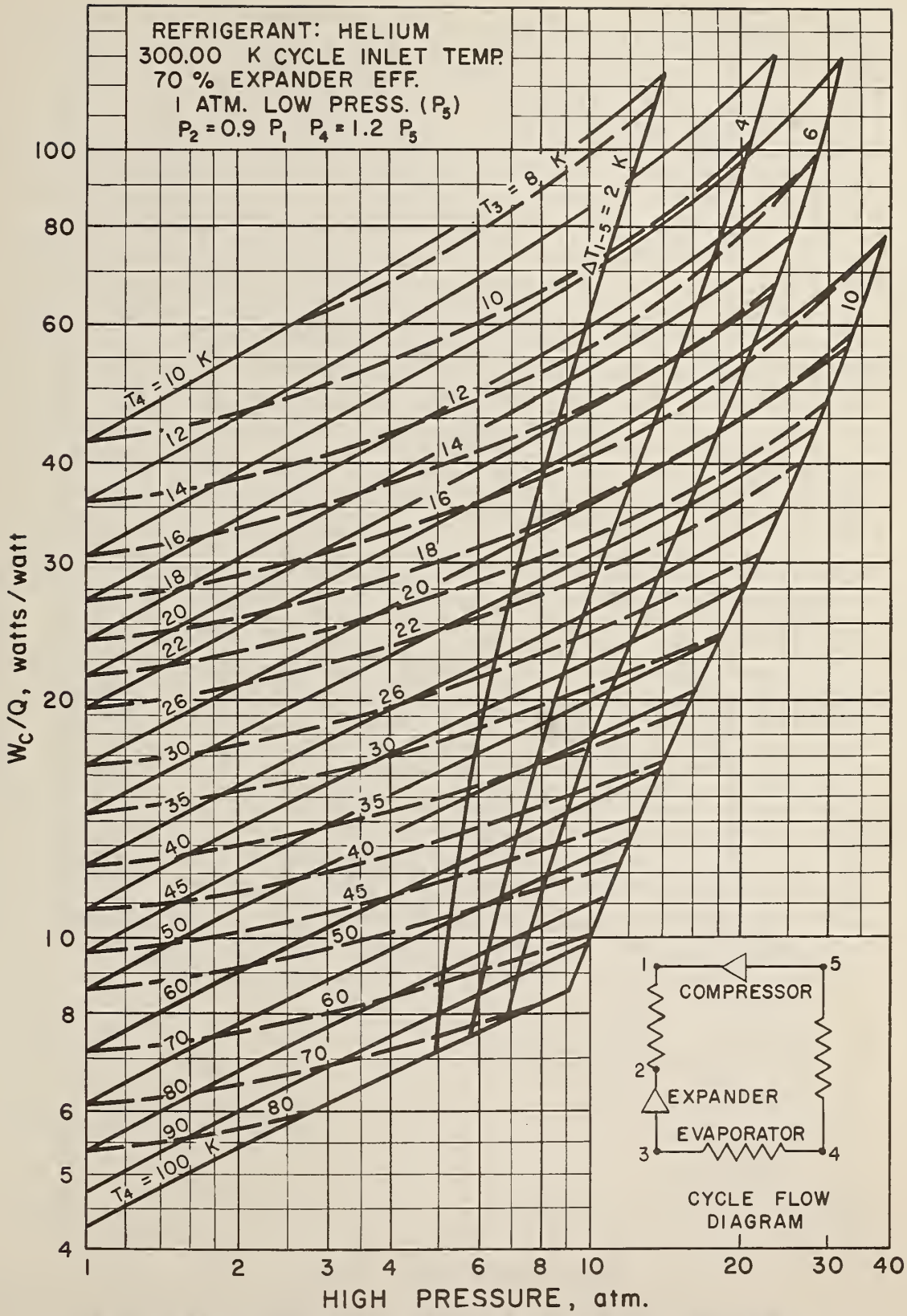

Figure 44. Brayton Refrigerator Performance - Helium Refrigerant - 300 K Cycle Inlet Temperature - 70% Expander Efficiency - Pressure Drop.

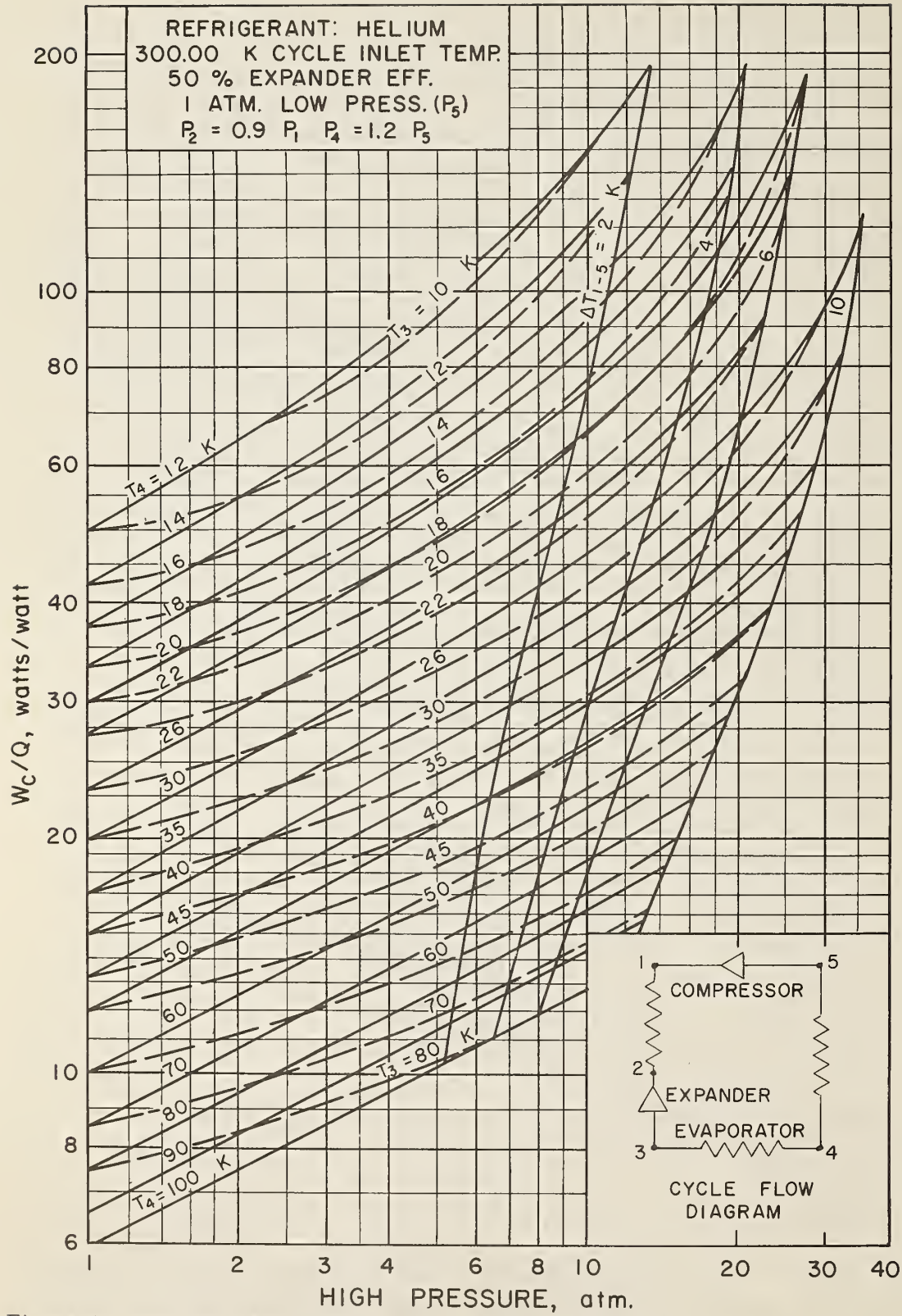

Figure 45. Brayton Refrigerator Performance - Helium Refrigerant - 300 K Cycle Inlet Temperature - 50% Expander Efficiency - Pressure Drop.

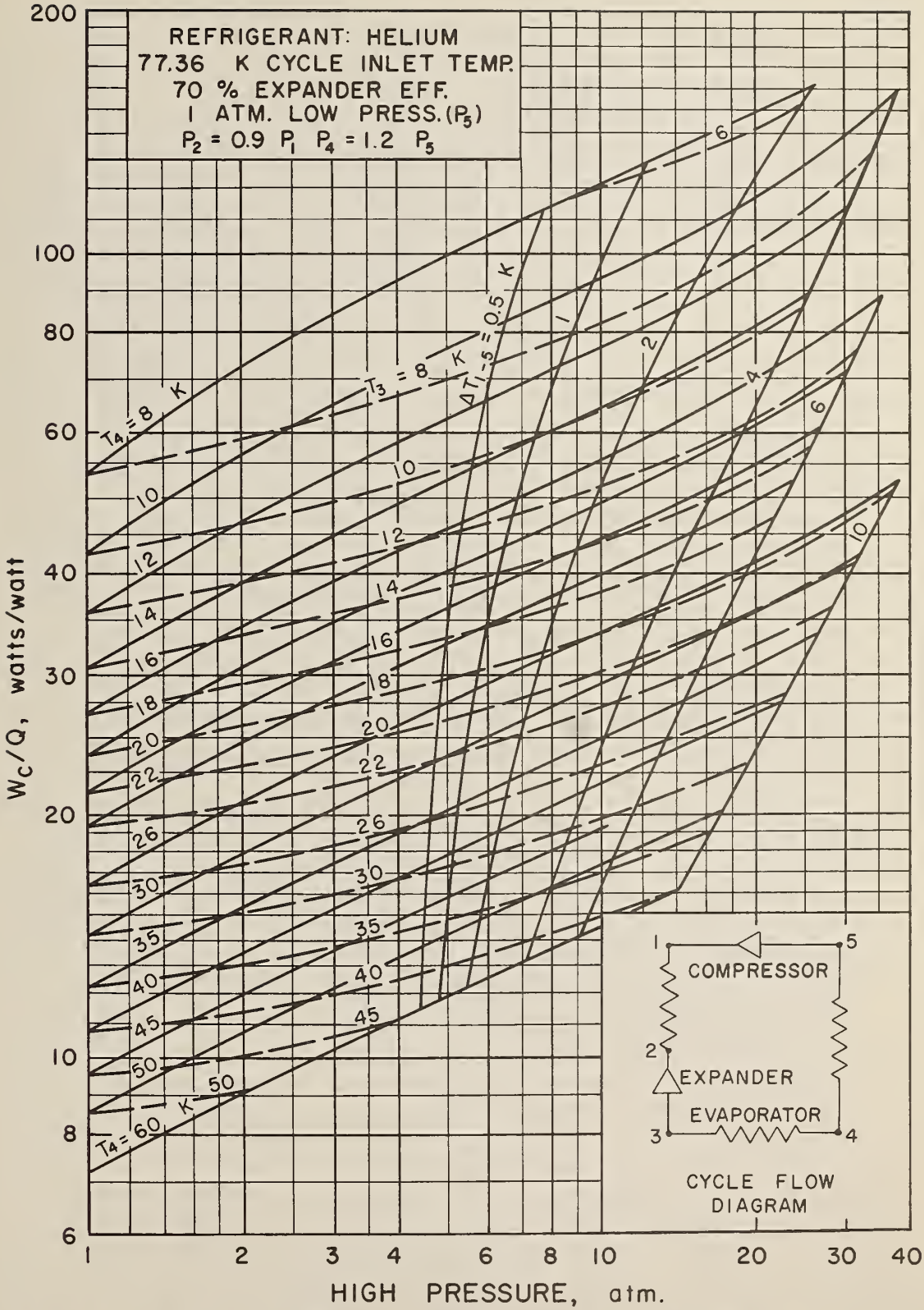

Figure 46. Brayton Refrigerator Performance - Helium Refrigerant - 77.36 K Cycle Inlet Temperature - 70% Expander Efficiency - Pressure Drop.

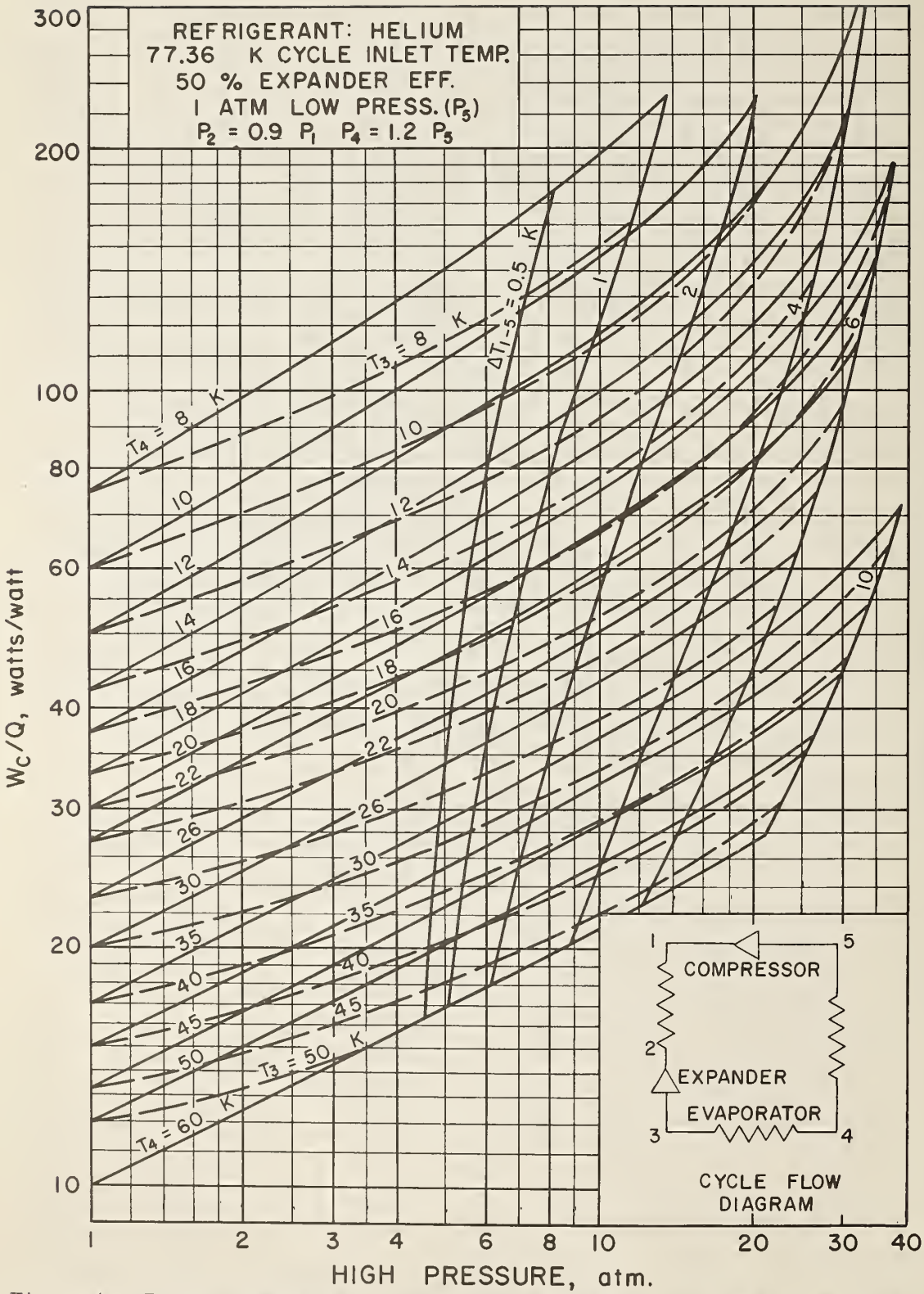

Figure 47. Brayton Refrigerator Performance - Helium Refrigerant - 77.36 K Cycle Inlet Temperature - 50% Expander Efficiency - Pressure Drop.

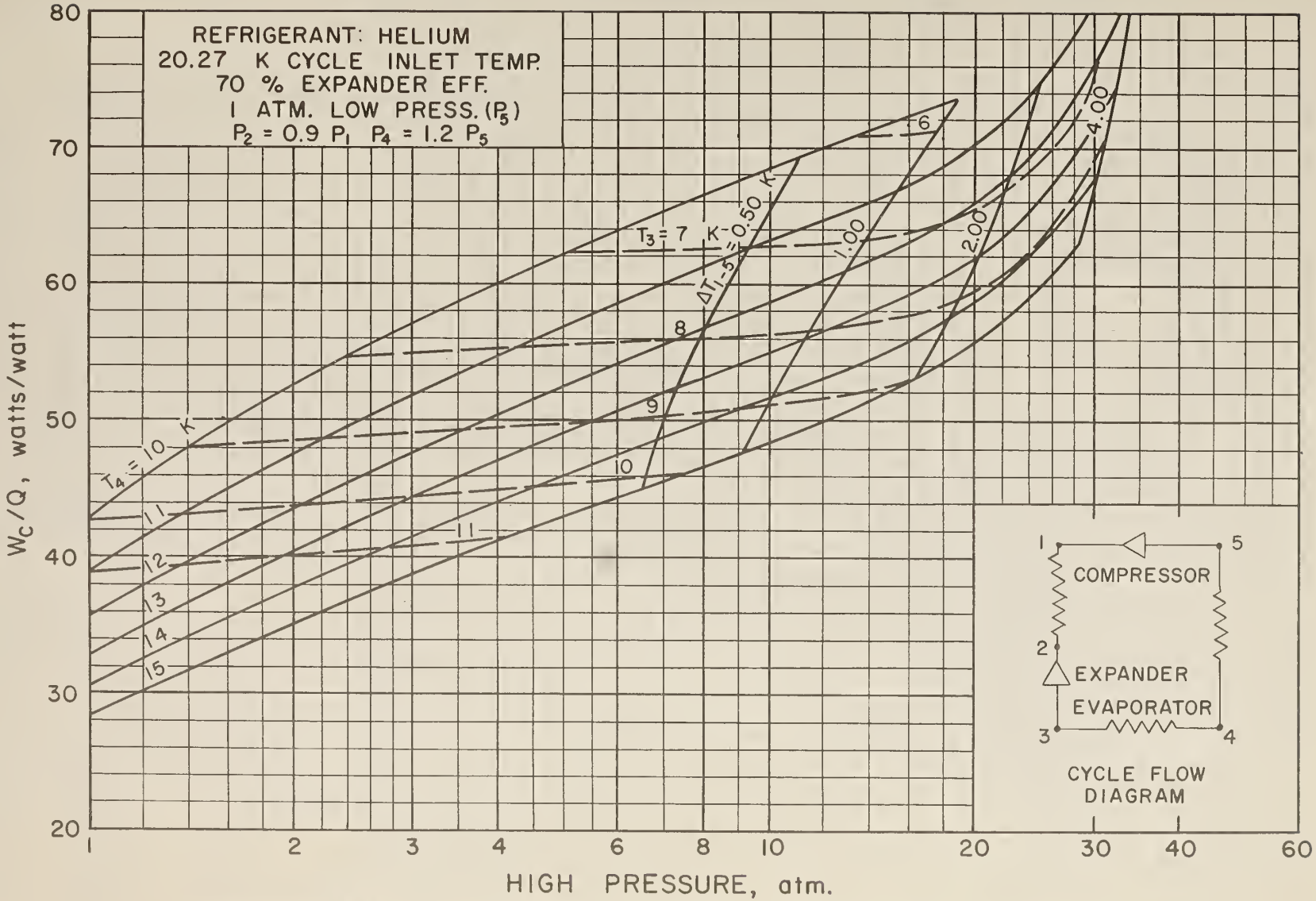

Figure 48. Brayton Refrigerator Performance - Helium Refrigerant - 20.27 K Cycle Inlet Temperature - 70% Expander Efficiency - Pressure Drop.

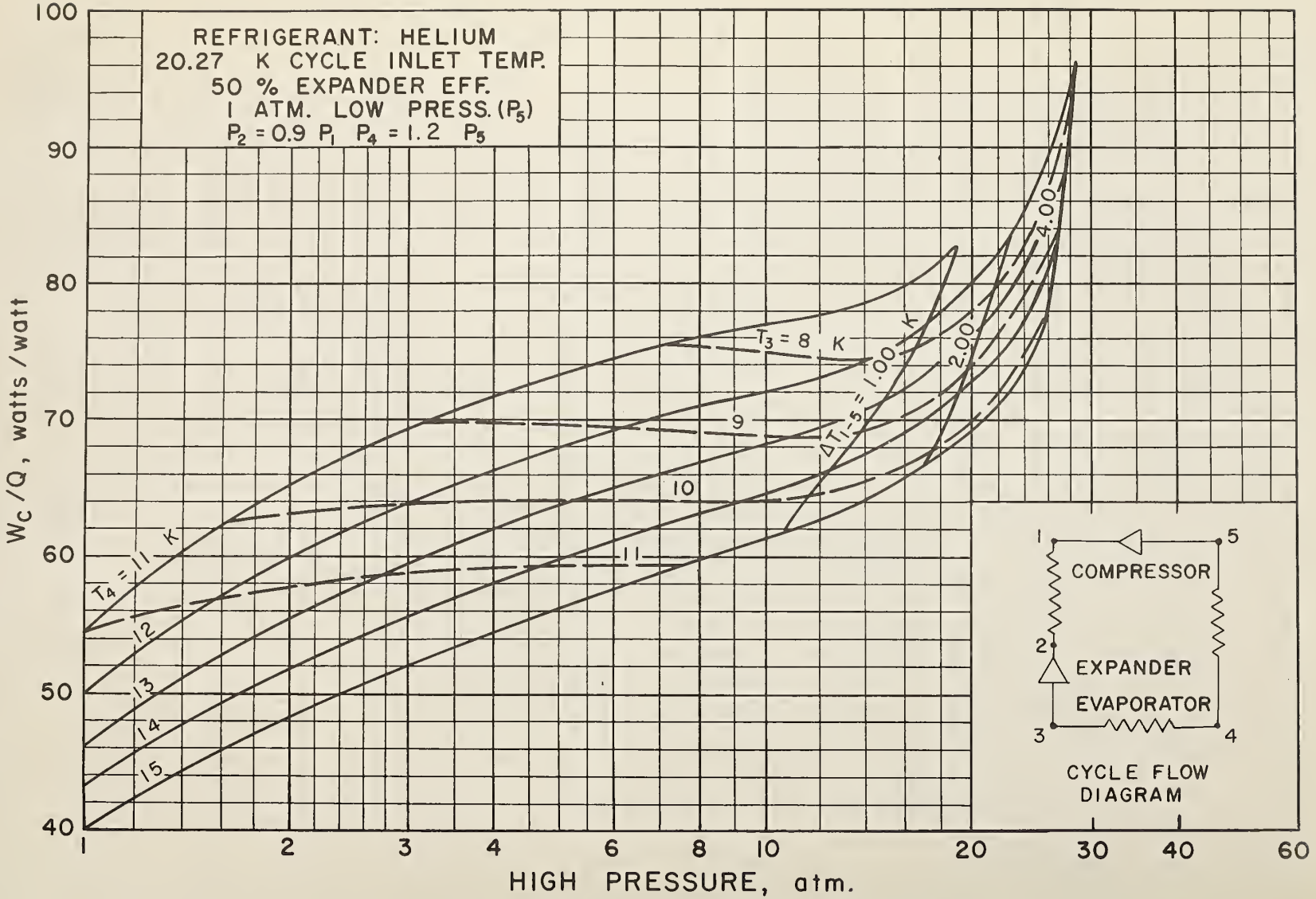

Figure 49. Brayton Refrigerator Performance - Helium Refrigerant - 20.27 K Cycle Inlet Temperature - 50% Expander Efficiency - Pressure Drop.

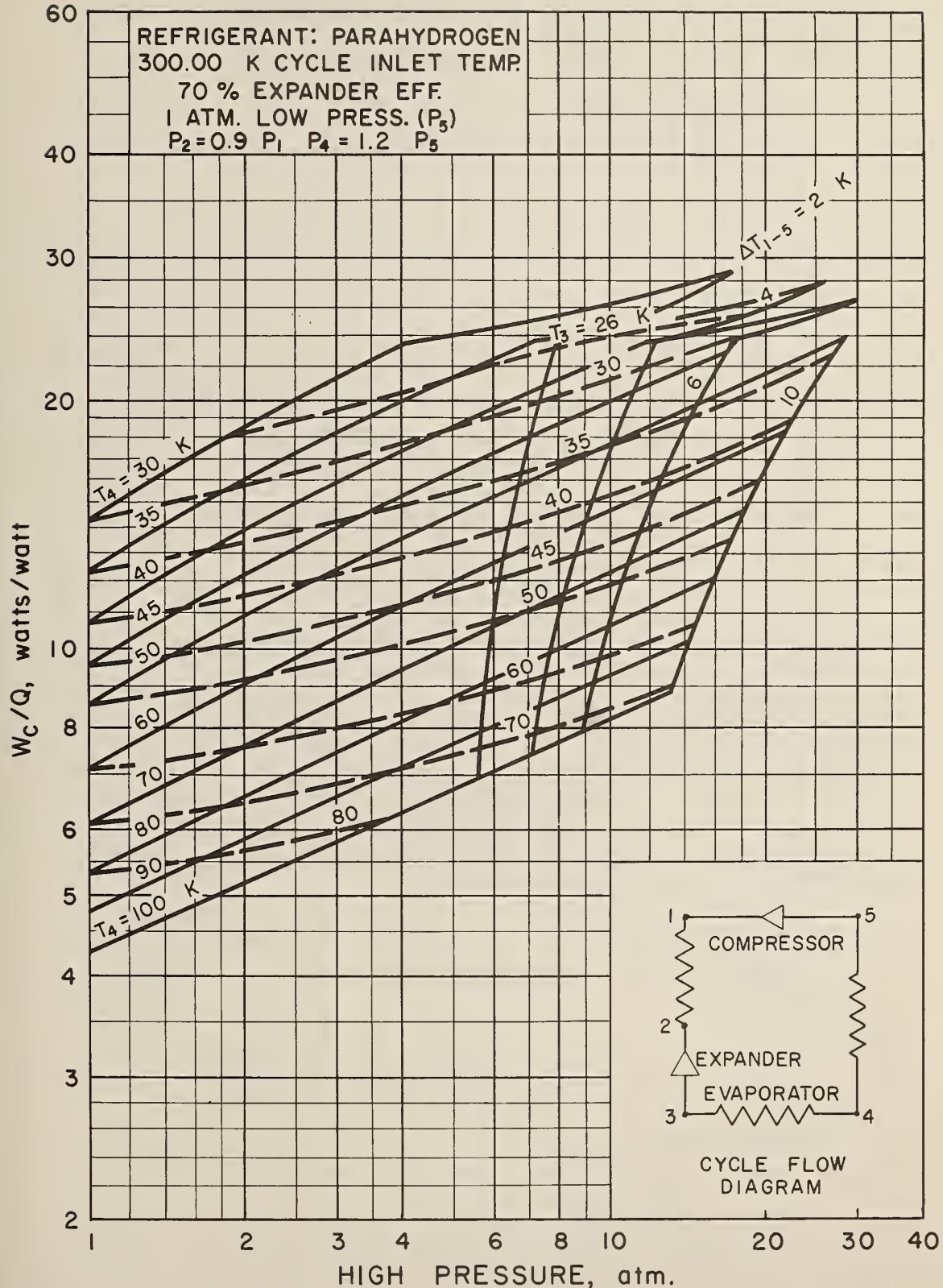

Figure 50. Brayton Refrigerator Performance - Parahydrogen Refrigerant - 300 K Cycle Inlet Temperature - 70% Expander Efficiency - Pressure Drop.

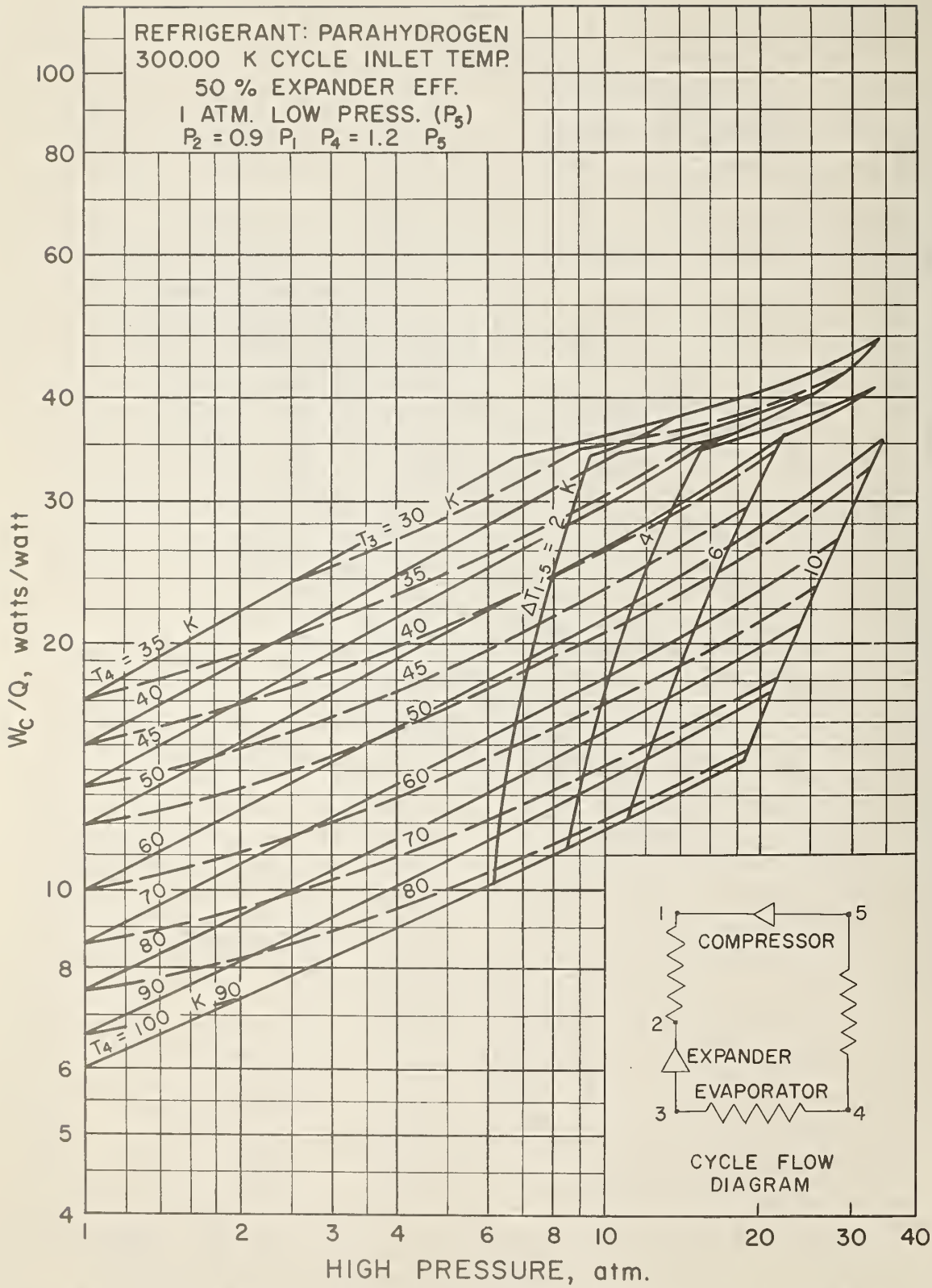

Figure 51. Brayton Refrigerator Performance - Parahydrogen Refrigerant - 300 K Cycle Inlet Temperature - 50% Expander Efficiency - Pressure Drop.

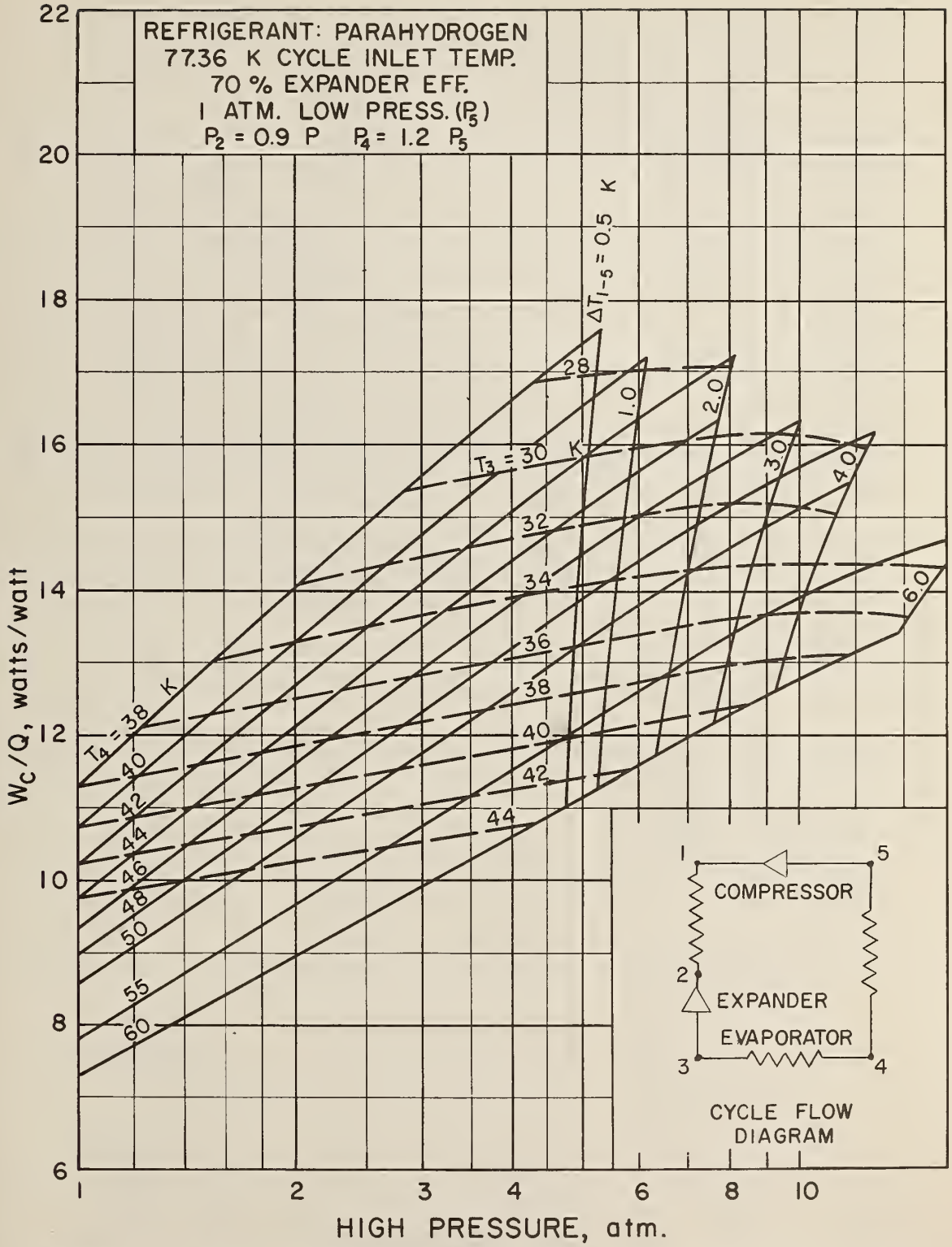

Figure 52. Brayton Refrigerator Performance - Parahydrogen Refrigerant - 77.36 K Cycle Inlet Temperature - 70% Expander Efficiency - Pressure Drop.

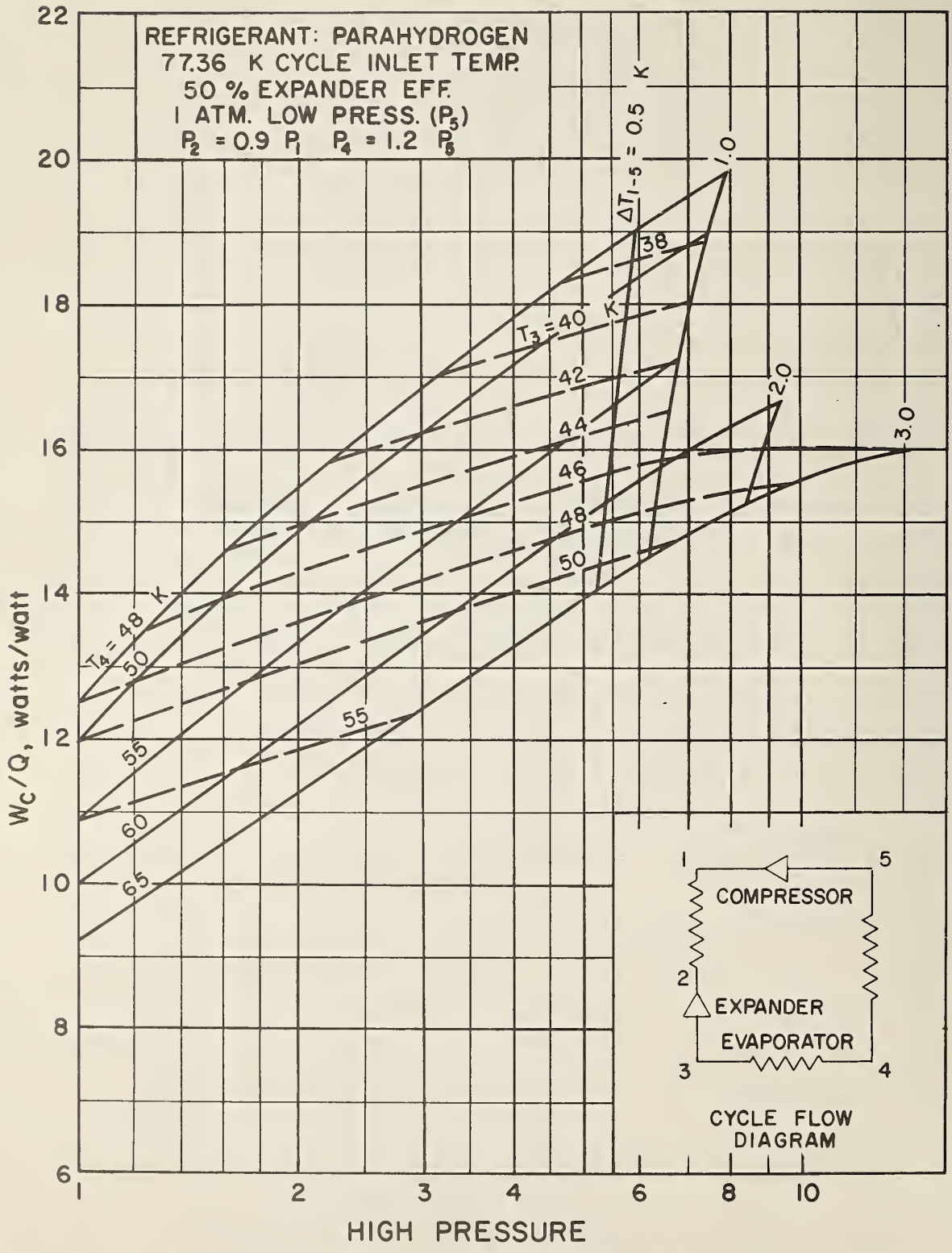

Figure 53. Brayton Refrigerator Performance - Parahydrogen Refrigerant - 77.36 K Cycle Inlet Temperature - 50% Expander Efficiency - Pressure Drop.

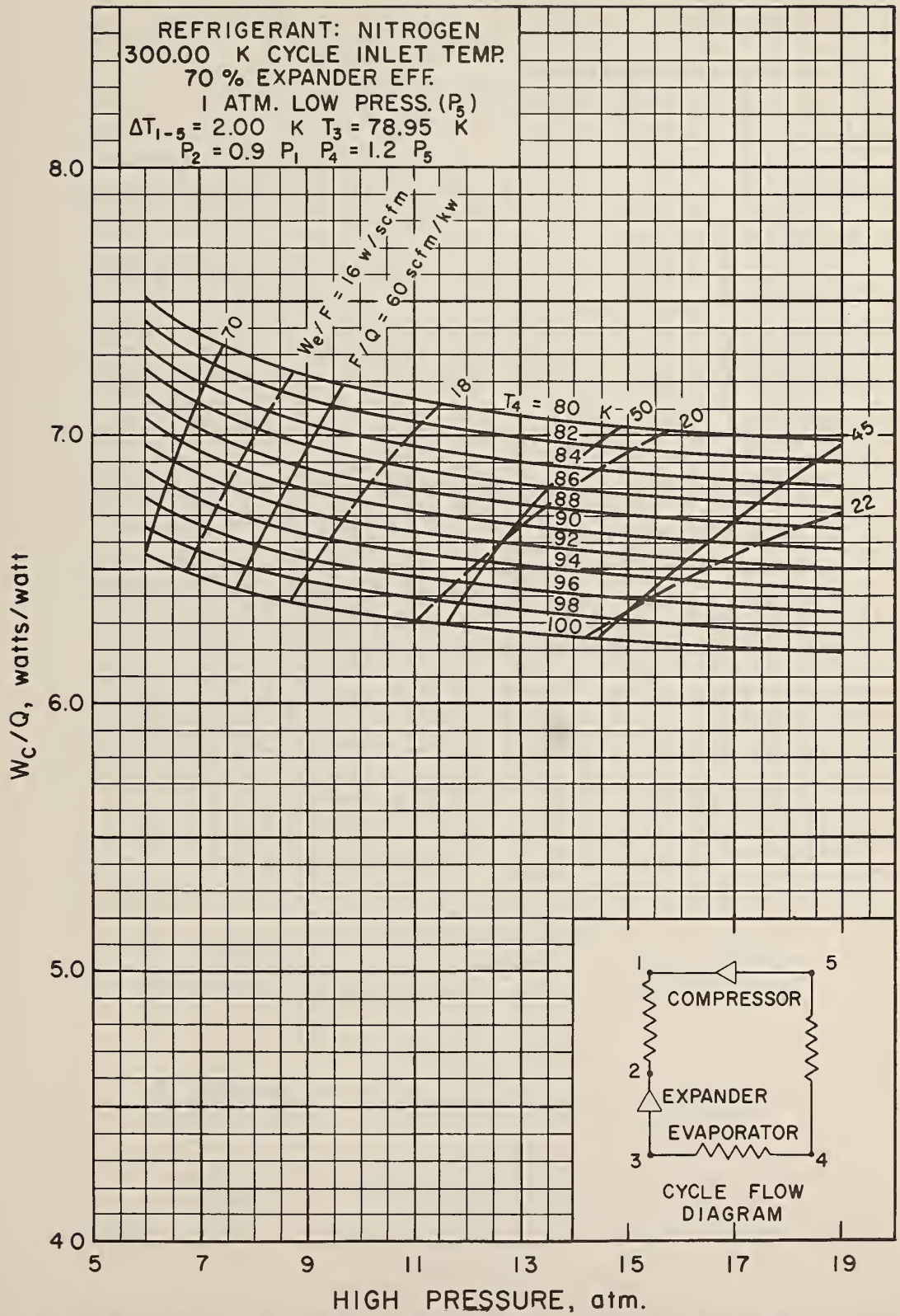

Figure 54. Brayton Refrigerator Performance - Nitrogen Refrigerant - 300 K Cycle Inlet Temperature - 70% Expander Efficiency - 2.0 K Heat Exchanger Temperature Difference - Pressure Drop.

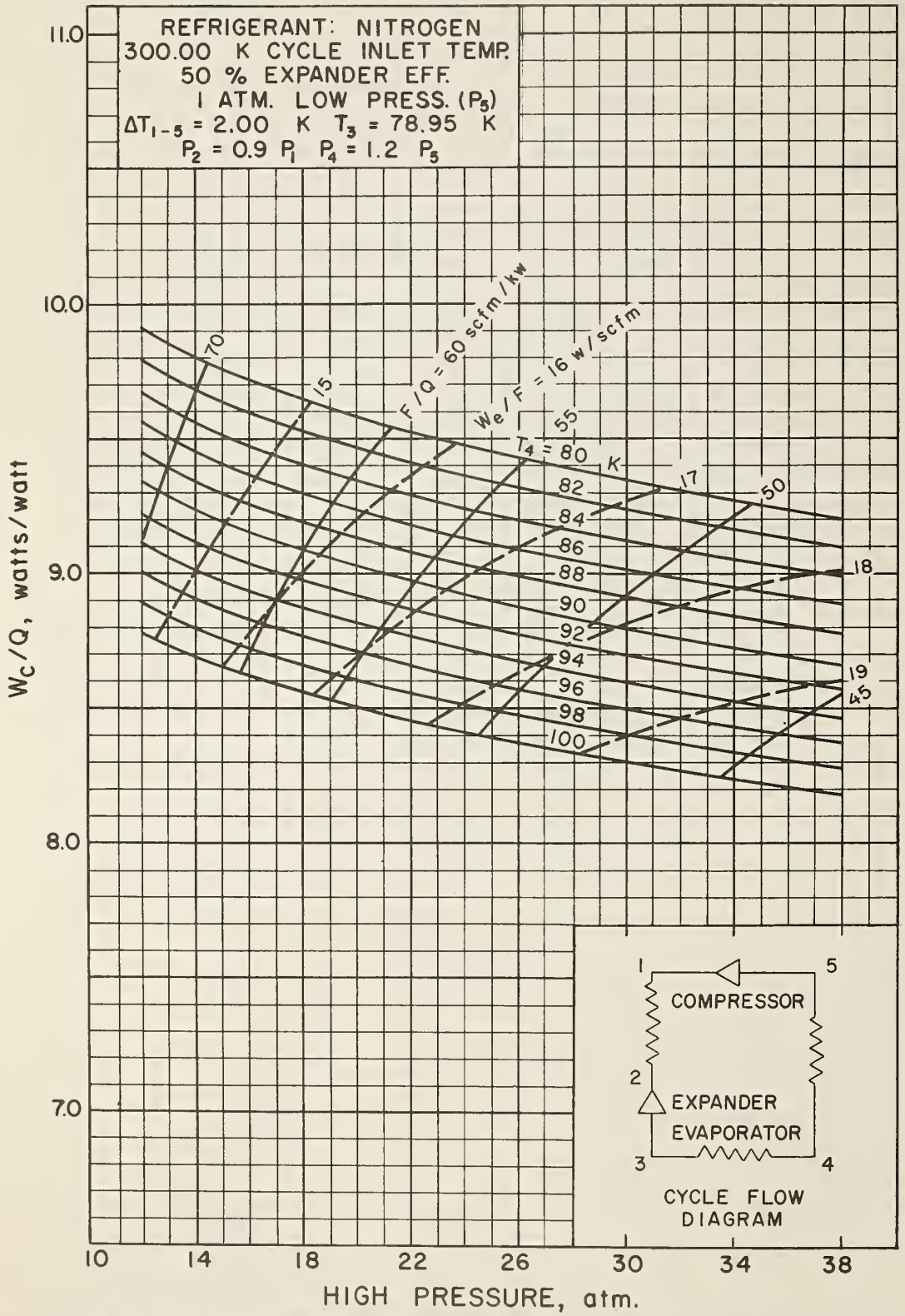

Figure 55. Brayton Refrigerator Performance - Nitrogen Refrigerant - 300 K Cycle Inlet Temperature - 50% Expander Efficiency - 2.0 K Heat Exchanger Temperature Difference - Pressure Drop.

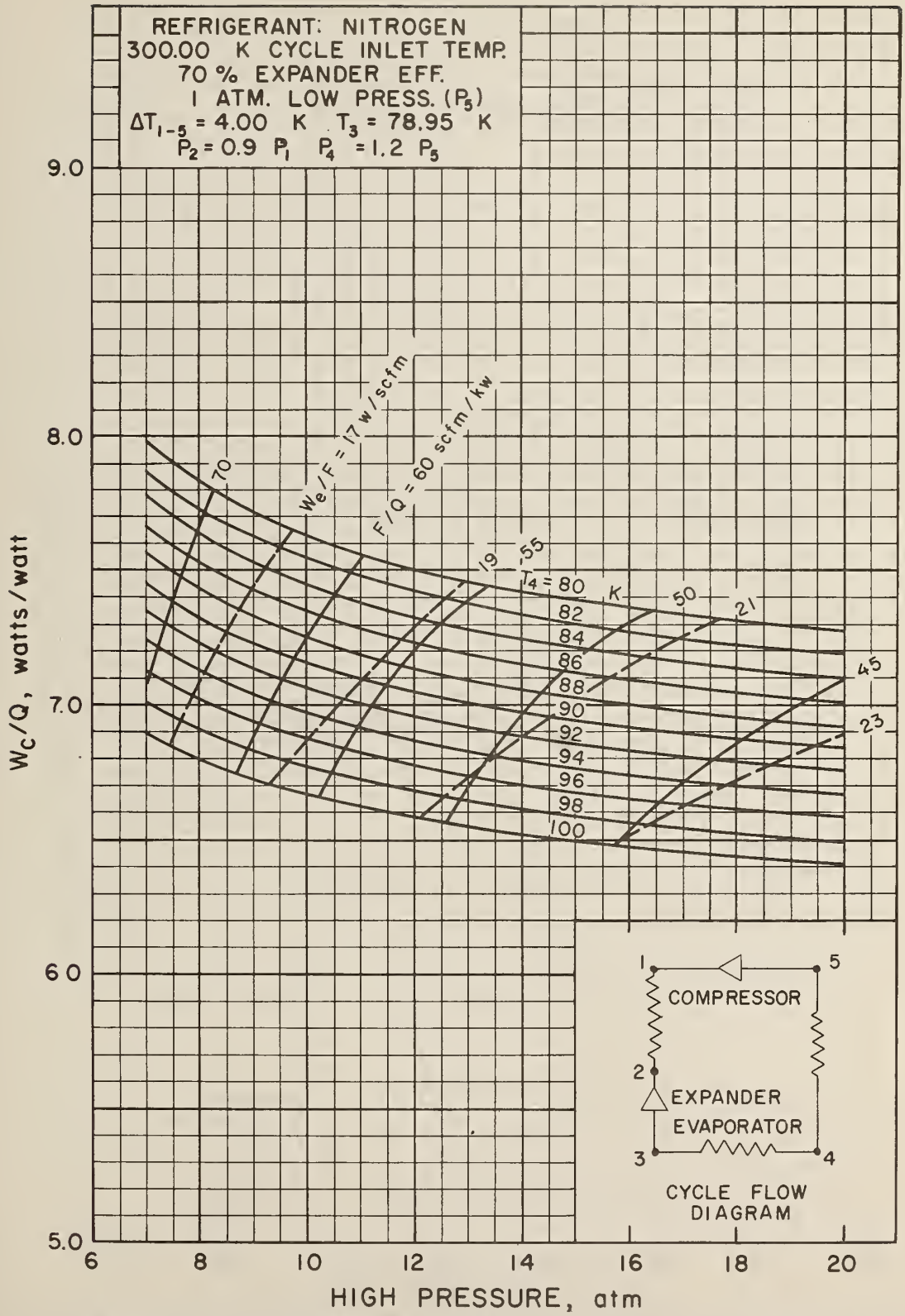

Figure 56. Brayton Refrigerator Performance - Nitrogen Refrigerant - 300 K Cycle Inlet Temperature - 70% Expander Efficiency - 4.0 K Heat Exchanger Temperature Difference - Pressure Drop.

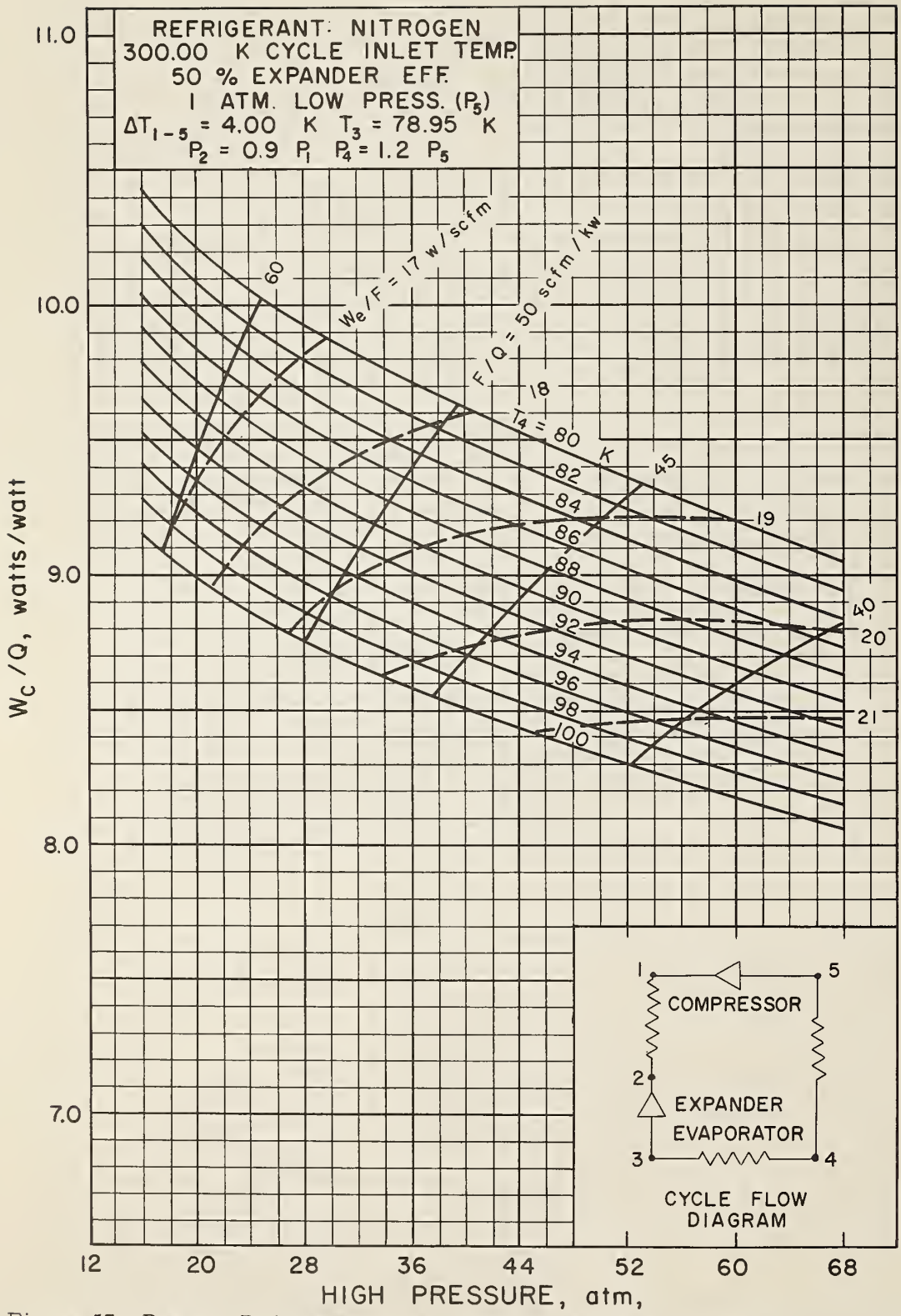

Figure 57. Brayton Refrigerator Performance - Nitrogen Refrigerant - 300 K Cycle Inlet Temperature - 50% Expander Efficiency - 4. 0 K Heat Exchanger Temperature Difference - Pressure Drop.

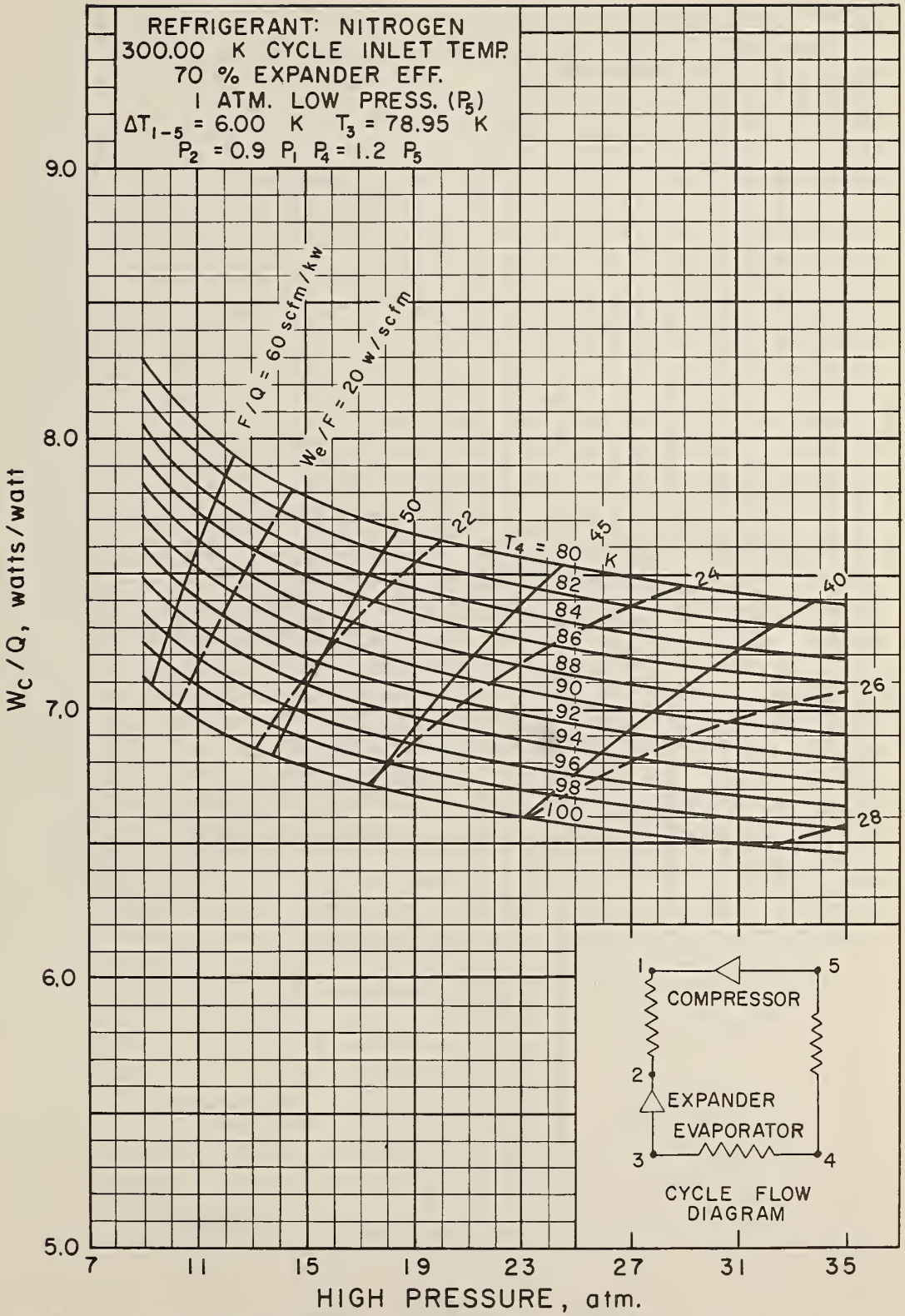

Figure 58. Brayton Refrigerator Performance - Nitrogen Refrigerant - 300 K Cycle Inlet Temperature - 70% Expander Efficiency - 6.0 K Heat Exchanger Temperature Difference - Pressure Drop.

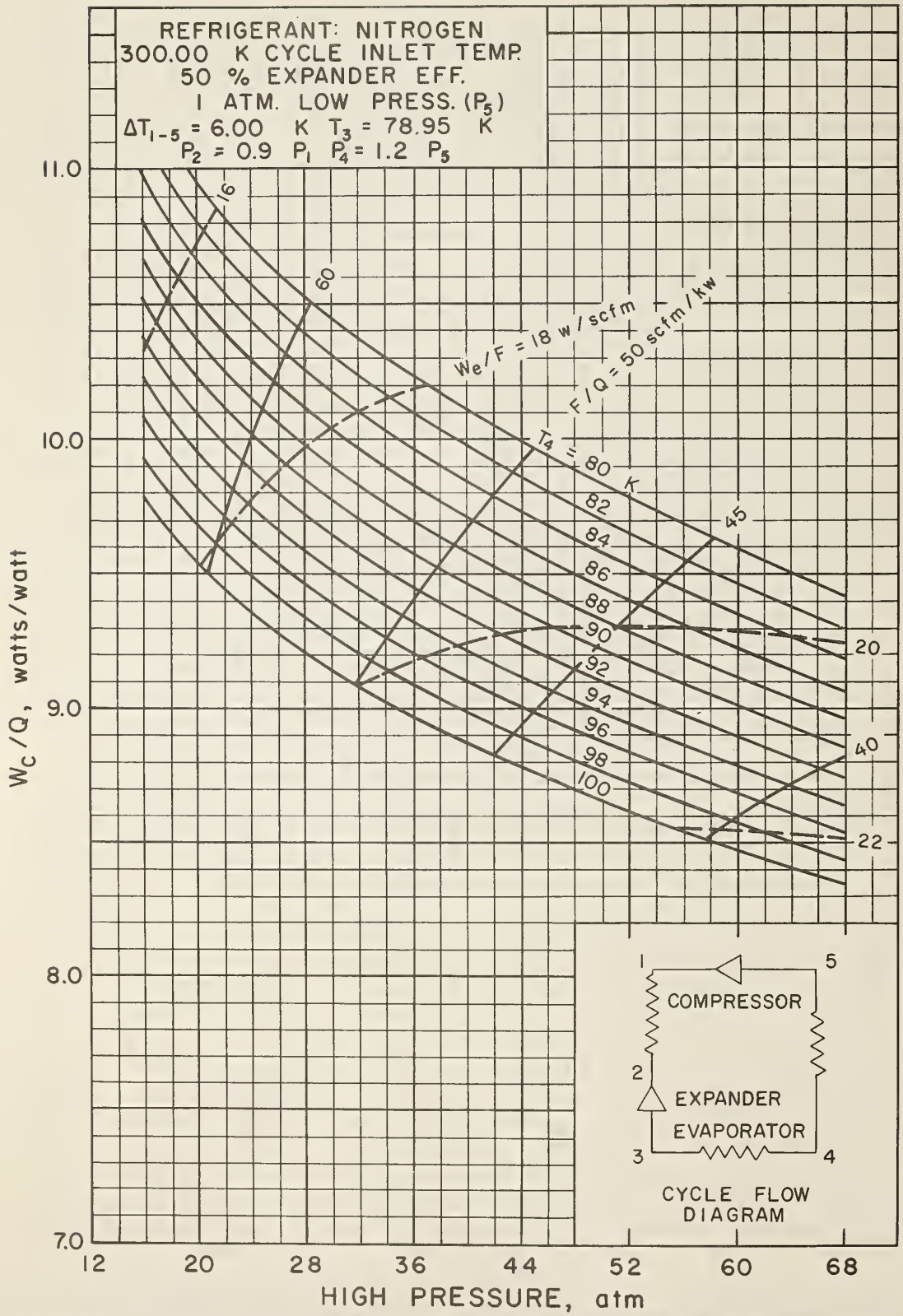

Figure 59. Brayton Refrigerator Performance - Nitrogen Refrigerant - 300 K Cycle Inlet Temperature - 50% Expander Efficiency - 6.0 K Heat Exchanger Temperature Difference - Pressure Drop.

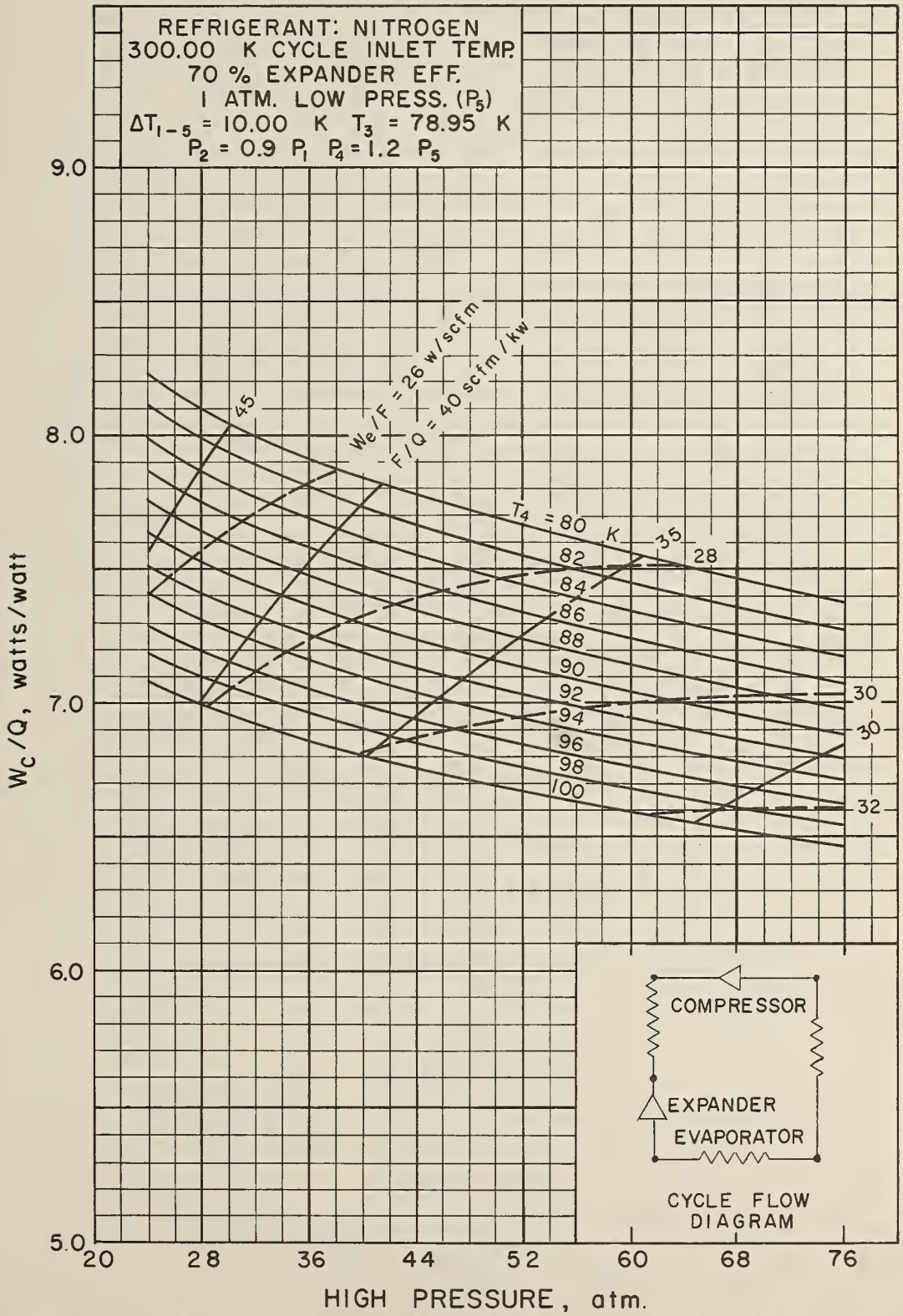

Figure 60. Brayton Refrigerator Performance - Nitrogen Refrigerant - 300 K Cycle Inlet Temperature - 70% Expander Efficiency - 10.0 K Heat Exchanger Temperature Difference - Pressure Drop.

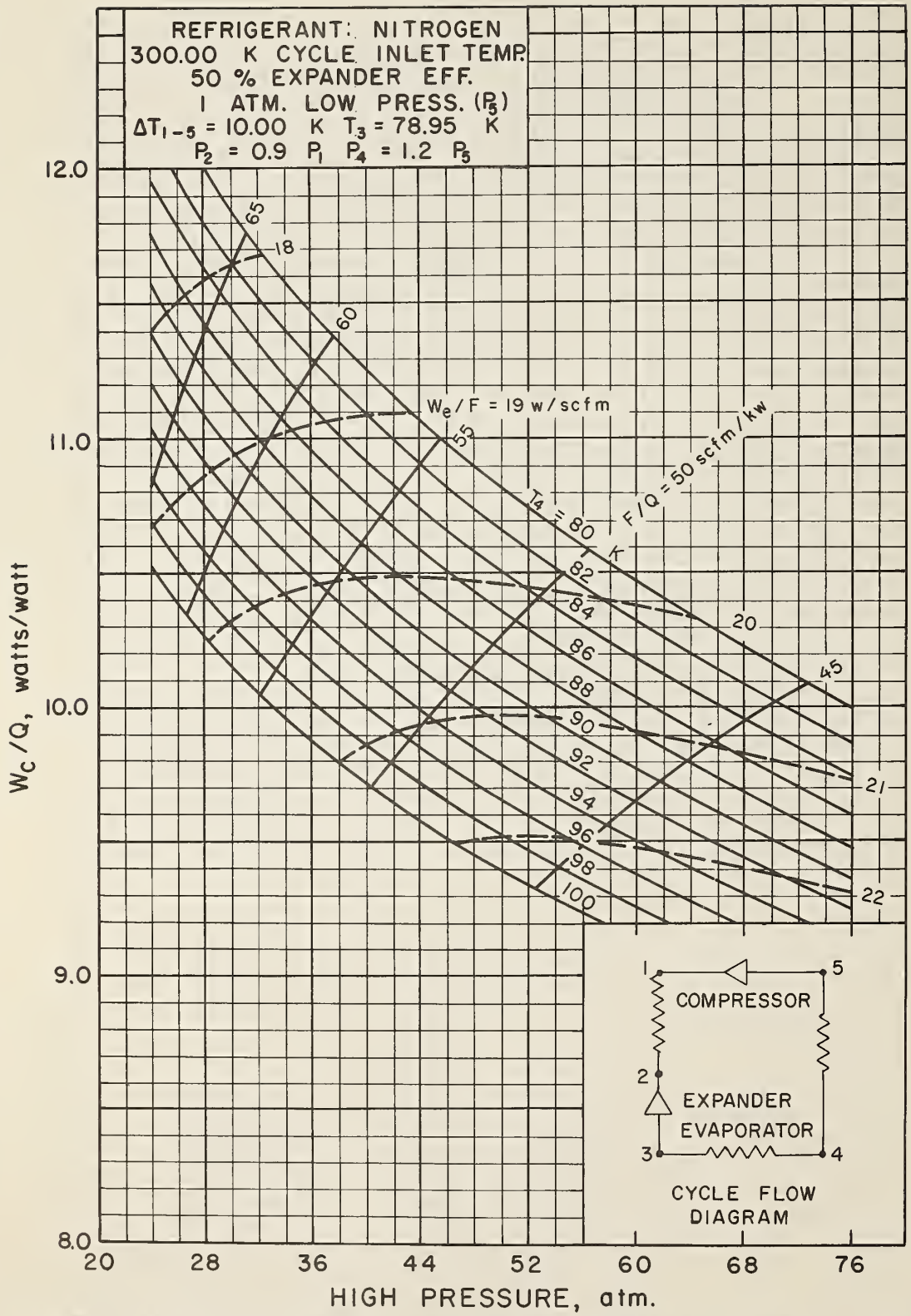

Figure 61. Brayton Refrigerator Performance - Nitrogen Refrigerant - 300 K Cycle Inlet Temperature - 50% Expander Efficiency - 10.0 K Heat Exchanger Temperature Difference - Pressure Drop.

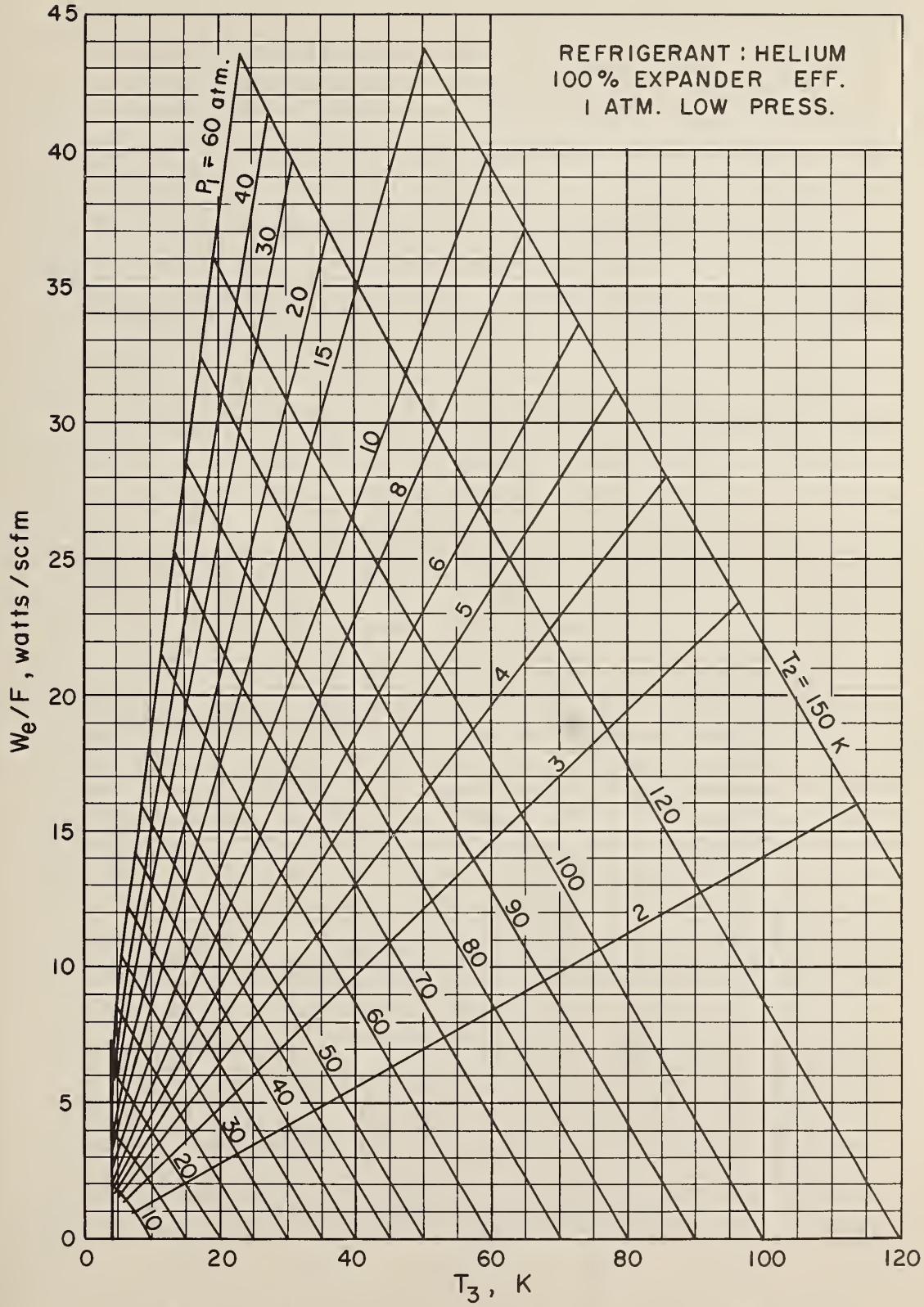

Figure 62. Expander Performance - Helium Refrigerant - 100% Expander Efficiency - No Pressure Drop.

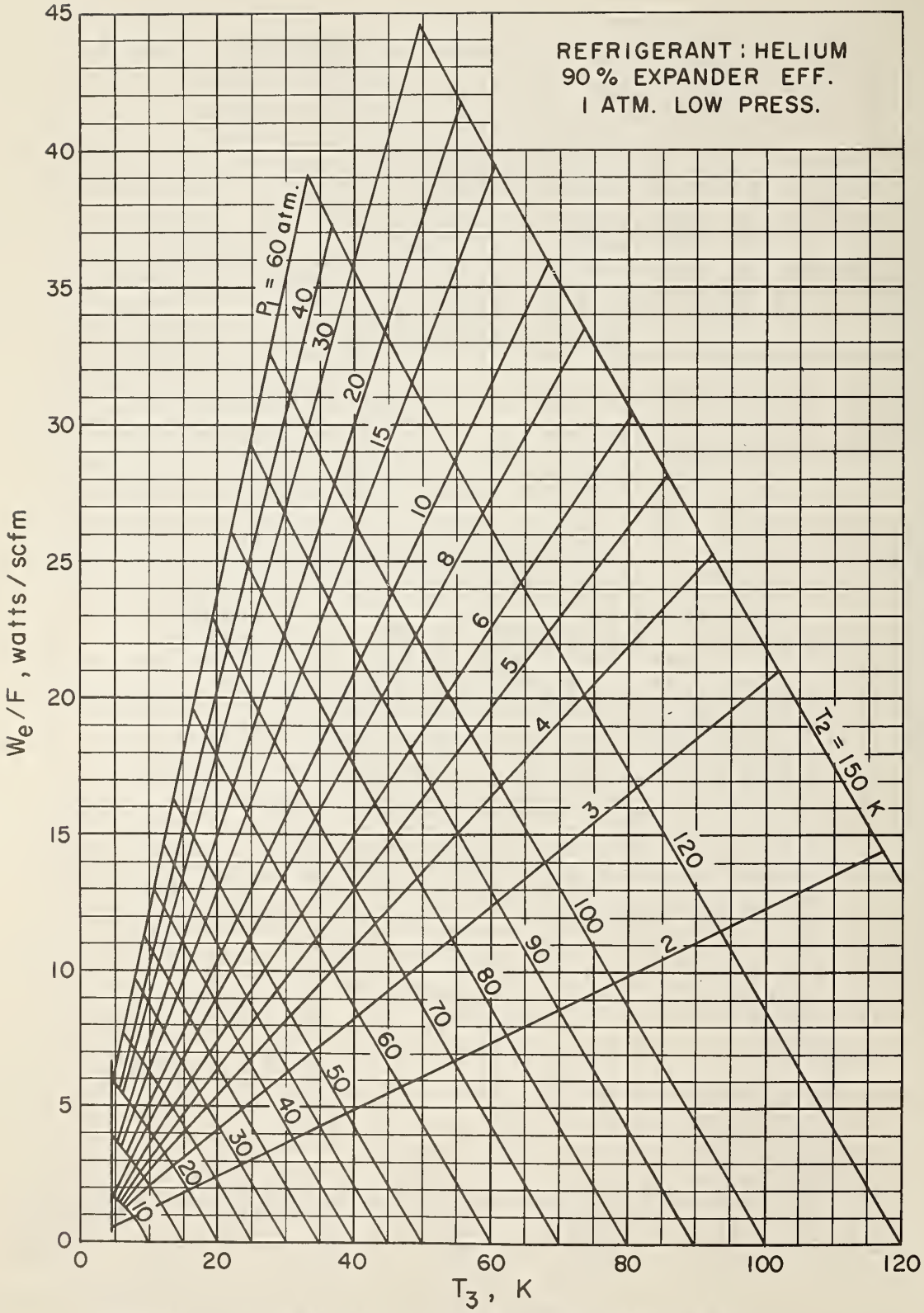

Figure 63. Expander Performance - Helium Refrigerant - 90% Expander Efficiency - No Pressure Drop.

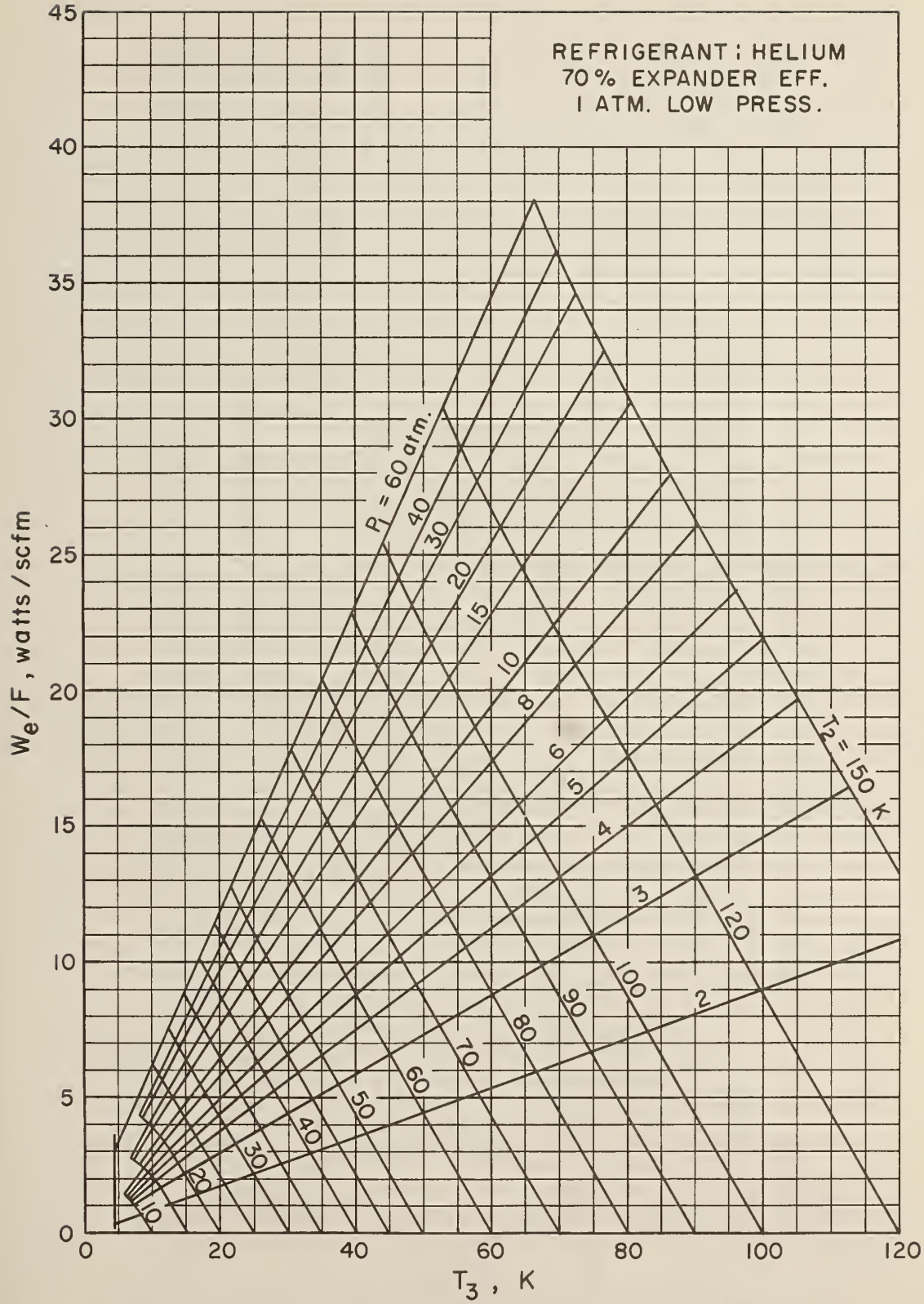

Figure 64. Expander Performance - Helium Refrigerant - 70% Expander Efficiency - No Pressure Drop.

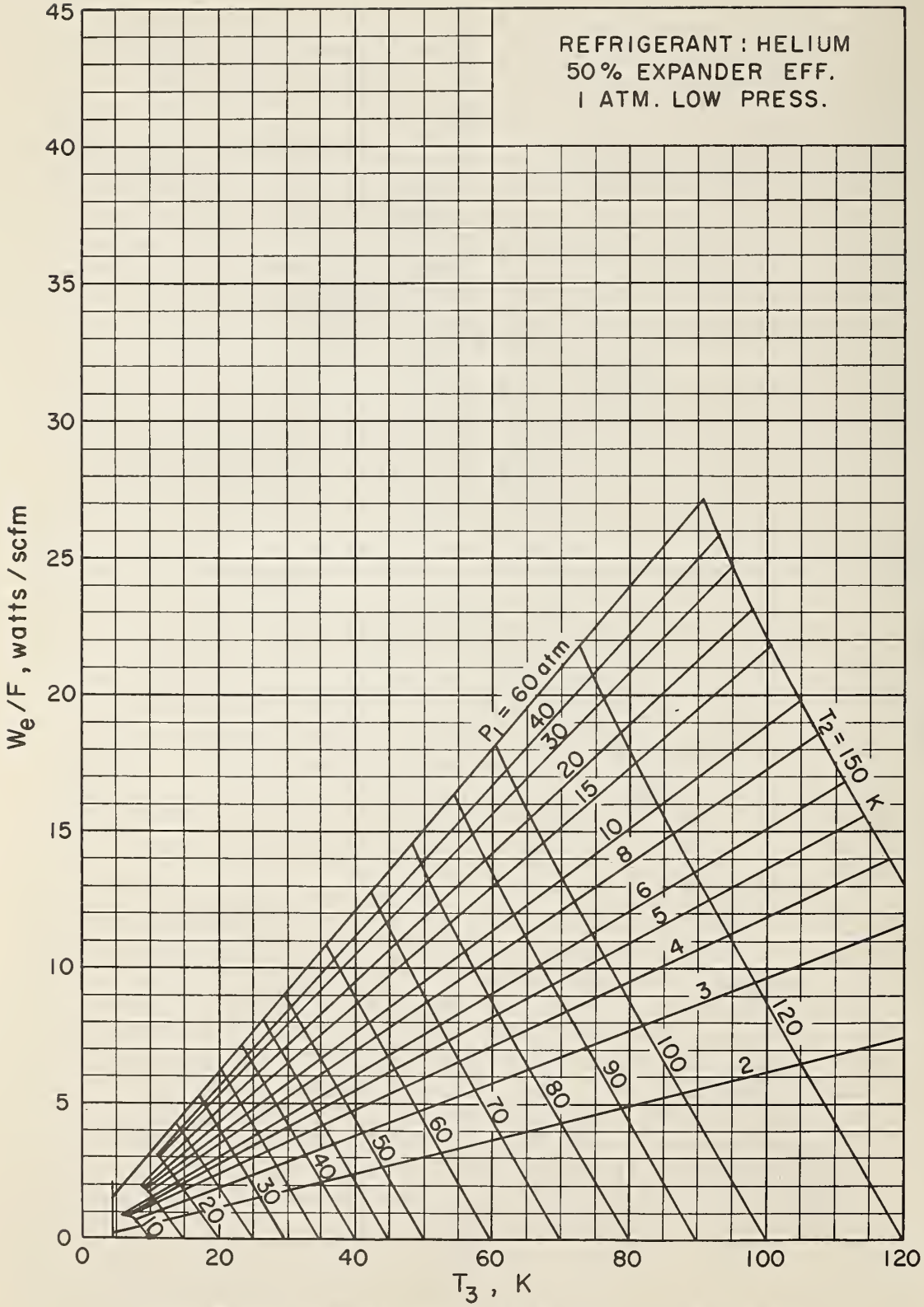

Figure 65. Expander Performance - Helium Refrigerant - 50% Expander Efficiency - No Pressure Drop.

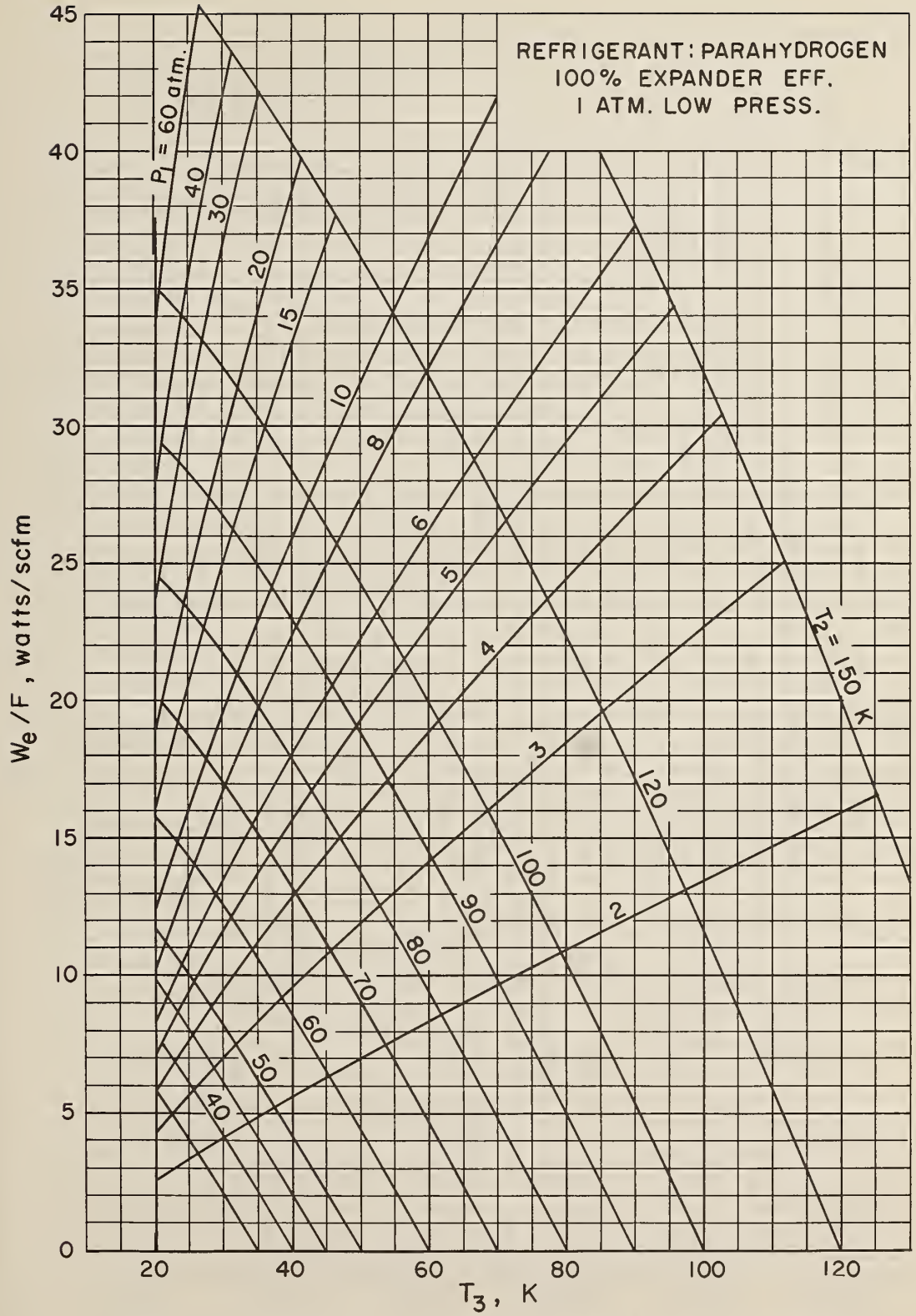

Figure 66. Expander Performance - Parahydrogen Refrigerant - 100% Expander Efficiency - No Pressure Drop.

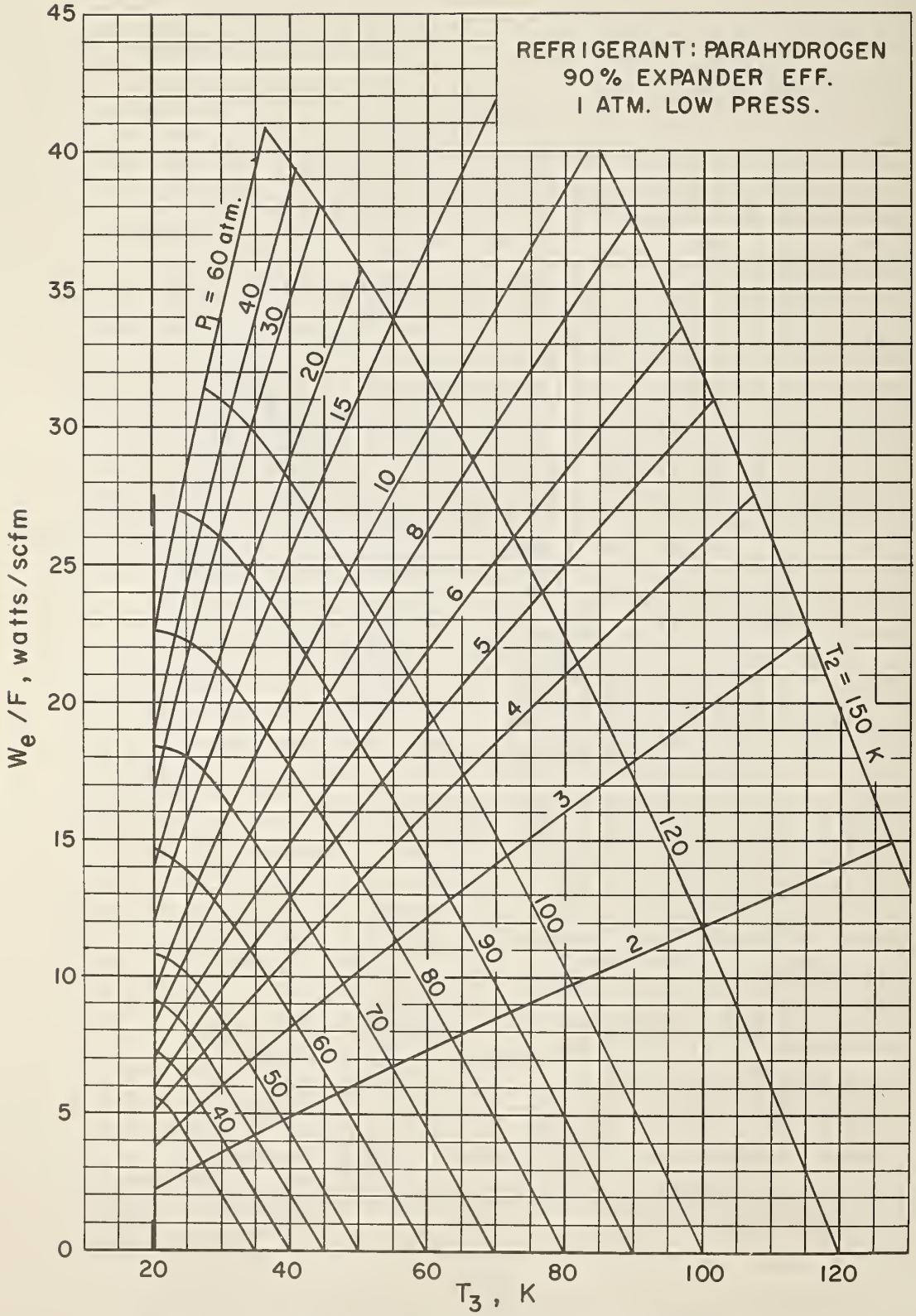

Figure 67. Expander Performance - Parahydrogen Refrigerant - 90% Expander Efficiency - No Pressure Drop.

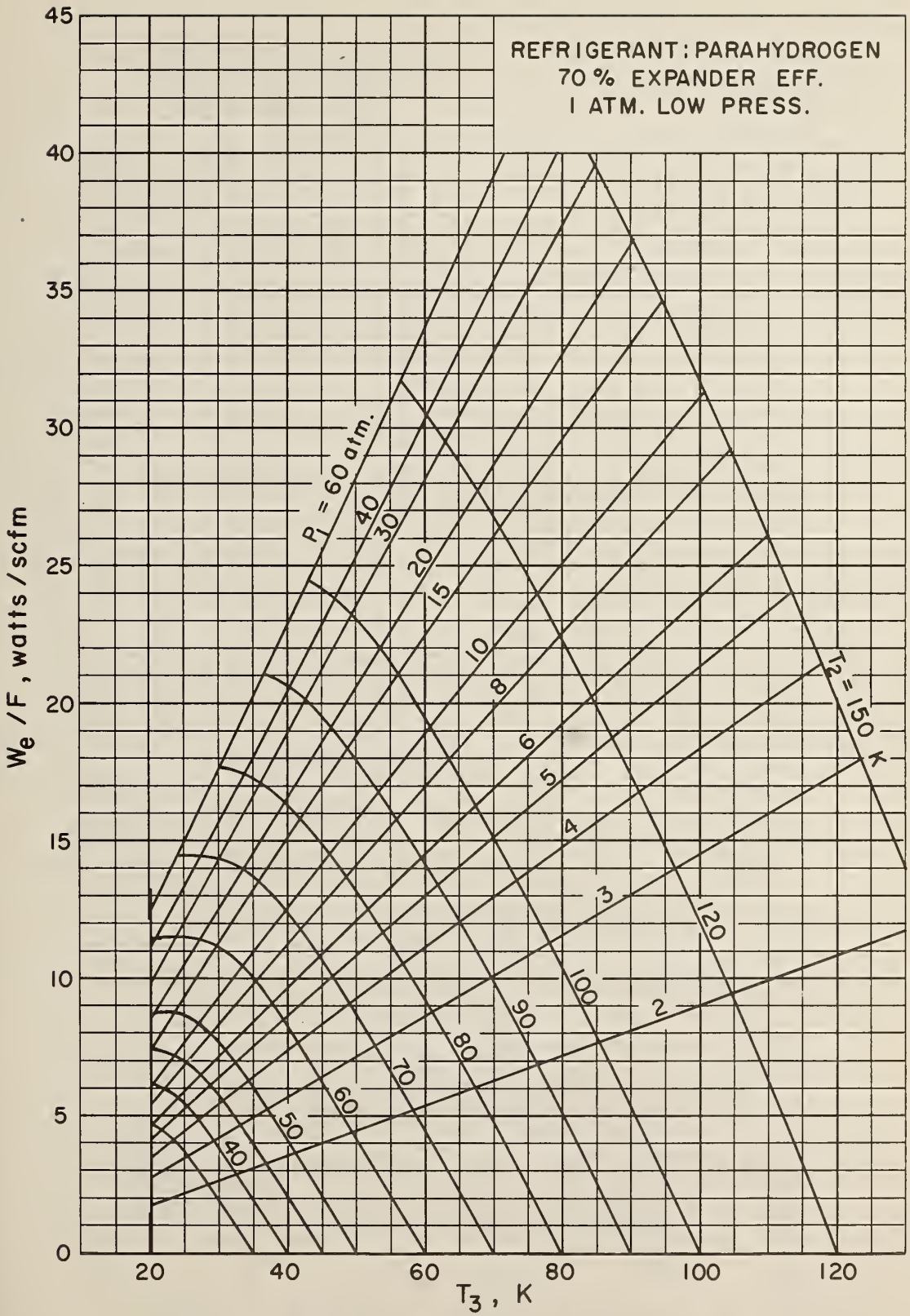

Figure 68. Expander Performance - Parahydrogen Refrigerant - 70% Expander Efficiency - No Pressure Drop.

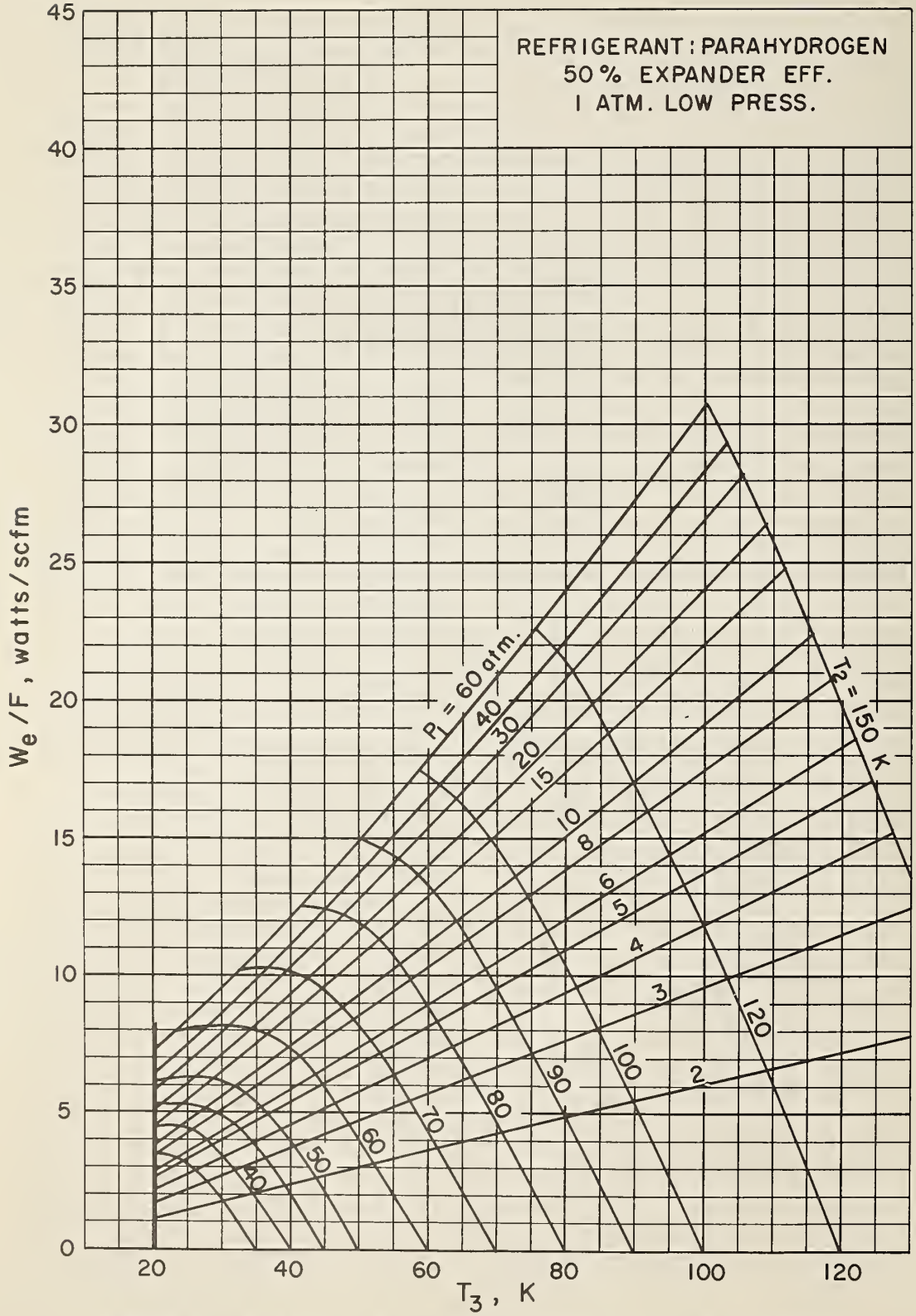

Figure 69. Expander Performance - Parahydrogen Refrigerant - 50% Expander Efficiency - No Pressure Drop.

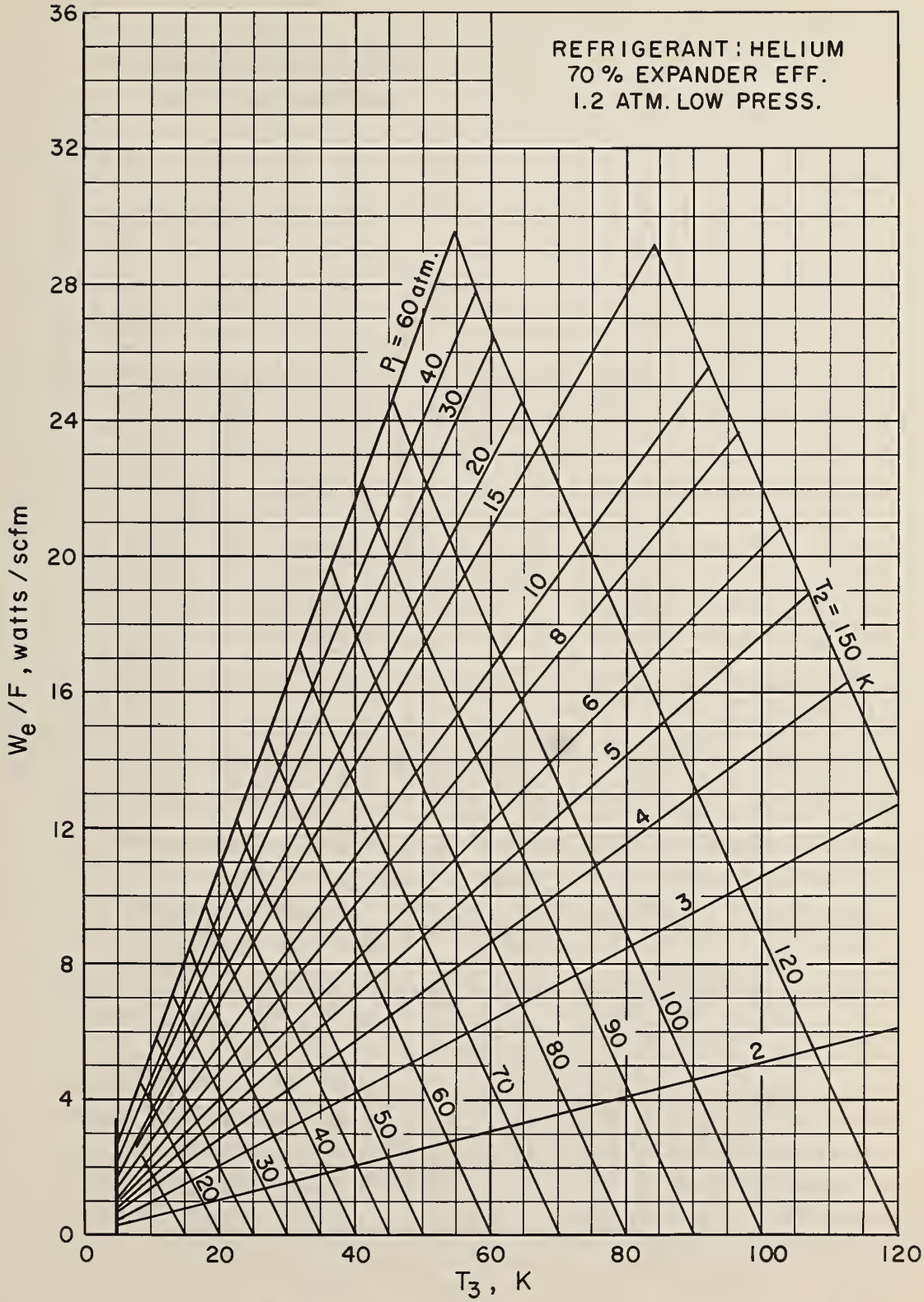

Figure 70. Expander Performance - Helium Refrigerant - 70% Expander Efficiency - Pressure Drop.

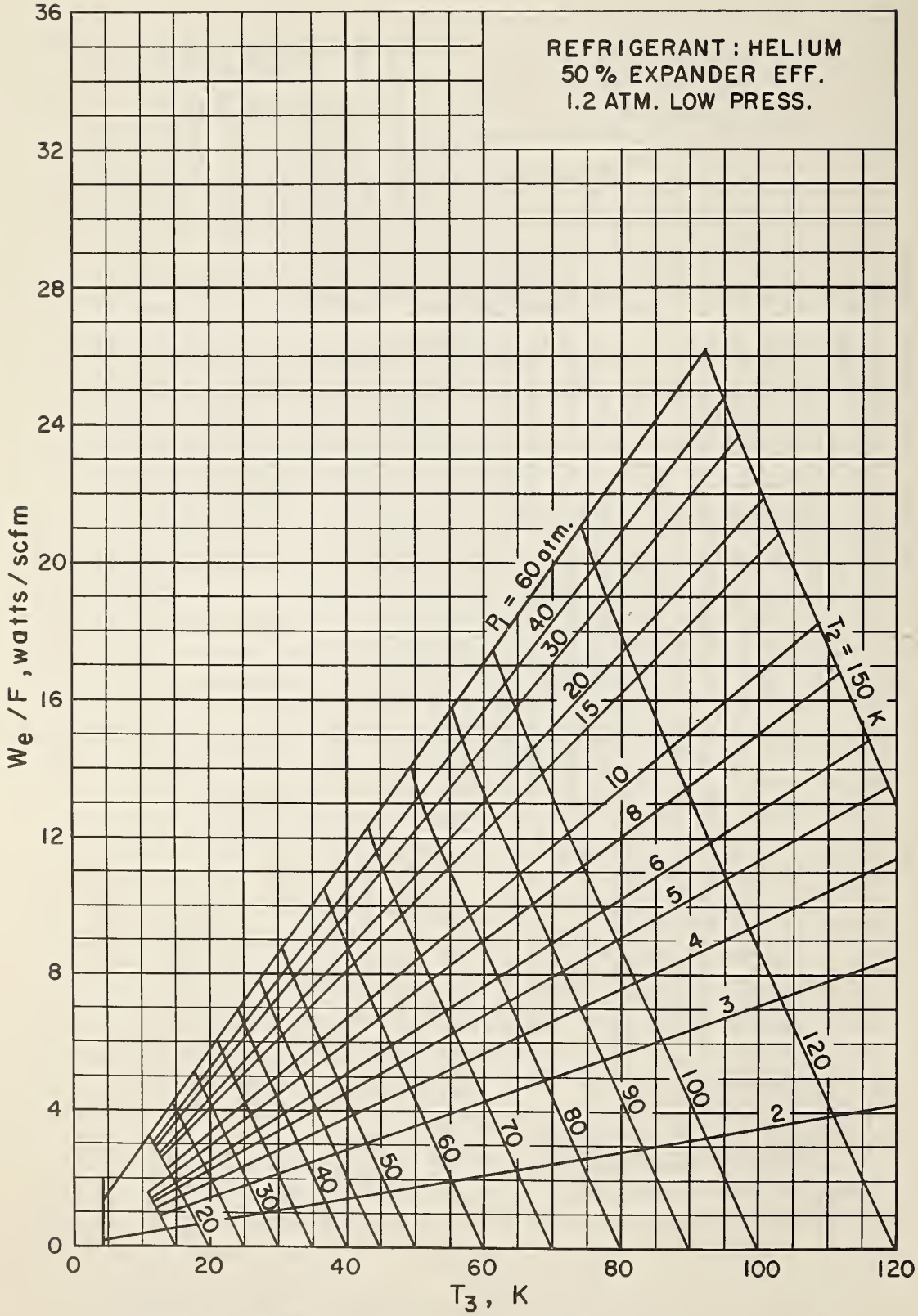

Figure 71. Expander Performance - Helium Refrigerant - 50% Expander Efficiency - Pressure Drop.

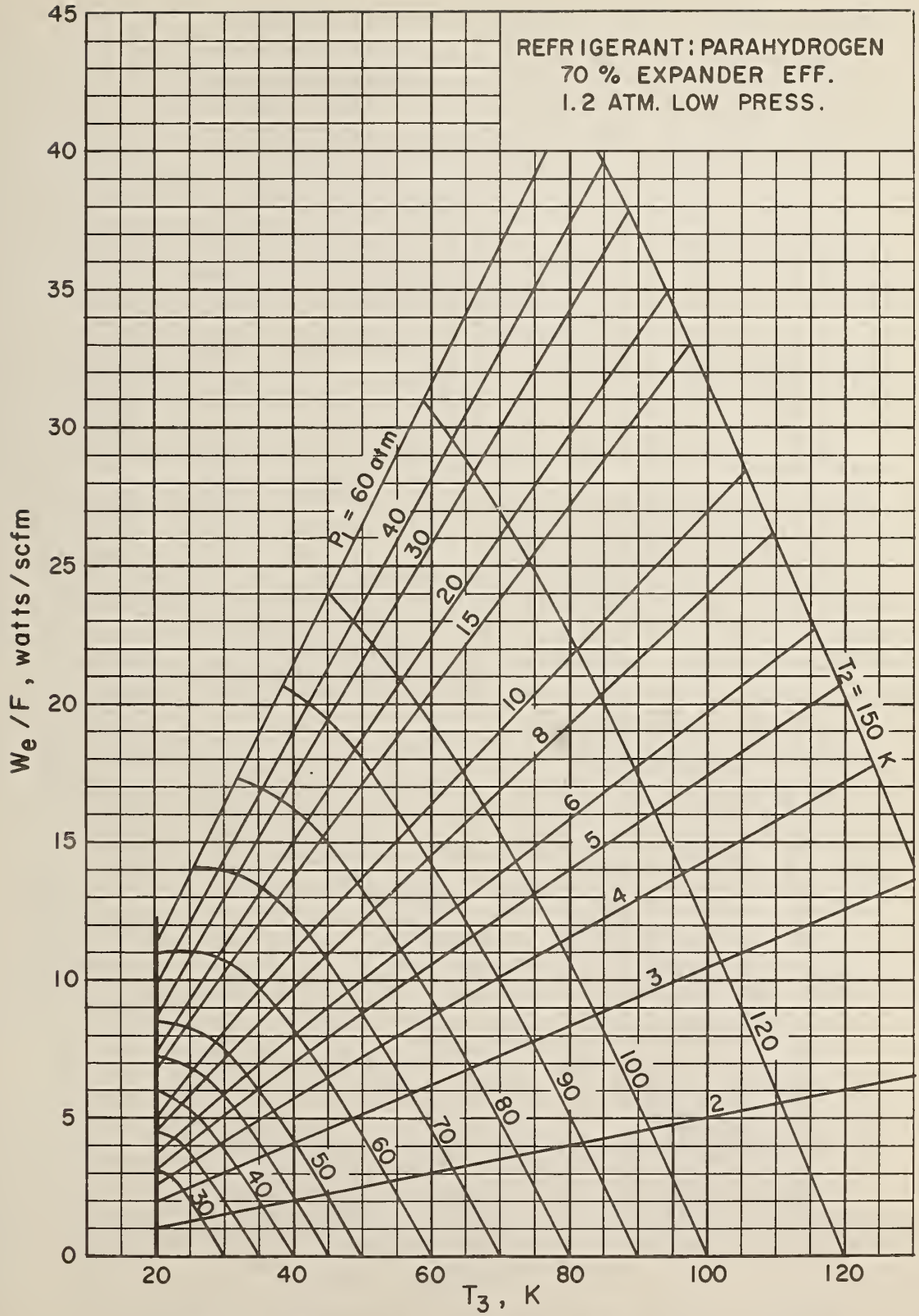

Figure 72. Expander Performance - Parahydrogen Refrigerant - 70% Expander Efficiency - Pressure Drop.

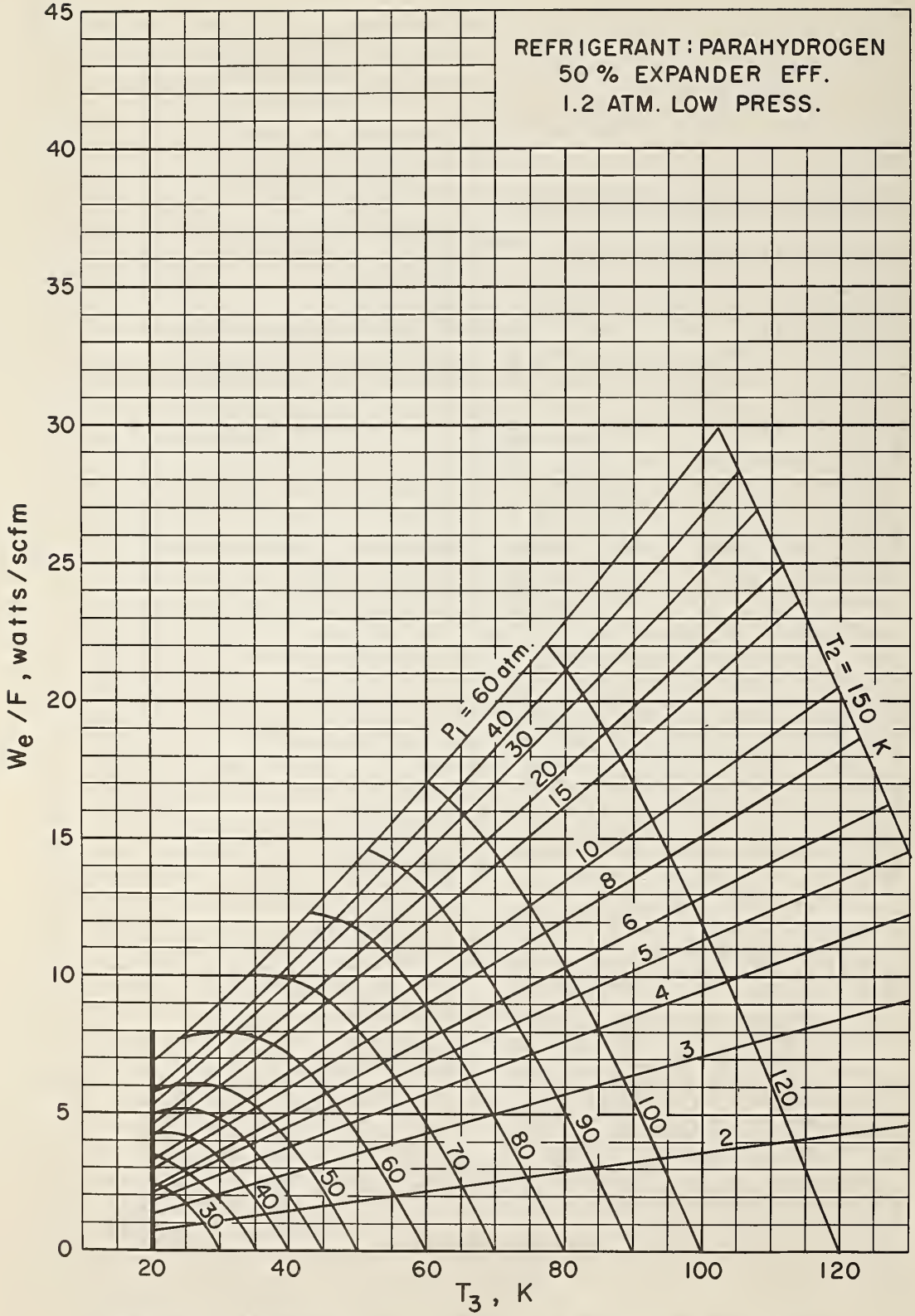

Figure 73. Expander Performance - Parahydrogen Refrigerant - 50% Expander Efficiency - Pressure Drop.

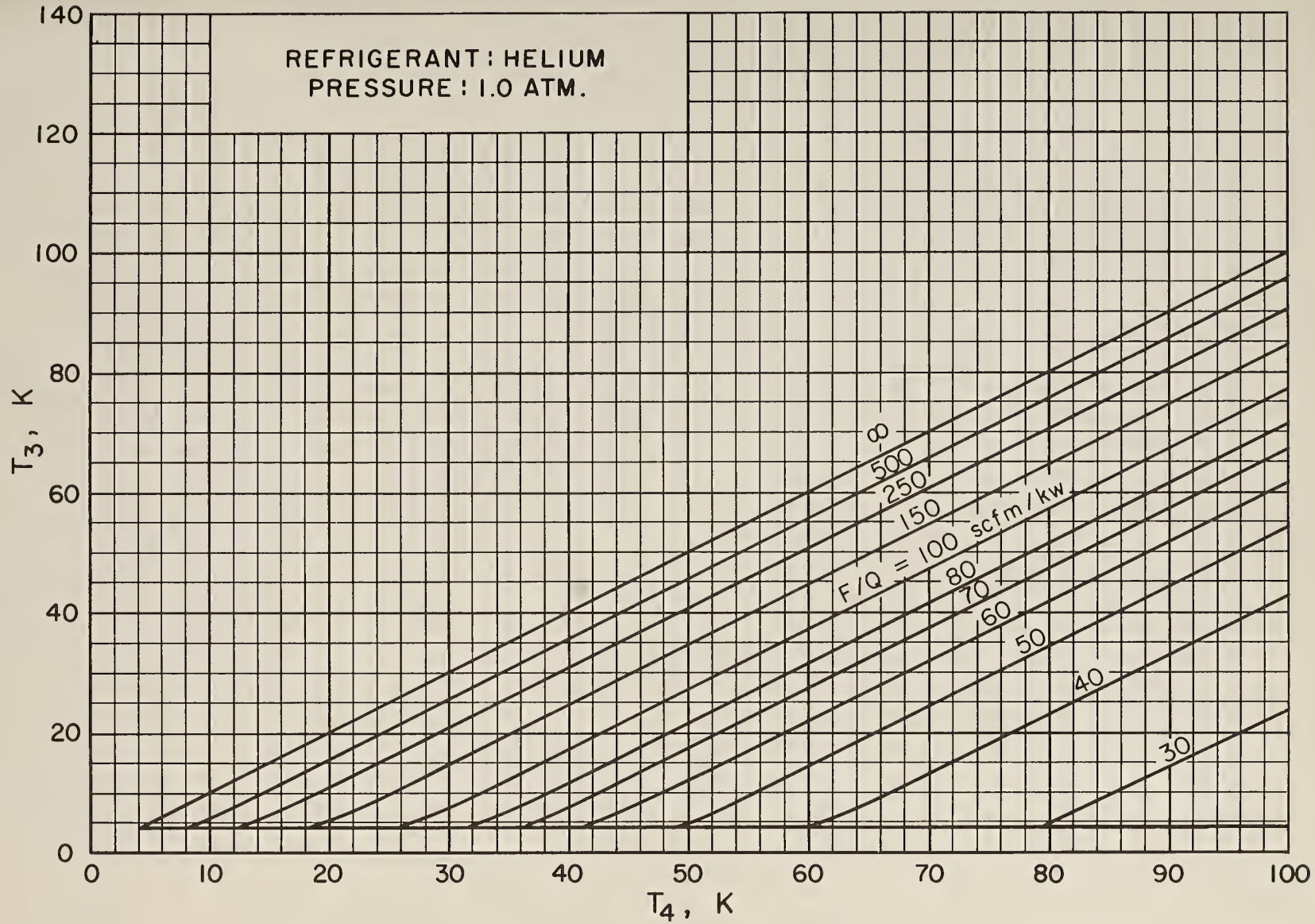

Figure 74. Specific Flow Rate - Helium Refrigerant.

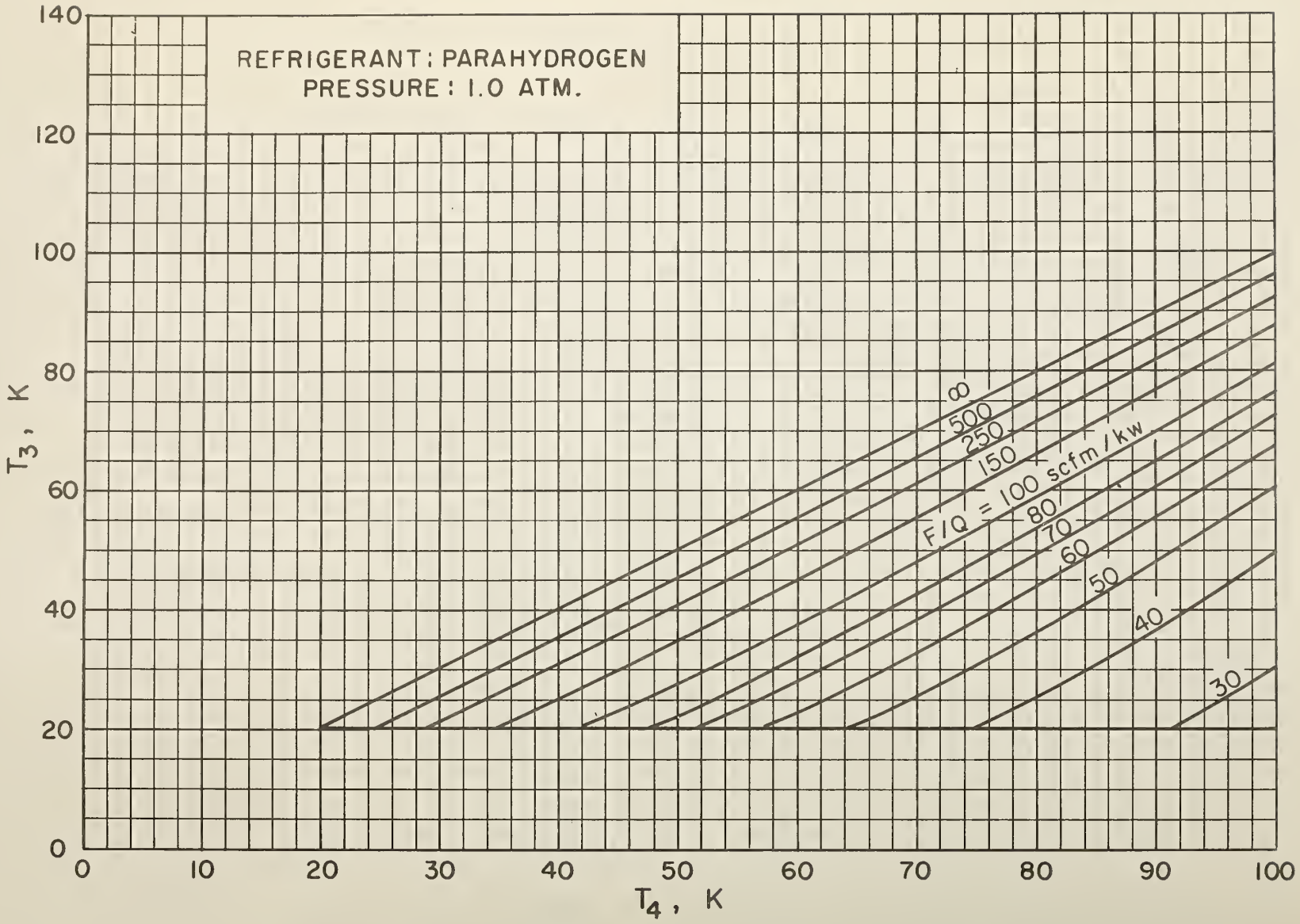

Figure 75. Specific Flow Rate - Parahydrogen Refrigerant.

GPO 845-449

NBS TECHNICAL PUBLICATIONS

PERIODICALS

JOURNAL OF RESEARCH reports National Bureau of Standards research and development in physics, mathematics, chemistry, and engineering. Comprehensive scientific papers give complete details of the work, including laboratory data, experimental procedures, and theoretical and mathematical analyses. Illustrated with photographs, drawings, and charts.

Published in three sections, available separately:

• Physics and Chemistry

Papers of interest primarily to scientists working in these fields. This section covers a broad range of physical and chemical research, with major emphasis on standards of physical measurement, fundamental constants, and properties of matter. Issued six times a year. Annual subscription: Domestic, $5.00; foreign, $6.00*.

• Mathematical Sciences

Studies and compilations designed mainly for the mathematician and theoretical physicist. Topics in mathematical statistics, theory of experiment design, numerical analysis, theoretical physics and chemistry, logical design and programming of computers and computer systems. Short numerical tables. Issued quarterly. Annual subscription: Domestic, $2.25; foreign, $2.75*.

• Engineering and Instrumentation

Reporting results of interest chiefly to the engineer and the applied scientist. This section includes many of the new developments in instrumentation resulting from the Bureau's work in physical measurement, data processing, and development of test methods. It will also cover some of the work in acoustics, applied mechanics, building research, and cryogenic engineering. Issued quarterly. Annual subscription: Domestic, $2.75; foreign, $3.50*.

TECHNICAL NEWS BULLETIN

The best single source of information concerning the Bureau's research, developmental, cooperative and publication activities, this monthly publication is designed for the industry-oriented individual whose daily work involves intimate contact with science and technology—*for engineers, chemists, physicists, research managers, product-development managers, and company executives.* Annual subscription: Domestic, $1.50; foreign, $2.25*.

*Difference in price is due to extra cost of foreign mailing.

NONPERIODICALS

Applied Mathematics Series. Mathematical tables, manuals, and studies.

Building Science Series. Research results, test methods, and performance criteria of building materials, components, systems, and structures.

Handbooks. Recommended codes of engineering and industrial practice (including safety codes) developed in cooperation with interested industries, professional organizations, and regulatory bodies.

Special Publications. Proceedings of NBS conferences, bibliographies, annual reports, wall charts, pamphlets, etc.

Monographs. Major contributions to the technical literature on various subjects related to the Bureau's scientific and technical activities.

National Standard Reference Data Series. NSRDS provides quantitative data on the physical and chemical properties of materials, compiled from the world's literature and critically evaluated.

Product Standards. Provide requirements for sizes, types, quality and methods for testing various industrial products. These standards are developed cooperatively with interested Government and industry groups and provide the basis for common understanding of product characteristics for both buyers and sellers. Their use is voluntary.

Technical Notes. This series consists of communications and reports (covering both other agency and NBS-sponsored work) of limited or transitory interest.

CLEARINGHOUSE

The Clearinghouse for Federal Scientific and Technical Information, operated by NBS, supplies unclassified information related to Government-generated science and technology in defense, space, atomic energy, and other national programs. For further information on Clearinghouse services, write:

Clearinghouse
U.S. Department of Commerce
Springfield, Virginia 22151

Order NBS publications from:
Superintendent of Documents
Government Printing Office
Washington, D.C. 20402

U.S. DEPARTMENT OF COMMERCE
WASHINGTON, D.C. 20230

OFFICIAL BUSINESS

POSTAGE AND FEES PAID
U.S. DEPARTMENT OF COMMERCE